



University of South Florida  
**Scholar Commons**

---

Graduate Theses and Dissertations

Graduate School

---

11-2-2009

# The Citric Acid Cycle of *Thiomicrospira crunogena*: An Oddity Amongst the Proteobacteria

Ishtiaque Quasem

*University of South Florida*

Follow this and additional works at: <http://scholarcommons.usf.edu/etd>

 Part of the [American Studies Commons](#)

---

## Scholar Commons Citation

Quasem, Ishtiaque, "The Citric Acid Cycle of *Thiomicrospira crunogena*: An Oddity Amongst the Proteobacteria" (2009). *Graduate Theses and Dissertations*.

<http://scholarcommons.usf.edu/etd/3680>

This Thesis is brought to you for free and open access by the Graduate School at Scholar Commons. It has been accepted for inclusion in Graduate Theses and Dissertations by an authorized administrator of Scholar Commons. For more information, please contact [scholarcommons@usf.edu](mailto:scholarcommons@usf.edu).

The Citric Acid Cycle of *Thiomicrospira crunogena*:

An Oddity Amongst the Proteobacteria

by

Ishtiaque Quasem

A thesis submitted in partial fulfillment  
of the requirements for the degree of  
Master of Science  
Department of Integrative Biology  
College of Arts and Sciences  
University of South Florida

Major Professor: Kathleen M. Scott, Ph.D.  
Jim Garey, Ph.D.  
Degeng Wang, Ph.D.

Date of Approval:  
November 2, 2009

Keywords: *Thiomicrospira crunogena*, central carbon metabolism, citric acid cycle,  
Proteobacteria, chemolithoautotroph

© Copyright 2009, Ishtiaque Quasem

## Acknowledgments

I would like to begin by acknowledging the USDA-CSREES program and NSF-MCB, which have provided the funds for my research assistantship. Their support was valuable in helping me progress as a researcher and independent thinker. I would also like to thank the University of South Florida Biology Department and the College of Arts and Science for a travel stipend to attend and present my research at the ASM meeting.

Most importantly, I would like to thank my committee for their advice on my project and help through the years. Dr. Jim Garey has taught me the fine art of molecular phylogenetics. Through thick and thin, his expertise was invaluable in helping me understand the phylogeny related to my bacterial genes and the many mechanisms of how to properly interpret such data. Dr. Degeng Wang was also invaluable in the techniques he had taught me in bioinformatics. Thanks to his thorough demonstrations of the many different ways to acquire and compare amino acid sequences, it allowed my data collection to be sensible and complete.

My years as a graduate student could not have been more productive nor as pleasant, had it not been for my persistent and wise major professor, Dr. Kathleen Scott. I would like to thank her for not only convincing me to take on a project entailing the genomic screening of the entire Proteobacterial phylum, but also directing and supporting me towards completing such a task. In addition, her experience and advice led me to not only complete this thesis, but also proposals, grants, and conference posters related to this project. It was through her compassion, understanding, and encouragements that helped me get through even the darkest of graduate school days. I am humbled and grateful for all the help and moral support she has given me during the time I have worked with her.

## Table of Contents

List of Tables .....	iii
List of Figures .....	iv
Abstract .....	v
Chapter 1 – Introduction .....	1
1.1 Hydrothermal Vent Habitat .....	1
1.2 Physiology .....	2
1.3 Phylogeny .....	3
1.4 Citric Acid Cycle Function .....	4
1.5 Steps of the Citric Acid Cycle .....	8
1.5.1 Pyruvate to Acetyl-coA .....	8
1.5.2 Acetyl-coA and Oxaloacetate to Citrate .....	10
1.5.3 Citrate to Isocitrate .....	11
1.5.4 Isocitrate to 2-oxoglutarate .....	11
1.5.5 2-oxoglutarate to Succinyl-coA .....	12
1.5.6 Succinyl-coA to Succinate .....	12
1.5.7 Succinate to Fumarate .....	13
1.5.8 Fumarate to Malate .....	14
1.5.9 Malate to Oxaloacetate .....	14
1.6 The Citric Acid Cycle in <i>T. crunogena</i> .....	15
1.7 Purpose .....	16
Chapter 2 – Methods .....	17
2.1 Finding Citric Acid Cycle Genes in Proteobacteria .....	17
2.2 Removing Genes with Apparent Alternative Function .....	18
2.3 Multiple Sequence Alignment and Phylogenetic Analysis .....	18
2.4 Enzyme Assays .....	20
Chapter 3 – Results and Discussion .....	24
3.1 Steps 1 – 4: Pyruvate to Oxoglutarate .....	25
3.2 Steps 5 – 9: Oxoglutarate to Oxaloacetate .....	34
3.3 Conclusion .....	42
References .....	43

Appendices.....	50
Appendix 1: Biochemically Characterized Genes of the Citric Acid Cycle Used as Query Sequences for BLAST Searches of IMG .....	51
Appendix 2: Paralogous Genes with an Alternative Function.....	57
Appendix 3: Active Site Residues for Alignment Verification .....	60
Appendix 4: Pfams Whose HMM Logos Were Used to Verify Alignments .....	63
Appendix 5: The Citric Acid Cycle of <i>T. crunogena</i> .....	66
Appendix 6: The Canonical Citric Acid cycle of <i>Gammaproteobacteria</i> .....	67
Appendix 7: The Canonical Citric Acid cycle of <i>Betaproteobacteria</i> .....	68
Appendix 8: The Canonical Citric Acid cycle of <i>Alphaproteobacteria</i> .....	69
Appendix 9: The Canonical Citric Acid cycle of <i>Epsilonproteobacteria</i> .....	70
Appendix 10: The Canonical Citric Acid cycle of <i>Delta-</i> and <i>Acido-Proteobacteria</i> .....	71
Appendix 11: Citric Acid Cycle Genes (Pyruvate to 2-Oxoglutarate) Present for Each Species in the <i>Gammaproteobacteria</i> .....	72
Appendix 12: Citric Acid Cycle Genes (Pyruvate to 2-Oxoglutarate) Present for Each Species in the <i>Betaproteobacteria</i> .....	75
Appendix 13: Citric Acid Cycle Genes (Pyruvate to 2-Oxoglutarate) Present for Each Species in the <i>Alphaproteobacteria</i> .....	77
Appendix 14: Citric Acid Cycle Genes (Pyruvate to 2-Oxoglutarate) Present for Each Species in the <i>Epsilon-</i> , <i>Delta-</i> , and <i>Acido-Proteobacteria</i> . .....	79
Appendix 15: Citric Acid Cycle Genes (2-Oxoglutarate to Oxaloacetate) Present for Each Species in the <i>Gammaproteobacteria</i> .....	80
Appendix 16: Citric Acid Cycle Genes (2-Oxoglutarate to Oxaloacetate) Present for Each Species in the <i>Betaproteobacteria</i> .....	83
Appendix 17: Citric Acid Cycle Genes (2-Oxoglutarate to Oxaloacetate) Present for Each Species in the <i>Alphaproteobacteria</i> .....	85
Appendix 18: Citric Acid Cycle Genes (2-Oxoglutarate to Oxaloacetate) Present for Each Species in the <i>Epsilon-</i> , <i>Delta-</i> , and <i>Acido-Proteobacteria</i> .....	87
Appendix 19: Phylogeny of Homodimeric Pyruvate Dehydrogenase Sequences.....	88
Appendix 20: Phylogeny of Isocitrate Dehydrogenase Sequences.....	92
Appendix 21: Phylogeny of Succinyl-coA Synthetase Sequences .....	96
Appendix 22: Phylogeny of Succinate Dehydrogenase/ Fumarate Reductase sequences.....	103
Appendix 23: Phylogeny of Class II Fumarase Sequences .....	109

## List of Tables

Table 1	Canonical Citric Acid Cycle Enzymes of Proteobacterial Classes.....	24
Table 2	Activities of Citric Acid Cycle Enzymes in <i>T. crunogena</i> .....	26

## List of Figures

Figure 1	Proteobacteria Phylogeny .....	3
Figure 2	16S RNA Tree of <i>Gammaproteobacteria</i> .....	3
Figure 3	Oxidative Citric Acid Cycle.....	5
Figure 4	Reverse Citric Acid Cycle .....	6
Figure 5	Reductive Citric Acid Pathway.....	7
Figure 6	Phylogeny of siCitrate Synthase Sequences .....	27
Figure 7	Effect of NADH on the Activities of Citrate Synthase in <i>T. crunogena</i> and <i>E. coli</i> .....	29
Figure 8	Phylogeny of Aconitase Sequences .....	31
Figure 9	Phylogeny of 2-Oxoglutarate: Acceptor Oxidoreductase Sequences .....	35
Figure 10	Phylogeny of Malate: Quinone Oxidoreductase Sequences .....	39

The Citric Acid Cycle of *Thiomicrospira crunogena*:  
An Oddity Amongst the Proteobacteria

Ishtiaque Quasem

ABSTRACT

*Thiomicrospira crunogena*, a deep-sea hydrothermal vent chemolithoautotroph, uses the Calvin-Benson-Bassham cycle to fix carbon. To meet its biosynthetic needs for oxaloacetate, oxoglutarate, and succinyl-coA, one would expect that this obligately autotrophic *Gammaproteobacterium* would use a ‘wishbone’ version of the citric acid cycle (CAC) to synthesize the intermediates necessary for biosynthesis, instead of the fully oxidative version to minimize carbon loss as carbon dioxide. However, upon examination of its complete genome sequence, it became apparent that this organism did not fulfill this expectation.

Instead of a wishbone pathway, *T. crunogena* appears to run a fully oxidative CAC. The cycle is ‘locked’ in the oxidative direction by replacement of the reversible enzyme malate dehydrogenase with malate: quinone oxidoreductase, which is capable only of operation in the oxidative direction. Furthermore, oxoglutarate decarboxylation is catalyzed by oxoglutarate: acceptor oxidoreductase. The presence of both oxidoreductases was confirmed via assays on *T. crunogena* cell extracts.

To determine whether this peculiar CAC was novel, complete genome sequences of ~340 Proteobacteria were examined via BLAST and COG searches in the Integrated



Microbial Genome database. Genes catalyzing steps in the CAC were collected from each organism and vetted for paralogs that had adopted an alternative, ‘non-CAC’ function through genome context and cluster analysis. Alignments were made with the remaining sequences and were verified by comparing them to curated alignments at Pfam database and examination of active site residues. Phylogenetic trees were constructed from these alignments, and instances of horizontal gene transfer were determined by comparison to a 16S tree.

These analyses verified that the CAC in *T. crunogena* is indeed unique, as it does not resemble any of the canonical cycles of the six classes of proteobacteria. Furthermore, three steps of the nine in its CAC appear to be catalyzed by enzymes encoded by genes that are likely to have been acquired via horizontal gene transfer. The gene encoding citrate synthase, and perhaps aconitase, are most closely affiliated with those present in the *Cyanobacteria*, while those encoding oxoglutarate: acceptor oxidoreductase cluster among the *Firmicutes*, and malate: quinone oxidoreductase clusters with the *Epsilonproteobacteria*.

## Chapter 1 - Introduction

*Thiomicrospira crunogena* was among the first obligate chemolithoautotrophic bacteria to have its genome sequenced [1]. One of the peculiarities identified during genome annotation was its bizarre citric acid cycle (CAC), which, unlike the wishbone-shaped citric acid pathway anticipated based on its autotrophic lifestyle, was locked in an oxidative direction with noncanonical enzymes [1]. The work conducted here explores the CAC of this organism in greater depth using genome comparisons, phylogenetic analyses, and enzyme assays.

### 1.1 Hydrothermal Vent Habitat

*Thiomicrospira crunogena* is a deep sea vent chemolithoautotrophic gammaproteobacterium [1], originally isolated from the East Pacific Rise [2] and detected through molecular methods in deep sea vents in both the Pacific and Atlantic oceans [3]. At these vents, warm hydrothermal vent fluid rich in redox substrates and dissolved inorganic carbon (DIC) is emitted [1]. The temperature difference of this warm vent fluid with the surrounding seawater ( $\sim 2^{\circ}\text{C}$ ) creates turbulent eddies as they mix; therefore the vent habitat fluctuates between dominance of the cold oxic bottom water and the warm anoxic vent fluid in short periods of time [1, 4].

Nonetheless, the deep sea hydrothermal vent is an ecosystem teeming with life, primarily due to chemolithoautotrophic microorganisms, like *T. crunogena*, producing

the bulk of the organic material. These primary producers are able to harness the energy released from the oxidation of reduced inorganic compounds (e.g.,  $\text{H}_2\text{S}$ ,  $\text{CH}_4$ ,  $\text{H}_2$ ,  $\text{Fe}^{+2}$ ) emitted from the vent and use it for carbon fixation [1, 5-8].

## 1.2 Physiology

*T. crunogena* is one of the most rapidly growing obligate autotrophs known, with a doubling time of approximately 1 hr under mesophilic conditions (20-30°C) [2]. This organism does not demonstrate an ability to use extracellular organic carbon compounds as electron donors or carbon sources [2]; growth on, and assimilation of, acetate, succinate, or glucose are not detectable (K. Scott, unpubl. data). Instead, it is capable of using reduced sulfur compounds ( $\text{H}_2\text{S}$ ,  $\text{S}_2\text{O}_4^{-2}$ ,  $\text{S}^0$ ) as electron donors, likely via a membrane-associated Sox system. Oxygen is the only electron acceptor supporting growth by *T. crunogena* [1]; growth is most rapid under low oxygen conditions, and its genome encodes a *cbb<sub>3</sub>*-type cytochrome c oxidase, which has a high affinity for oxygen, facilitating this microaerophilic lifestyle [1, 9]. This organism uses the energy from sulfur oxidation to fuel carbon fixation via the Calvin-Benson-Bassham cycle [1]. Despite the periodically high concentrations of dissolved inorganic carbon (DIC) present at hydrothermal vents, *T. crunogena* can grow rapidly even when the DIC concentration is as low as 20  $\mu\text{M}$ , apparently due to this organism's ability to accumulate intracellular DIC concentrations that are more than 100X higher than extracellular [10].

### 1.3 Phylogeny

*T. crunogena* is a member of the *Gammaproteobacteria*, one of the six classes into which the Proteobacteria are divided (*Alpha*, *Beta*, *Gamma*, *Delta*, *Epsilon*, and *Acidobacteria*; Fig. 1 [11, 12]). Based on 16S sequences, *T. crunogena* does not fall within any of the other clusters of *Gamma-proteobacteria* whose genomes have been sequenced at this point (Fig. 2).

**Figure 1: A generalized phylogenetic tree of the Proteobacterial classes, adapted from [11, 12].**

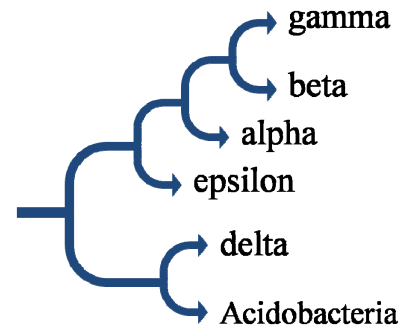
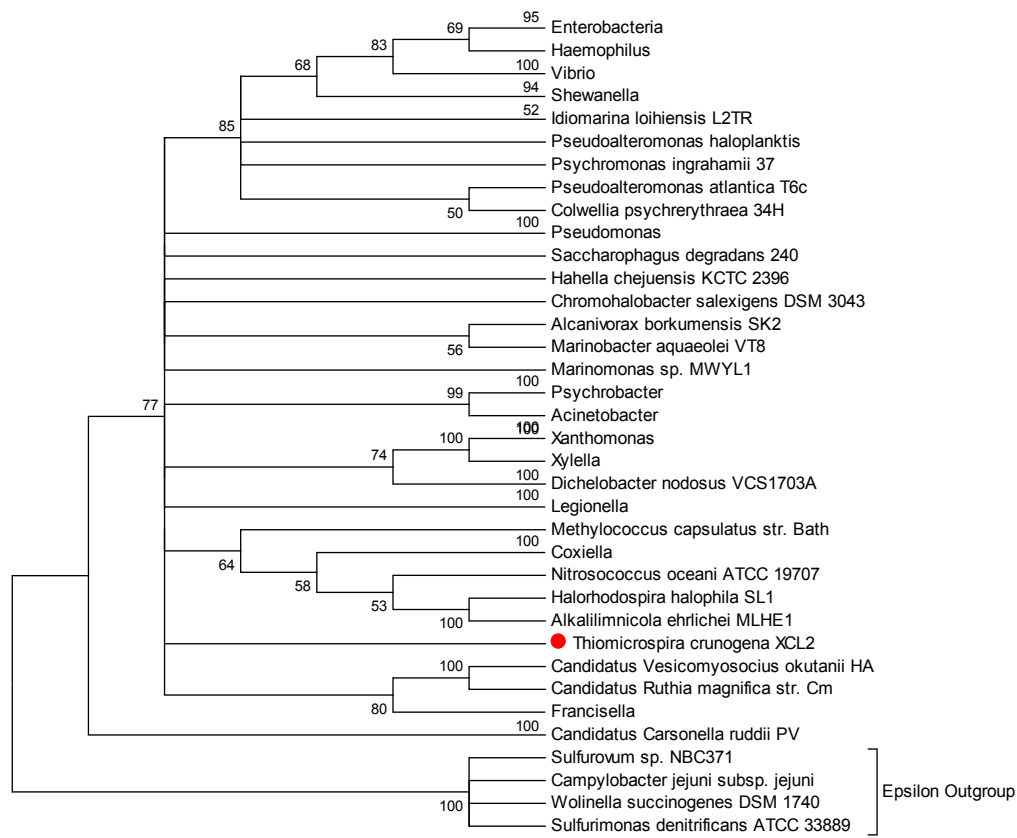


**Figure 2: 16S RNA tree of *Gammaproteobacteria* whose genomes have been sequenced. The inferred evolutionary relatedness is based on 16S rRNA gene sequences. Complete 16S sequences were aligned via RNACAD, implemented via RDP 2, version 10, using a model for secondary structure based on bacterial 16S [13]. Neighbor-joining trees were constructed with MEGA 4.0, with bootstrap values based on 1000 replicate samplings of the alignments, pairwise deletions for gaps and missing data, a maximum composite likelihood model, and the assumption of uniform rates among sites [14]. Only those bootstrap values larger than 50 are included on this tree. To simplify the figure, the Enterobacteria and some monogenic clades have been collapsed and are listed in the tree as a genus name.**



## 1.4 Citric Acid Cycle Function

Organisms with different physiologies have adopted different modes of the CAC to meet their metabolic needs. In the oxidative CAC (Fig. 3), oxaloacetate and acetyl-coA are condensed to synthesize citrate, which is oxidized and decarboxylated twice to regenerate oxaloacetate, and produce NADH, which can feed electrons into the electron transport chain (ETC) [15]. In the process of running this cycle, metabolic intermediates necessary for biosynthesis are generated [16, 17]. Oxoglutarate is formed, which is necessary for glutamate synthesis [18]. Succinyl-coA is also produced, which in many organisms is necessary for porphyrin synthesis [19]. Oxaloacetate is also synthesized, which is necessary for aspartate and nucleobase synthesis [17]. In some autotrophic bacteria and archaea, the CAC can also operate in a reverse, reductive, CO<sub>2</sub>-fixing direction (Fig. 4) as a primary carbon fixation pathway [20, 21].

Many cyanobacteria and other autotrophs using the Calvin-Benson-Bassham cycle for carbon fixation have a wishbone shaped version of the citric acid cycle [22], which minimizes decarboxylations. In this wishbone-shaped reductive citric acid pathway (Fig. 5), the metabolic requirements for oxoglutarate are met by decarboxylation of citrate, as in the oxidative CAC, while succinyl-coA and oxaloacetate are synthesized from pyruvate by carboxylation and reduction [1, 15, 22]; by circumventing the decarboxylation of oxoglutarate, these organisms conserve the energy they have expended in forming this carbon-carbon bond.

Figure 3: The oxidative citric acid cycle. The numbers correspond to the following enzymes: 1. Pyruvate dehydrogenase 2. Citrate synthase 3. Aconitase 4. Isocitrate dehydrogenase 5. 2-oxoglutarate dehydrogenase 6. Succinyl-coA synthetase 7. Succinate dehydrogenase 8. Fumarase 9. Malate dehydrogenase

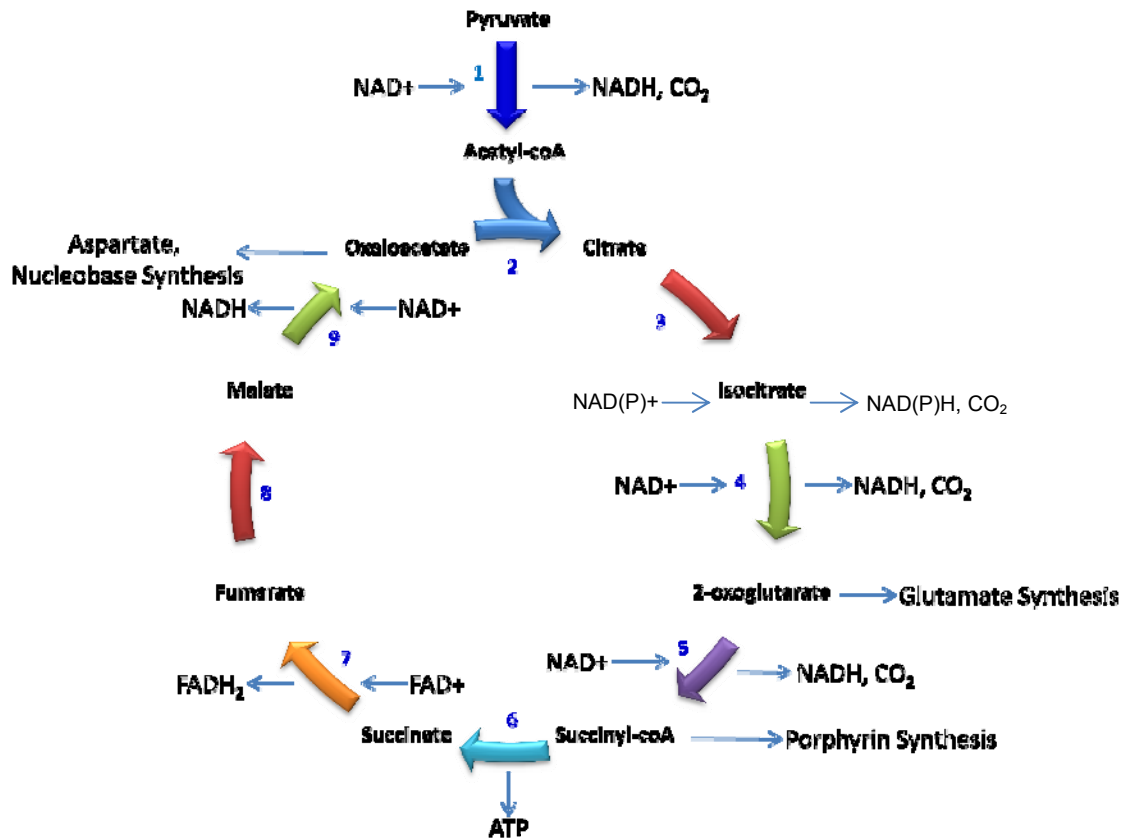


Figure 4: The reverse citric acid cycle, adapted from [23], which is utilized, instead of the Calvin-Benson-Bassham cycle, by some autotrophs to fix carbon. The numbers correspond to the following enzymes: 1. ATP-dependent citrate lyase; 2. Pyruvate: acceptor oxidoreductase, 3. Phosphoenolpyruvate synthase, 4. Phosphoenolpyruvate carboxykinase, 5. Malate dehydrogenase, 6. Fumarase, 7. Fumarate reductase, 8. Succinyl-coA ligase, 9. Oxoglutarate: acceptor oxidoreductase, 10. Isocitrate dehydrogenase, 11. Aconitase.

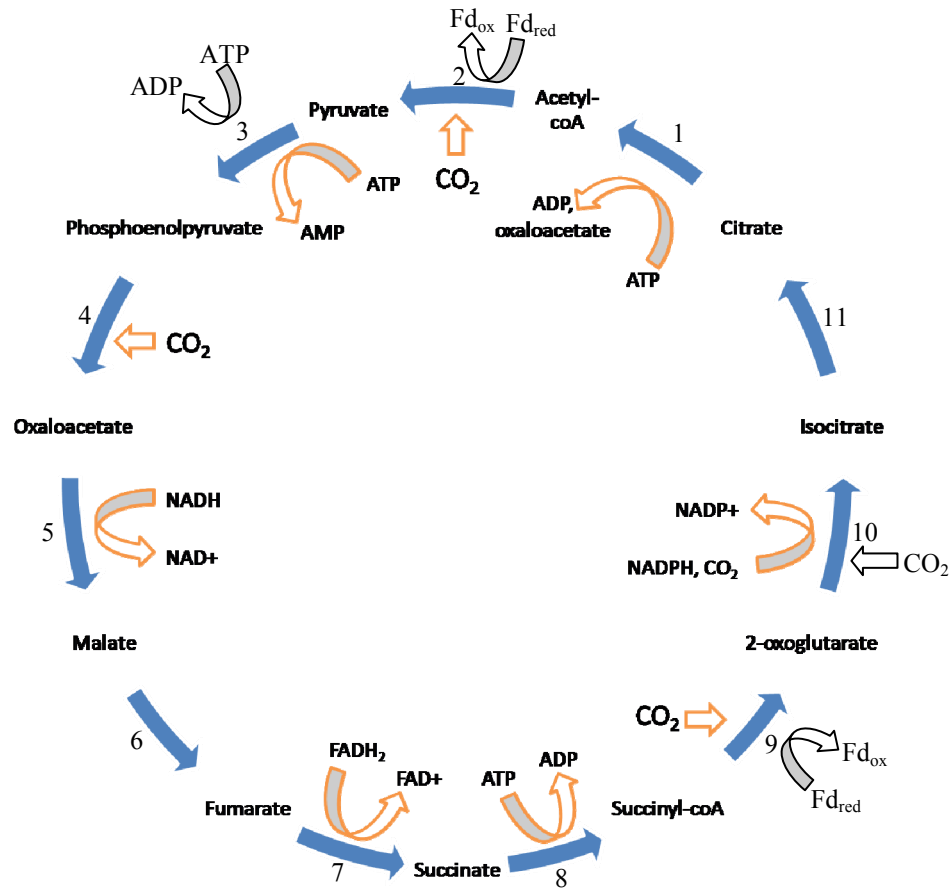
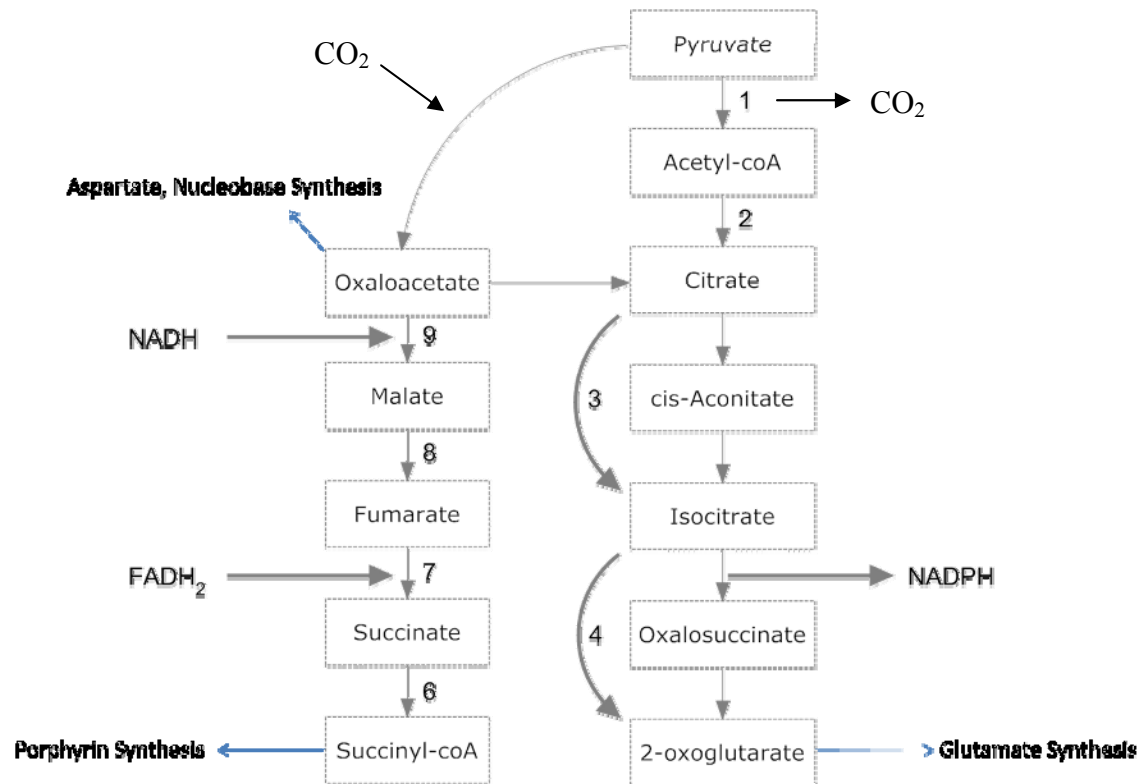


Figure 5: The wishbone shaped reductive citric acid pathway, adapted from [24]. This pathway provides no net reduction or oxidation, and allows lithoautotrophic organisms which do not use organic carbon as their major electron donor to still produce intermediates necessary for biosynthesis. The numbers represent enzymes catalyzing each reaction, and are as listed in Fig. 3. In this pathway, the interconversion of succinyl-coA and 2-oxoglutarate does not occur.





## 1.5 Steps of the citric acid cycle

1.5.1 Pyruvate to Acetyl-coA. Three complexes are capable of interconverting pyruvate and acetyl-coA (pyruvate dehydrogenase, pyruvate: acceptor oxidoreductase, and pyruvate: formate lyase). The pyruvate dehydrogenase complex (PDH) catalyzes the irreversible decarboxylation of pyruvate to form acetyl-coA. This complex exists in homodimeric and heterodimeric forms. The homodimeric PDH consists of the enzymes pyruvate dehydrogenase/decarboxylase (E1), dihydrolipoyl acetyltransferase (E2) and dihydrolipoyl dehydrogenase (E3) and is octahedral in symmetry [25-27]. Heterodimeric PDH does not have an E1 subunit homologous to the one present in homodimeric PDH. Instead, the evolutionarily distinct heterodimeric PDH E1 consists of an  $\alpha$  and  $\beta$  subunit, and holoenzyme is a heterotetramer (E1 $\alpha$  and E1 $\beta$ , E2, E3) with icosahedral symmetry [26]. The subunits of the PDH complex act in concert to produce acetyl-coA. E1 or E1 $\alpha\beta$  decarboxylates pyruvate and links the remaining two carbon unit to thiamine pyrophosphate. The E2 subunits transfer the two carbon unit from thiamine pyrophosphate to coA via lipoic acid prosthetic groups. The E3 subunit reoxidizes the E2-bound lipoic acid [27]. The E2 subunit forms the structural core of the complex [27-29], while the E1 and E3 subunits form a shell around it [29]. The genetic organization of this complex varies across species, but in general the E1/E1 $\alpha\beta$  and E2 subunits are present in an operon [25]. E3 can be shared by other complexes and thus the gene is sometimes present on the genome far from the PDH operon [25]. PDH is particularly useful for aerobic organisms, since unlike the other enzymes capable of converting pyruvate to acetyl-coA, it is not sensitive to oxygen and can contribute electrons to the

ETC [30].

Pyruvate: Acceptor Oxidoreductase (PAOR) catalyzes the reversible conversion of pyruvate to acetyl-coA. Thus far, four forms of this enzyme have been described: single subunit, two-subunit, four subunit, and five subunit [31, 32]. The four types are phylogenetically homologous; the ancestral form is believed to have had four subunits, and the other forms may have arisen from them via gene fusion [31-34]. The fifth subunit of the five-subunit form appears to be unique to that form [32]. The PAOR complex contains 1–3 iron-sulfur clusters and thiamine pyrophosphate [35], which aid in the oxidative decarboxylation of pyruvate. In general, PAOR is oxygen sensitive, although the homodimeric PAOR from *Desulfovibrio africanus* is not [36]. The PAOR reaction is reversible because the cellular electron acceptors this complex uses have extremely low midpoint potentials (e.g., ferredoxin and flavodoxin; [32, 37, 38]. The reversibility of this enzyme lends it a degree of versatility [37]. For instance, in autotrophs that utilize the reductive citric acid cycle as their primary carbon fixation pathway, PAOR functions to carboxylate acetyl-coA [35]. In many anaerobes, the PAOR complex catalyzes the decarboxylation of pyruvate as the first step of the phosphoroclastic system, in which acetyl-coA that PAOR produces is converted to acetyl-phosphate via a phosphotrans-acetylase, which in turn can be used to phosphorylate ADP via substrate-level phosphorylation [32, 37]. Furthermore, sulfate reducers, nitrogen fixers and acetogenic bacteria can use the extremely low-potential electrons produced by the PAOR complex for a variety of biosynthetic processes [37].

The third complex, pyruvate formate lyase (PFL), is found in many organisms

growing anaerobically and aids in fermentative glucose metabolism [39]. It is a homodimer and, like PAOR, catalyzes a reversible decarboxylation of pyruvate. Unique to PFL, a glycy radical intermediate is used, and the one-carbon unit removed from pyruvate is released as formate instead of carbon dioxide. Therefore, unlike both PAOR and PDH, no reduced cellular electron carrier (e.g., NADH or ferredoxin) is produced [40, 41]. This oxygen-sensitive enzyme is particularly useful for organisms growing without an ETC, as it does not produce reduced electron carriers.

1.5.2 Acetyl-coA and Oxaloacetate to Citrate. The condensation of acetyl-coA and oxaloacetate to form citrate is unique as it is the only reaction in the CAC that results in the formation of a carbon-carbon bond [42]. Two physiologically dissimilar enzymes catalyze this irreversible reaction: the ubiquitous si-citrate synthase (siCS) and the less common re-citrate synthase (reCS) [43]. The prefixes refer to the stereospecificity of the carboxymethyl group of oxaloacetate to which the acetyl-coA is incorporated [43].

Two forms of siCS exist: Type 1 and Type 2. In general, Type 1 is dimeric, regulated by ATP, and prevalent among eukaryotes, archaea, and gram-positive bacteria, whereas Type 2 is hexameric and common among the gram-negative bacteria [44-46]. Most Type 2 siCS enzymes are allosterically inhibited by NADH [44]. However, cyanobacterial siCS enzymes are insensitive to NADH [47-49], as is that of *Acetobacter aceti* [50]. This irreversible enzyme differs structurally across domains of life, but studies suggest that all forms (Types 1 & 2) have similar active sites [44, 50]. Due to its oxygen insensitivity, it could be useful for aerobic organisms that have an ETC for ATP generation. Facultative anaerobes allosterically inhibit the activity of this enzyme when

growing anaerobically to prevent excess NADH formation [50].

Although the subunit composition and molecular mass have not yet been reported in reCS, the unusual stereospecificity of its reaction, need for  $Mn^{+2}$  or  $Co^{+2}$ , and sensitivity to oxygen make it quite distinct from siCS [43]. These characteristics restrict this enzyme to anaerobes such as *Clostridia* and *Desulfovibrio* [43].

1.5.3 Citrate to Isocitrate. The interconversion of citrate to isocitrate proceeds via an intermediate dehydration product (cis-aconitate) [51]. This reversible isomerization reaction is catalyzed by aconitase [52], of which three forms exist. Aconitase A (AcnA) and aconitase B (AcnB) are distantly related iron-sulfur proteins [53]. AcnA is relatively oxygen-stable, while AcnB is oxygen-sensitive [53, 54]. Some organisms have genes encoding both enzymes, and express them under conditions reflecting their oxygen sensitivity [53, 54].

A third form, aconitase X (AcnX), was predicted via comparative genomics [55]. In some species of Archaea, genes encoding aconitase A and B are absent, but some form of aconitase must be active for the cells to be viable. A bioinformatics-informed examination of their genomes uncovered a gene predicted to bind citrate that was distantly related to AcnA and AcnB [55]. Catalytic activity by aconitase X has yet to be measured.

1.5.4 Isocitrate to 2-oxoglutarate. The interconversion of isocitrate to 2-oxoglutarate is catalyzed by isocitrate dehydrogenase (IDH), a reversible enzyme. Thus far, only NADP-dependent IDH's have been detected in bacteria [56], and of these there are two forms: monomeric and multimeric. The monomeric IDH is approximately 80-

100kDa, while the multimeric form (usually found as a dimer) is approximately 40-75kDa [56, 57]. Analyses of the sequences of these two types reveal conserved primary structures [57].

1.5.5 2-oxoglutarate to Succinyl-coA. The interconversion of 2-oxoglutarate to succinyl-coA can be catalyzed by two enzyme complexes. One enzyme that can accomplish this feat is the irreversible 2-oxoglutarate dehydrogenase (2-OGDH) enzyme. It belongs to a family of multienzyme complexes that includes PDH [58]; accordingly, they possess an E1, E2, and E3 subunit with the structural and catalytic core in E2 [58-60]. These subunits can be found in a gene cluster, although the E3 subunit can be found in other operons. Gene sequences encoding the subunits of 2-OGDH do not appear to diverge from each other as substantially as those encoding PDH [59].

The other complex capable of converting oxoglutarate to succinyl-coA is the 2-oxoglutarate: acceptor oxidoreductase (OAOR). Unlike 2-OGDH this enzyme is reversible [61]. This complex is homologous to PAOR, and is similarly sensitive to oxygen [62] but occurs in only three forms: two subunit, four subunit, and five subunit [63, 64].

1.5.6 Succinyl-CoA to Succinate. The interconversion of succinyl-coA to succinate is a reversible reaction catalyzed by the succinyl-coA synthetase enzyme, which couples the removal of coA to the phosphorylation of ADP [65]. Due to the reversible nature of this enzyme it can also function in the other direction for anabolic purposes [65]. This enzyme exists as a heterotetramer of two different subunits,  $\alpha$  and  $\beta$  [66], which are usually found in an operon. The  $\alpha$ -subunit binds ATP and catalyzes

phosphoryl group transfer, while the  $\beta$ -subunit contains at least part of the coA and succinate binding sites [67].

1.5.7 Succinate to Fumarate. The interconversion of succinate to fumarate is catalyzed by enzymes generally referred to as the succinate dehydrogenases/fumarate reductases (Sdh-Frd). These enzymes either oxidize succinate to fumarate, and transfer the electrons to quinone [68], or do the reverse reduction/oxidation. They consist of two hydrophilic subunits (A and B) as well as membrane-spanning hydrophobic subunits (C and D). Subunits A and B contain the catalytic core of the enzyme; subunit A carries a covalently linked FAD, and subunit B has three Fe-S clusters [69, 70]. Subunits C and D transfer electrons to, or accept electrons from, the membrane quinone/quinol pool [69, 70]. There are five types of this enzyme complex (A-E) which can be distinguished by their C and D subunits, which vary in their prosthetic groups and copy number per complex [70]. Types A, B, and C contain 2, 2, and 1 haem groups respectively. Types A, C, D, and E have two anchor subunits, while B has only one. The anchor subunits from type E complexes are particularly unusual, as they resemble heterodisulphide reductase from methanogenic archaea [68]. A phylogenetic analysis of the A and B subunits is consistent with clustering these complexes based on their C and D subunit structure [70]. The five types of Sdh-Frd complex are also distinguished by their catalytic directionality. Types A and E act as irreversible succinate dehydrogenases, while Type D is only capable of catalyzing fumarate reduction. Types B and C can operate bidirectionally [68].

Organisms with different physiologies tend to have (Sdh-Frd) complexes that are

consistent with their lifestyles. For example, *E. coli*, which is a facultative anaerobe, expresses two different forms of Sdh/Frd; one during aerobic growth for succinate oxidation (Type C), and the other during anaerobic growth for fumarate reduction (Type D) [71].

1.5.8 Fumarate to Malate. Fumarase catalyzes the reversible interconversion of fumarate and malate. Two classes of fumarase enzymes have been described so far (I and II) [72]. Dimeric class I fumarases are oxygen sensitive, heat inactivated, and iron-dependent, whereas tetrameric class II fumarases are iron-independent and thermo-stable [72]. Accordingly, oxygen sensitivity restricts class I to anaerobes, while aerobes possess class II fumarases [73-77]. Facultative anaerobes *Bacillus stearothermophilus*, *E. coli* and *Bradyrhizobium japonicum* all possess genes encoding both forms of this enzyme [78]. In *E. coli*, class II fumarase is expressed as part of the *soxR* regulatory system, which operates during oxidative stress to maintain cellular redox balance [78].

1.5.9 Malate to Oxaloacetate. The interconversion of malate and oxaloacetate acts to replenish the oxaloacetate necessary to complete the citric acid cycle. Oxaloacetate formation from malate can be carried out in bacteria by two enzymes: malate dehydrogenase (MDH) and malate: quinone oxidoreductase (MQO). MDH is a cytoplasmic enzyme while MQO is membrane associated [79]. MDH is a multimeric enzyme that can be present as dimers or tetramers of identical subunits [80]. This enzyme couples malate oxidation to NAD reduction, and is reversible [81], enabling it to play a role in the wishbone-shaped citric acid pathway [82].

MQO, which also has a single subunit, uses quinones instead of NAD as the

electron acceptor [79, 81]. These quinones are subsequently oxidized in the ETC [81]. Unlike MDH, malate oxidation catalyzed by MQO is irreversible, as the relatively positive midpoint potential of the quinols produced preclude the reverse reaction under physiological conditions [83].

### 1.6 The Citric Acid Cycle in *T. crunogena*

Based on the initial genome annotation, the *T. crunogena* genome encodes enzymes that could catalyze a complete citric acid cycle [1]. Particularly surprising was the presence of 2-oxoglutarate oxidoreductase genes as well as those encoding malate:quinone oxidoreductase. A citric acid cycle constructed from the enzymes encoded by these genes would be ‘locked’ in the oxidative direction by malate:quinone oxidoreductase, as the transfer of electrons from malate to quinones (ubiquinone for *T. crunogena*) is irreversible under physiological conditions due to the relatively positive midpoint potential of quinones [83]. *T. crunogena* also lacks pyruvate carboxylase and phosphoenolpyruvate carboxylase genes, leaving malate oxidation as the only route available in this organism for oxaloacetate biosynthesis [1]. Consequently, the biosynthesis of this key metabolic intermediate requires three oxidative decarboxylations (via pyruvate dehydrogenase, isocitrate dehydrogenase, and oxoglutarate dehydrogenase), which seems rather inefficient for an obligate autotroph, which expends considerable cellular energy fixing and reducing carbon via the Calvin-Benson-Bassham cycle.



## 1.7 Purpose

The purpose of this study was to verify and expand upon the results from the initial annotation of the *T. crunogena* genome. The genome was exhaustively searched for enzymes encoding each step of the citric acid cycle. Genes predicted to encode CAC enzymes were scrutinized via alignments, cluster analysis, and genome context to strengthen function predictions (and verified, when particularly surprising, via enzyme assays: citrate synthase allosteric regulation; presence of OAOR and MQO; absence of MDH). To examine the possible acquisition of genes via horizontal gene transfer, placement of *T. crunogena* CAC genes within phylogenetic trees was compared to *T. crunogena*'s 16S-based phylogeny. Lastly, the citric acid cycle assembled from these genes was compared to the citric acid cycles encoded by the genomes of 340 proteobacteria to determine whether any other organism has a CAC similar to the peculiar CAC present in *T. crunogena*.

## Chapter 2 - Methods

### 2.1 Finding Citric Acid Cycle Genes in Proteobacteria

In order to strengthen predictions of CAC gene function in *T. crunogena*, as well as to elucidate patterns of CAC gene presence and absence among a phylogenetically and physiologically diverse group of bacteria, complete genomes of 340 Proteobacteria present in the IMG database (<http://img.jgi.doe.gov/cgi-bin/pub/main.cgi>), were searched for genes encoding enzymes catalyzing steps of the citric acid cycle. Several tools present at the IMG website were used to query each genome. BLAST searches were undertaken using the amino acid sequences of biochemically characterized enzymes as query sequences (Appendix 1). The list of sequence matches ('target genes') resulting from these BLAST searches were then supplemented with sequences retrieved via searches of the target genomes for members of the appropriate COG (Clusters of Orthologous Groups of Proteins, Appendix 1) and KEGG pathways (Kyoto Encyclopedia of Genes and Genomes). Genomes were also queried using E.C. numbers and keyword searches. For multisubunit enzymes, the genes encoding the largest, most informative subunits were used for BLAST and COG-based queries of IMG. For those *Thiomicrospira crunogena* genes that did not fall clearly within the *Gammaproteobacteria*, a BLAST-based query of all genomes (draft and complete; bacterial, archaeal, and eukaryotic) was undertaken to find genes most closely related to those from *T. crunogena*.

## 2.2 Removing Genes with Apparent Alternative Function

Paralogous genes with apparent alternative function were removed from the list of target genes based on genome context, phylogenetic cluster analysis, and protein size. Gene context was visualized using the “View Neighborhood” function in IMG, and surrounding genes in an apparent operon were examined to determine whether the target gene might play a role outside of the citric acid cycle (Appendix 2).

Genes were also vetted via phylogenetic cluster analysis. Amino acid sequences predicted from paralogous genes with alternative function were aligned with those predicted from target genes and biochemically characterized genes using the Clustal W program implemented in MEGA 4.0 (Molecular Evolutionary Genetics Analysis software, [14]). A neighbor-joining tree [14] was then constructed by MEGA 4.0 using default parameters, and target genes were classified as likely to have an alternative function if they clustered with the paralogous genes of alternative function. Predicted protein size was also used to identify pseudogenes. Genes predicted to encode “oversized” proteins were scrutinized to determine whether they might be fusion proteins in multisubunit enzymes or bifunctional enzymes.

## 2.3 Multiple Sequence Alignment and Phylogenetic Analysis

Amino acid sequences predicted from the vetted genes were re-aligned via Clustal W implemented in MEGA 4.0 (Blosum62 matrix, default parameters). Alignments were verified by checking them for aligned active site residues (Appendix 3). To further verify the alignments, alignment logos were generated from them using Weblogo

(<http://weblogo.berkeley.edu/>, [84]), and were compared with curated PFAM HMM logos (<http://pfam.sanger.ac.uk/>, [85]) to ensure that other conserved regions besides active site residues were appropriately aligned (Appendix 4). For multisubunit enzymes, alignments for each subunit were generated, and then concatenated.

The neighbor-joining method was then used to construct phylogenetic trees in MEGA 4.0 from each alignment. Bootstrap values for each clade resulted from resampling the alignments 1000 times [14]. To maximize the number of sites available for analysis and account for gaps and missing data, pairwise deletion was used [14]. When possible, paralogous genes with apparent alternative function were used as outgroups. If this was not possible, orthologous genes from distant relatives were used instead. Apparent horizontal gene transfer events were identified as incongruences between the trees generated from enzyme-encoded genes and those generated from 16S sequences.

To highlight patterns of citric acid cycle enzyme presence/absence among Proteobacteria, as well as to identify possible instances of horizontal gene transfer, phylogenetic trees of 16S genes were constructed. 16S rRNA sequences were collected from IMG and aligned via RNACAD, implemented via RDP 2 (<http://rdp.cme.msu.edu/>), version 10, using a model for secondary structure based on bacterial 16S [86]. Neighbor-joining trees were constructed with MEGA 4.0, with bootstrap values based on 1000 replicate samplings of the alignments, pairwise deletions for gaps and missing data, a maximum composite likelihood model, and the assumption of uniform rates among sites.

## 2.4 Enzyme Assays

Enzyme activities were measured in *T. crunogena*, as well as *Escherichia coli* when warranted as a control. *T. crunogena* was grown in thiosulfate-supplemented artificial seawater medium in 5L chemostats under ammonia limitation [2, 10]. *E. coli* cells were cultivated in Luria broth supplemented with 50 mg/L kanamycin. Cells from both species were harvested via centrifugation (5000 g, 4°C, 10 min), and stored at -80°C until use.

Citrate synthase activity and allosteric inhibition were measured in cell extracts prepared from *T. crunogena* and *E. coli*. Wild-type *E. coli* have two enzymes capable of condensing oxaloacetate and acetyl-coenzyme A: citrate synthase, as well as methylcitrate synthase [87]. In order to prevent any methylcitrate synthase, which can also catalyze the citrate synthase reaction, from interfering with the assay, the *E. coli* strain used, JW0324-1 ([88]; obtained from the *E. coli* Genetic Stock Center at Yale University), has its methylcitrate synthase gene interrupted with a kanamycin resistance cartridge. To prepare cell extracts, frozen cell pellets were thawed and suspended in 5ml PBS (0.5 M NaCl, 0.01 M Na<sub>2</sub>HPO<sub>4</sub>, pH 7.5) supplemented with lysozyme (1 mg/ml). B-PER II detergent (5 ml; Thermo Scientific) was mixed in to the suspended cells, and the lysate was sonicated with glass beads on ice with 15 sec pulses until viscosity was reduced. Cell lysate was then centrifuged (10,000 g, 4°C, 15 min) to remove cell debris. To remove cofactors, supernatant (=cell extract) was desalted using PD-10 columns (GE Healthcare) equilibrated with PBS. Citrate synthase activity was measured spectrophotometrically at 412 nm via 5-thio-2-nitrobenzoic acid (DTNB) reduction, using a

citrate synthase assay kit (Sigma-Aldrich, Inc.) as per the manufacturer's recommendations, with measurements every 60 sec over a 5 min timecourse. Potential allosteric effectors were added to the assay as necessary (ATP: 1 mM, 10 mM; NADH: 2.5 mM; 5 mM; 10 mM; oxoglutarate: 1 mM; 10 mM). Substrate-free control reactions (lacking either oxaloacetate or acetyl-coenzyme A) were also run to uncover any background DTNB reduction present in the cell extracts.

To prepare cell extracts for oxoglutarate: acceptor oxidoreductase (OAOR) activity measurements, frozen *T. crunogena* and *E. coli* cell pellets were resuspended in 5 ml assay buffer (100 mM Tris/HCl, 4 mM dithioerthritol, 5 mM MgCl<sub>2</sub>, pH 7.8; Hugler et al., 2003) supplemented with 1 mg/ml lysozyme. Suspended cells were refrozen for 20 min at -80°C, thawed under a stream of N<sub>2</sub> gas, and sonicated and centrifuged as described above for citrate synthase assays. Assay conditions were similar to [89], but OAOR activity was measured in the reducing, rather than the oxidizing, direction via <sup>14</sup>CO<sub>2</sub> incorporation. Assay buffer was supplemented with methylviologen (4 mM) to act as an electron donor, and 0.9 ml portions were injected into 2 ml glass autosampler vials sealed with gastight silicon septa. Cell-free extract (0.1 ml) and succinyl-coenzyme A (to test for OAOR activity) or acetyl-coenzyme A (to test for pyruvate: acceptor oxidoreductase activity) were added to a concentration of 1 mM. Vial headspace was sparged three times for 20 sec with N<sub>2</sub> gas, and dithionite was injected to a final concentration of 0.5 mM to reduce the methylviologen and remove dissolved O<sub>2</sub>. Reactions were begun by injecting 0.01 ml H<sup>14</sup>CO<sub>3</sub> (55mCi/mmol). Samples of 0.2 ml were removed at 1 min intervals over a 4 min timecourse and injected into scintillation

vials primed with 0.2 ml glacial acetic acid to halt the reaction and remove  $\text{H}^{14}\text{CO}_3$ .

After sparging each sample overnight with air, 3 ml scintillation cocktail was added and oxoglutarate was quantified via scintillation counting.

To measure malate: quinone oxidoreductase (MQO) activity, *T. crunogena* cells were fractionated to generate a cytoplasmic and membrane fraction, as MQO, while not an integral membrane protein, is membrane-associated (e.g., [90-92]). Frozen *T. crunogena* cells were thawed in 10 ml MQO sonication buffer (50 mM HEPES, 10 mM potassium acetate, 10 mM  $\text{CaCl}_2$ , 5 mM  $\text{MgCl}_2$ , pH 7.5; [91]) supplemented with 1 mg/ml lysozyme. Cells were frozen, thawed, and sonicated as described above for the OAOR assay. Lysate was gently centrifuged to remove cell debris (6000 g, 4°C, 30 min). Supernatant was then centrifuged to pellet the membranes (75,000 g, 4°C, 1 hr). The high-speed supernatant was removed, and the pellet (=membrane fraction) was resuspended in 10 ml MQO sonication buffer, washed twice, and resuspended in 0.5 ml 0.05 mM HEPES, 10 mM  $\text{CaCl}_2$ , 5 mM  $\text{MgCl}_2$ , pH 7.5. To prepare to assay MQO activity spectrophotometrically via dichlorophenolindophenol (DCPIP) reduction, 0.95 ml assay buffer (100 mM  $\text{K}_2\text{HPO}_4$ , 10 mM KCN, 1 mM phenazine methosulfate, 0.1 mM 0.1 mM DCPIP, 10  $\mu\text{M}$  FAD, 50  $\mu\text{M}$  ubiquinone) was added to a cuvette, followed by 0.05 ml membrane fraction. Malate was added to a final concentration of 10 mM to commence the reaction, and the  $A_{600}$  was monitored over 3 min timecourse [90, 91]. Reactions were also conducted in the absence of malate, to measure any background DCPIP reduction that might be present in the membrane fraction.

Malate dehydrogenase activity was assayed on *T. crunogena* and *E. coli* cell

extracts prepared as for OAOR activity. Enzyme activity was assayed spectrophotometrically by measuring malate-stimulated NADH oxidation at 340 nm [92].

All enzyme activities were normalized to the protein concentration present in the assay. Protein concentrations were quantified via the RC DC Protein Assay (Biorad, Hercules, CA).



### Chapter 3 - Results and Discussion

*T. crunogena* has a unique CAC (Table 1; Appendix 5), unlike the “canonical” cycles of the six classes of Proteobacteria (Table 1; Appendix 6-10), which were constructed based on the most common enzyme(s) catalyzing each step in each class. Furthermore, no individual bacterial species sampled here had a CAC similar to that present in *T. crunogena*. Genes found in each individual genome are presented in Appendices 11 – 18.

**Table 1: Canonical Citric Acid Cycle Enzymes of Proteobacterial Classes**

Steps of the CAC	<i>T. crunogena</i>	<i>Gamma-Proteobacteria</i>	<i>Beta-Proteobacteria</i>	<i>Alpha-Proteobacteria</i>	<i>Epsilon-Proteobacteria</i>	<i>Delta-, Acido-Proteobacteria</i>
Pyruvate to Acetyl-coA	Homodimeric PDH	Homodimeric PDH	Homodimeric PDH	Heterodimeric PDH	4-subunit & Single subunit PAOR	Heterodimeric PDH & Single subunit PAOR
Acetyl-coA, Oxaloacetate to Citrate	siCitrate Synthase Type 2	siCitrate Synthase Type 2	siCitrate Synthase Type 2	siCitrate Synthase Type 2	siCitrate Synthase Type 2	siCitrate Synthase Type 2
Citrate to Isocitrate	Aconitase B	Aconitase A & B	Aconitase A & B	Aconitase A	Aconitase B	Aconitase A & B
Isocitrate to Oxoglutarate	Monomeric IDH	Monomeric & Multimeric IDH	Monomeric & Multimeric IDH	Multimeric IDH	Monomeric IDH	Multimeric IDH
Oxoglutarate to Succinyl-coA	2-subunit OAOR	2-OGDH	2-OGDH	2-OGDH	4-subunit OAOR	2-OGDH & 4-subunit OAOR
Succinyl-coA to Succinate	Succinyl-coA Synthetase	Succinyl-coA Synthetase	Succinyl-coA Synthetase	Succinyl-coA Synthetase	Succinyl-coA Synthetase	Succinyl-coA Synthetase
Succinate to Fumarate	SDH-FRD Type C	SDH-FRD Type C & D	SDH-FRD Type C	SDH-FRD Type C	SDH-FRD Type B & E	SDH-FRD Type B
Fumarate to Malate	Fumarase Class II	Fumarase Class I & II	Fumarase Class I & II	Fumarase Class II	Fumarase Class II	Fumarase Class I & II
Malate to Oxaloacetate	MQO	MDH & MQO	MDH	MDH	MDH & MQO	MDH

To simplify, the steps of the CAC in *T. crunogena* will be discussed in two parts; steps 1 – 4 (pyruvate to oxoglutarate) will be discussed first, followed by steps 5 – 9 (oxoglutarate to oxaloacetate).

### 3.1 Steps 1 – 4: Pyruvate to Oxoglutarate

In *T. crunogena*, the conversion of pyruvate to acetyl-coA is likely to be catalyzed by homodimeric PDH, as genes encoding this enzyme were present in the genome, but none of the others were (e.g., heterodimeric PDH, PFL, PAOR). Genes encoding homodimeric PDH are present in many other *Gammaproteobacteria* (Appendix 11). The top hits resulting from a BLAST-based query of IMG using the *T. crunogena* PDH E1 subunit gene were all gammaproteobacterial sequences. In addition, phylogenetic analysis places the *T. crunogena* gene within a clade with other members of *Gammaproteobacteria* (Appendix 19), and the overall topology of the tree is similar to the 16S tree, suggesting that the genes encoding this enzyme have primarily been vertically transmitted within the Proteobacteria. Interestingly, homodimeric PDH is also widely distributed among the *Betaproteobacteria*, but only a few representatives of this enzyme were found amongst members of the *Alpha*-, *Delta*-, or *Epsilonproteobacteria*, or *Acidobacteria* (Appendix 12, 13, 14), which suggests that homodimeric PDH may have been acquired by the shared ancestor of the *Beta*- and *Gammaproteobacteria*.

*T. crunogena* has a gene encoding a Type II siCS to catalyze the condensation of acetyl-coA and oxaloacetate to form citrate, and has moderate activities of citrate synthase in cell extracts (Table 2). However, it does not appear that the Type II gene present in the *T. crunogena* genome shares a long history within the *Gamma-proteobacteria*. A BLAST-based query of IMG using the amino acid sequence predicted from the *T. crunogena* Type II siCS gene had top hits dominated by members of the phyla *Cyanobacteria* and *Aquificales*. Consistent with the distribution of these top hits,

phylogenetic analysis placed the *T. crunogena* gene, as well as those from several other chemolithoautotrophic and methylotrophic bacteria, within a clade dominated by cyanobacteria (Fig. 6). Furthermore, this clade was outside of the clade of proteobacterial Type II CSs, which is consistent with acquisition of this gene within the lineage leading to *T. crunogena* via horizontal transfer, perhaps from a member of the *Cyanobacteria*. A possible selective advantage resulting from the acquisition of a cyanobacterial-like siCS gene is suggested from patterns of allosteric regulation of cyanobacterial citrate synthases. In these organisms, type II siCS enzymes are insensitive to NADH [48, 49]. This insensitivity is a boon to organisms that use the citric acid cycle primarily for biosynthetic purposes, as inhibition by excess cellular reductant is counterproductive under these circumstances. Indeed, *T. crunogena* citrate synthase was found to be insensitive to NADH (Fig. 7), as well as ATP and oxoglutarate (data not shown).

**Table 2: Activities of Citric Acid Cycle Enzymes Measured in *T. crunogena*.**

Enzyme	Fraction	Activities ( $\mu\text{mol}/\text{min mg protein}$ )	
		+ substrate	- substrate*
Citrate synthase	Cell-free extract	0.41	0.01
Oxoglutarate: acceptor oxidoreductase	Cell-free extract	2.3 E-05	0.5 E-05
Malate: quinone oxidoreductase	Membrane	0.19	0.01
Malate dehydrogenase	Cell-free extract	ND**	N/A***

\*Negative controls in which substrate was omitted were included in each assay. For citrate synthase assay, the omitted substrate was oxaloacetate. Similar results were measured in the absence of acetyl-coA. For OAOR, the omitted substrate was succinyl-coA. For MQO and MDH, the omitted substrates were malate and oxaloacetate, respectively.

\*\*ND=none detected. Assays of *E. coli* cell-free extract had activities of 8  $\mu\text{mol}/\text{min mg protein}$ .

\*\*\* N/A = not applicable.

**Figure 6: Phylogeny of si-citrate synthase sequences, with 2-methylcitrate synthase as the outgroup. Branches in blue indicate chemolithoautotrophs, while green branches indicate cyanobacteria. The red dot indicates *T. crunogena*, while the branches in green indicate cyanobacteria.**

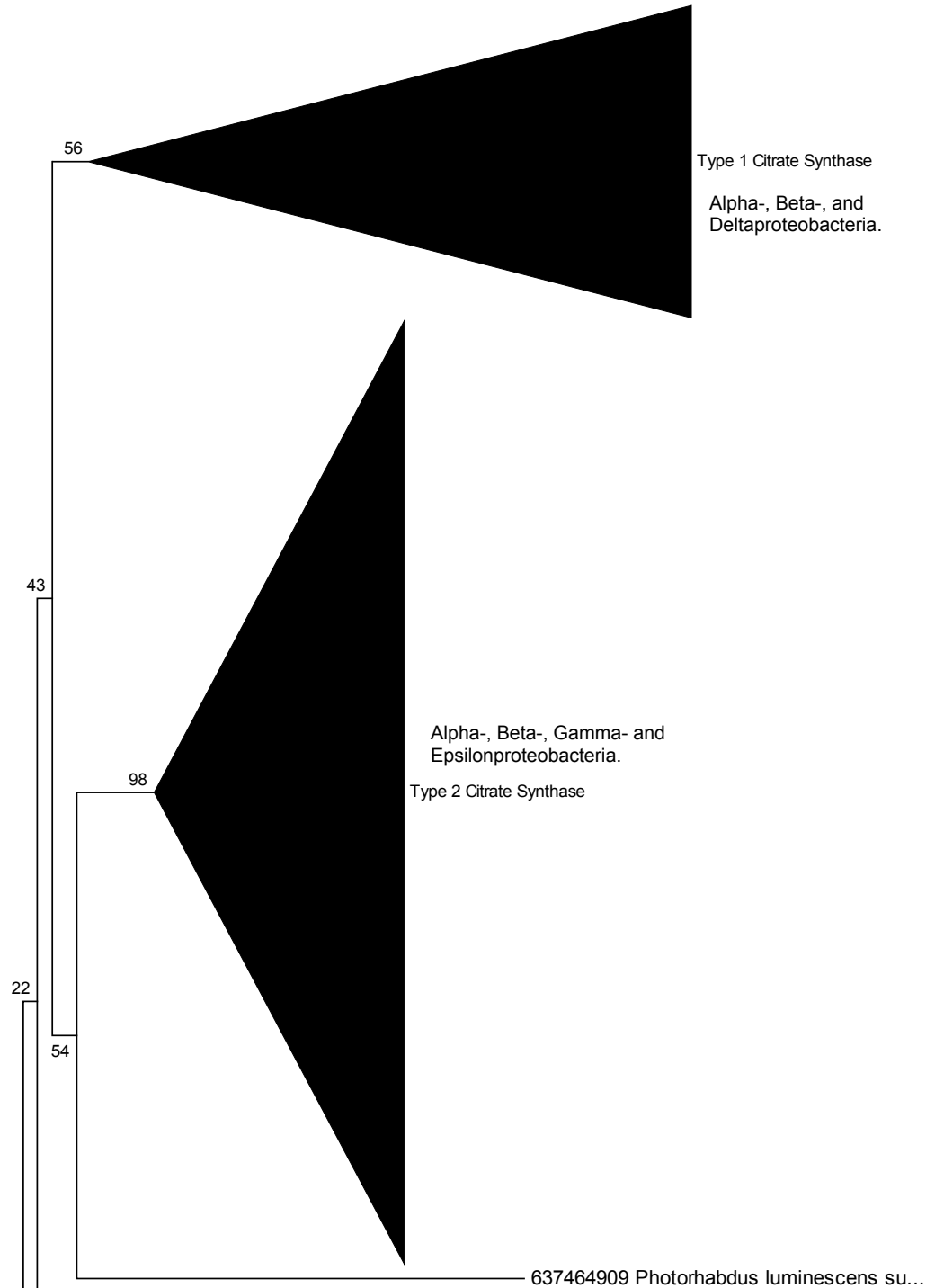


Figure 6 (continued):

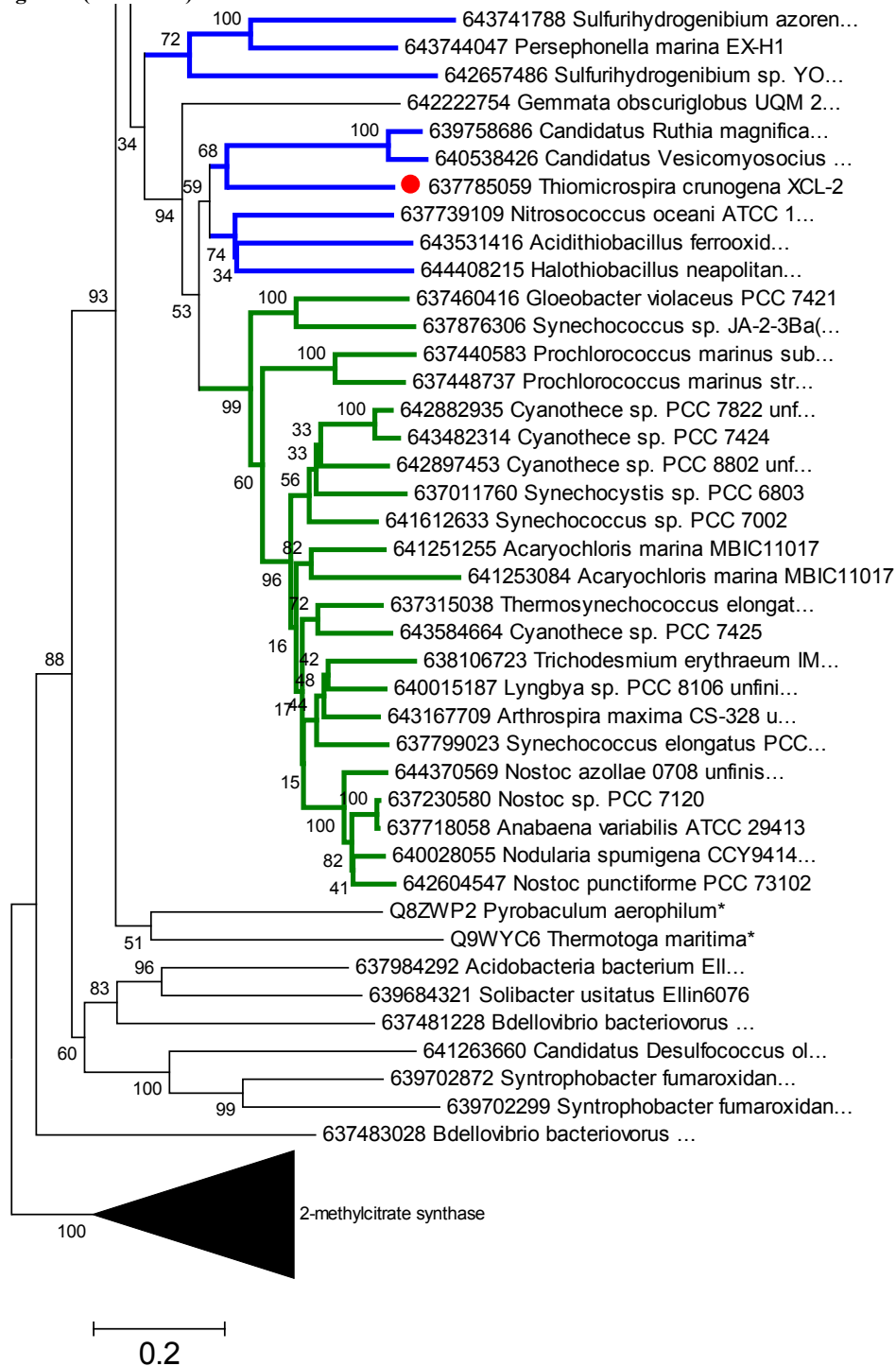
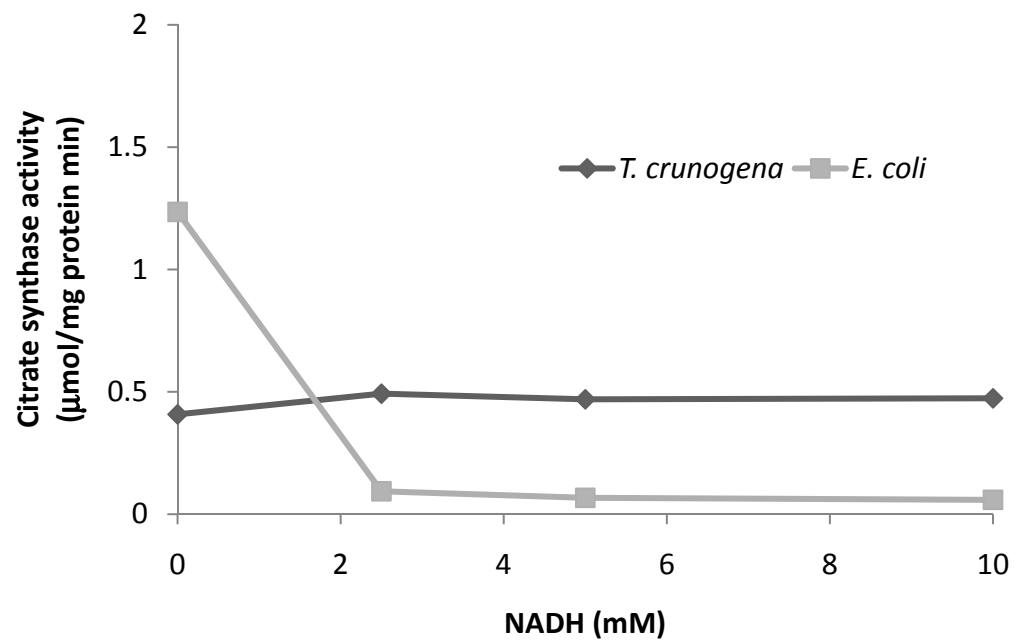


Figure 7: Effect of NADH on the activity of citrate synthase from *T. crunogena* and *E. coli*.



A gene encoding the more oxygen-sensitive version of aconitase, AcnB, is present in the *T. crunogena* genome, suggesting that this enzyme is used to catalyze the conversion of citrate to isocitrate, as is the case for many *Gamma*-, *Beta*- and *Epsilonproteobacteria* (Appendix 11, 12, 14). *T. crunogena* lives in a microaerophilic environment, and is likely to be subject to lower levels of oxidative stress. AcnA is more resistant to oxidative damage; under the low-oxygen conditions under which *T. crunogena* grows, the higher catabolic efficiency of AcnB may provide more of a selective advantage [53]. Similarly to siCS, a BLAST-based query of IMG using the amino acid sequence predicted from the *T. crunogena* AcnB gene had top hits primarily from the cyanobacteria and falls among sequences of other chemolithoautotrophs and methylotrophs. A phylogenetic analysis clustered the *T. crunogena* gene separate from a clade dominated by cyanobacteria (Fig. 8); both clades however were nested deep within the clade of proteobacterial AcnB. Thus, a direct link of descent cannot be established between the *T. crunogena* gene and the cyanobacterial genes due to low statistical significance (poor bootstrap values) and because the clade was not separate from the clade of proteobacterial AcnB.

**Figure 8: Phylogeny of aconitase sequences, with isopropylmalate synthase as the outgroup. Branches in blue indicate chemolithoautotrophs, while branches in orange indicate methylotrophs, and green branches indicate cyanobacteria. The red dot indicates *T. crunogena*.**

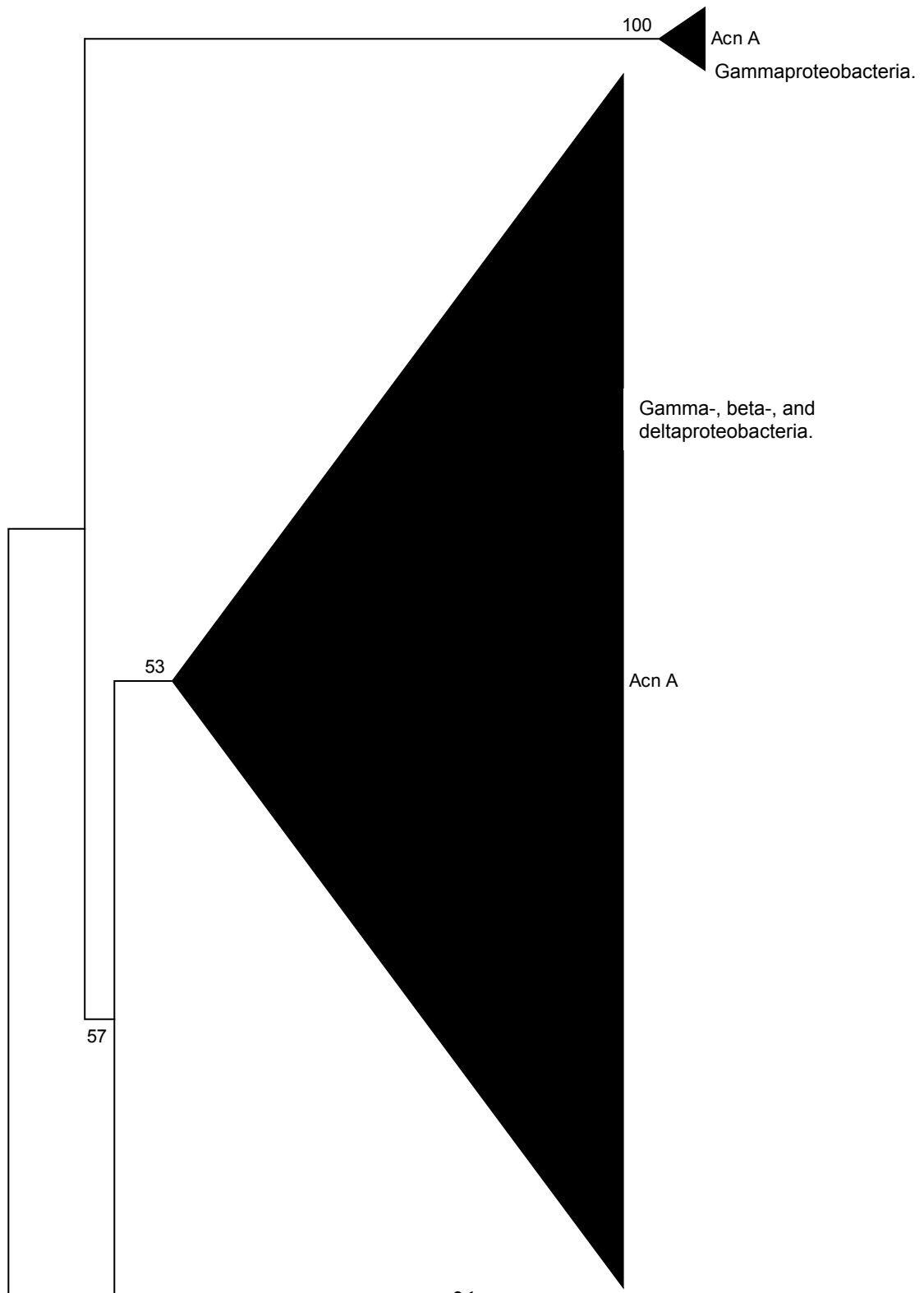
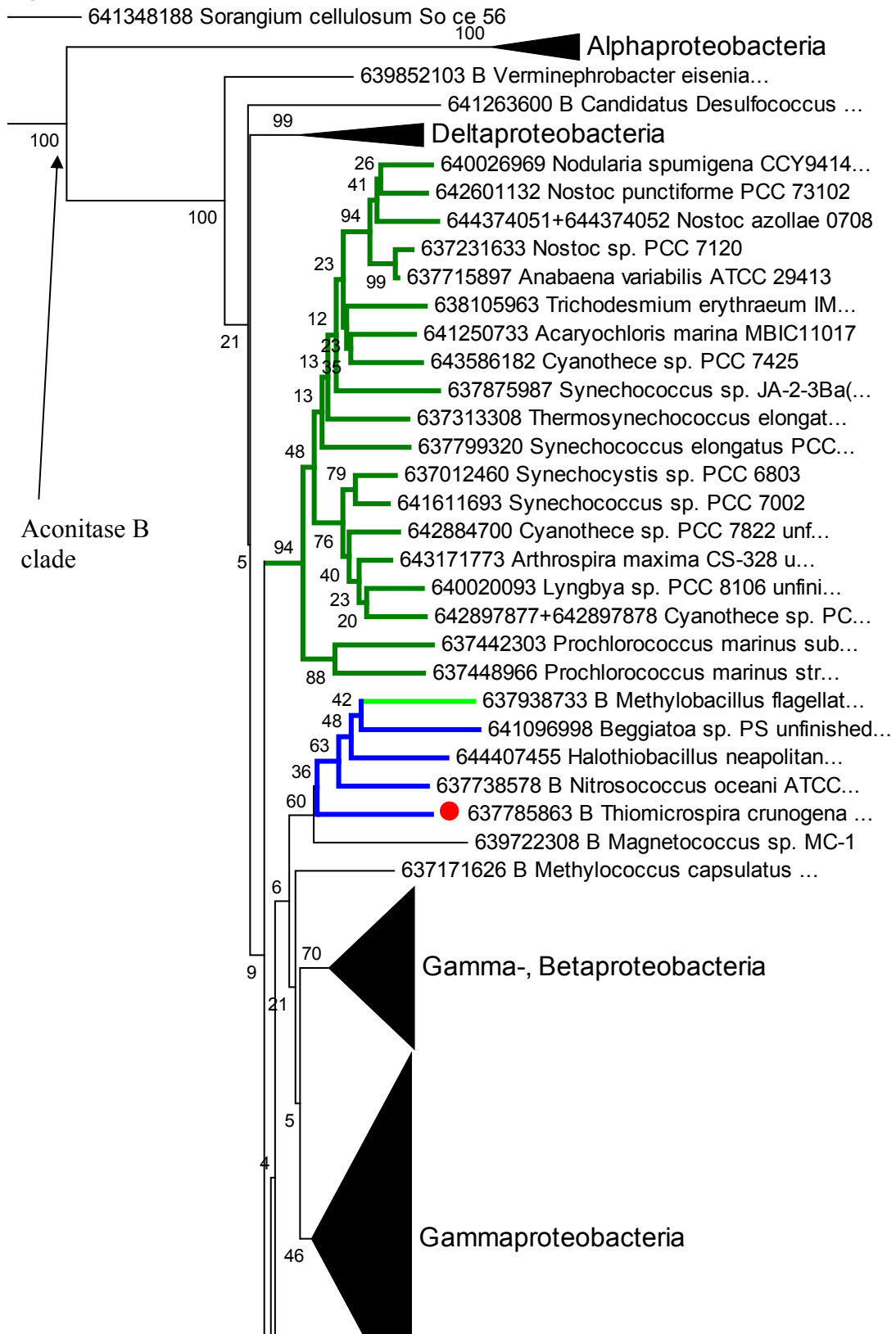
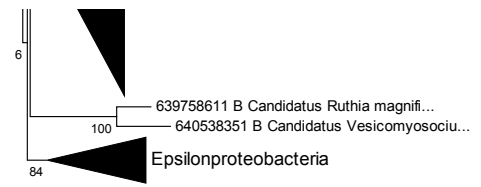
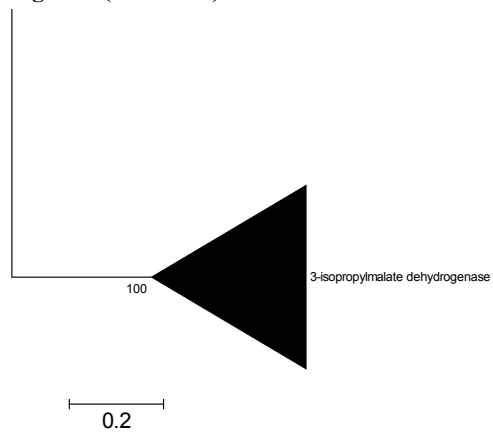




Figure 8 (continued):



**Figure 8 (continued):**



A gene encoding monomeric IDH is present in the *T. crunogena* genome, whose product could catalyze the interconversion of isocitrate to 2-oxoglutarate. An abundance of gammaproteobacterial top hits from a BLAST search of IMG, as well as phylogenetic analysis (Appendix 20), are consistent with vertical transmission within the *Gammaproteobacteria*.

### 3.2 Steps 5 – 9: Oxoglutarate to oxaloacetate

Unlike most *Gammaproteobacteria*, in which OGDH catalyzes the conversion of 2-oxoglutarate to succinyl-coA, in *T. crunogena*, genes encoding a 2-subunit OAOR are present (Appendix 15). Indeed, a BLAST query of IMG using the *T. crunogena* OAOR alpha and beta subunit amino acid sequence produced top hits dominated by members of the phylum *Firmicutes*, and phylogenetic analysis of the concatenated alpha-beta subunit sequence placed the *T. crunogena* gene apart from the clade containing most of the proteobacterial sequences. Instead, it falls within a small clade of proteobacterial facultative and obligate autotrophs (*Rhodospirillum rubrum*, *Alkali ehrlichei*, *Rhodopseudomonas palustris*, *Magnetospirillum magneticum*), with some support (60% bootstrap value) for inclusion in a clade with *Firmicutes* (Fig. 9). Given the rarity of OAOR genes among other proteobacteria (Appendices 16-18; Fig. 9) and the clustering of this gene near a clade of firmicutes, it is possible that the OAOR genes in *T. crunogena* are a recent acquisition from another lineage. It is interesting that *T. crunogena*, an obligate autotroph, has an enzyme that catalyzes this step (Table 2) because many obligate autotrophs, such as cyanobacteria, use the wishbone pathway,

which lacks this step [22].

**Figure 9: Phylogeny of 2-oxoglutarate: oxidoreductase sequences, with pyruvate: acceptor oxidoreductase as the outgroup.**

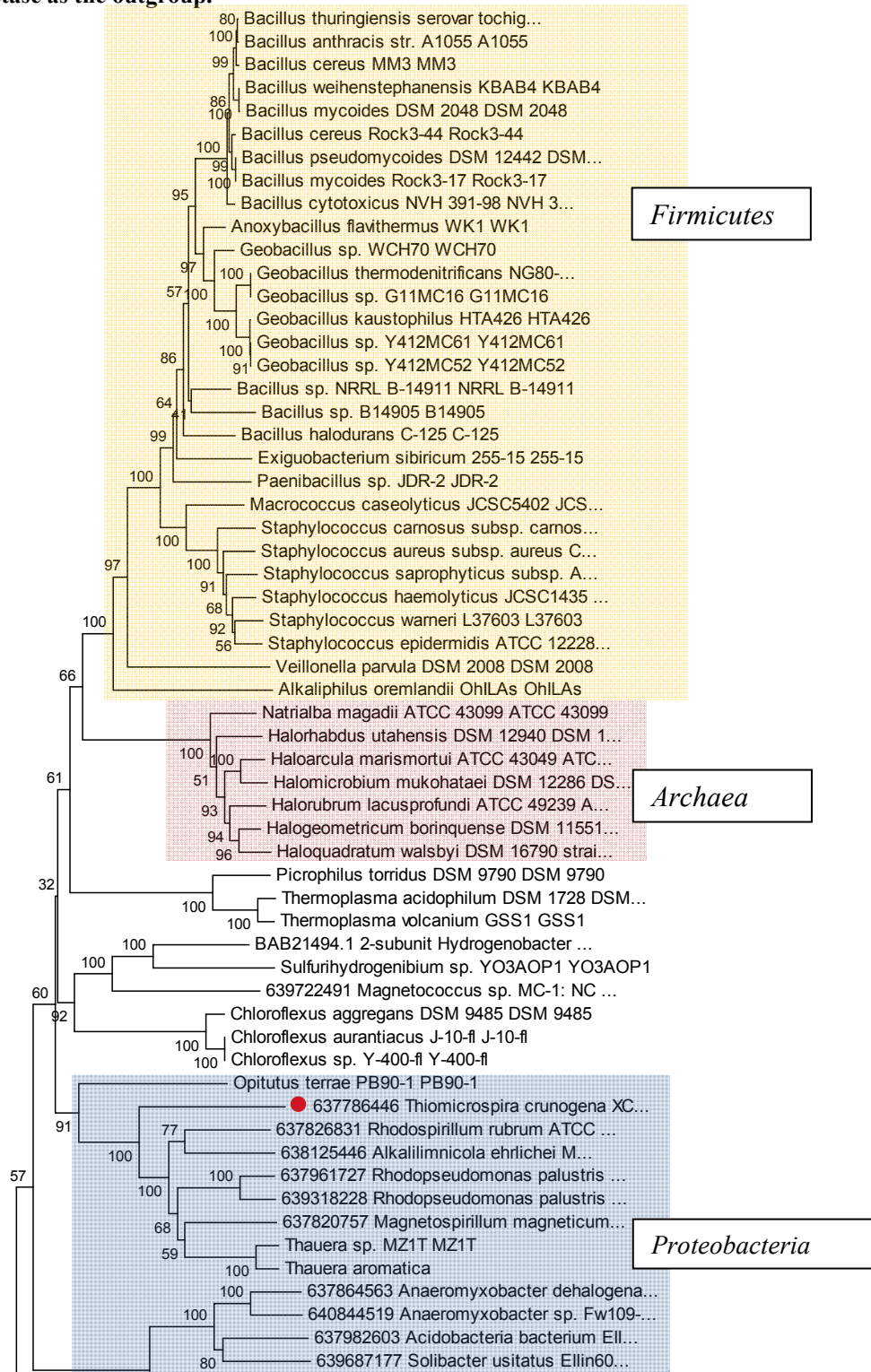
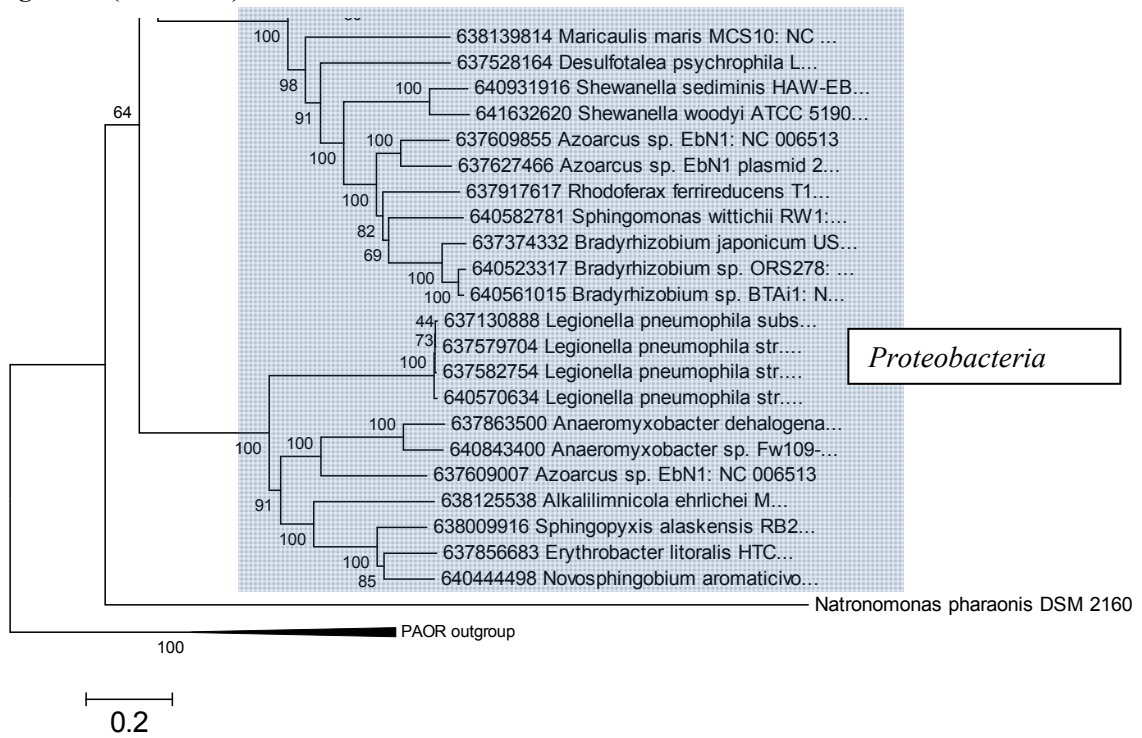


Figure 14 (continued):



Genes encoding succinyl-coA synthetase are present in the *T. crunogena* genome, suggesting that this enzyme catalyzes the interconversion of succinyl-coA to succinate in this organism. Genes encoding this enzyme are ubiquitous among proteobacteria (Appendices 15-18). Based on a BLAST search of IMG and phylogenetic analysis, both the alpha and beta subunit genes for this enzyme from *T. crunogena* cluster among succinyl-coA synthetase genes from other *Gammaproteobacteria* (Appendix 21), indicating that these genes were primarily vertically transmitted within the *Gammaproteobacteria*.

Like many proteobacteria (Appendices 15-18), the *T. crunogena* genome encodes the four subunits of a type C SDH-FRD, which could catalyze the interconversion of succinate to fumarate, as well as a class two fumarase, which is likely to convert fumarate to malate. SDH-FRD Type C, unlike SDH type A, D, or E, is a reversible enzyme [70] found in many *Gammaproteobacterial* facultative anaerobes (Appendix 15). SDH-FRD Type B, the other reversible enzyme catalyzing this step [70], is predominant among the microaerophiles in our sample. It is interesting that *T. crunogena*, which is an obligate microaerophile, does not follow this trend.

A BLAST search of IMG using the sequences of alpha and beta subunits of SDH-FRD Type C and fumarase, as well as phylogenetic analysis of the genes encoding both enzymes (using concatenated alpha and beta subunits for the SDH-FRD Type C) indicates that these sequences are most closely affiliated with those from other *Gammaproteobacteria* (Appendices 22-23), consistent with vertical transmission within the *Gammaproteobacteria*.

Based on gene presence and supported by enzyme assays, *T. crunogena* uses MQO, and not malate dehydrogenase, to convert malate to oxaloacetate (Table 2). Although this enzyme, which catalyzes the irreversible oxidation of malate to oxaloacetate via reduction of quinone [83], is common among the *Gammaproteobacteria* (Appendix 9), BLAST searches of IMG as well as phylogenetic analysis suggests relatively recent acquisition by the lineage leading to *T. crunogena* from the *Epsilonproteobacteria*, where it is also widely distributed (Fig. 15; Appendix 12). Furthermore, this enzyme is not widely distributed among methylotrophic and autotrophic proteobacteria; the few that have it (*Methylobacterium extorquens*, *Methylobacterium radiotolerans*, *Methylobacillus flagellates*, *Rhodobacter palustris*, *Sulfurimonas denitrificans*) also have genes encoding malate dehydrogenase. Given the irreversibility of MQO, as well as the energy loss resulting from introducing electrons into the electron transport chain at the redox level of quinol instead of NADH, it is difficult to understand why this enzyme is the sole mechanism for malate-oxaloacetate interconversion in *T. crunogena*. Perhaps an irreversible reaction ensures that oxaloacetate is always reasonably abundant, which might be necessary to ensure that sufficient quantities of this key metabolic intermediate are available to fuel the unusually rapid growth of this organism.

**Figure 10: Phylogeny of malate: quinone oxidoreductase sequences, with FAD dependent oxidoreductase and sarcosine oxidase as an outgroup.**

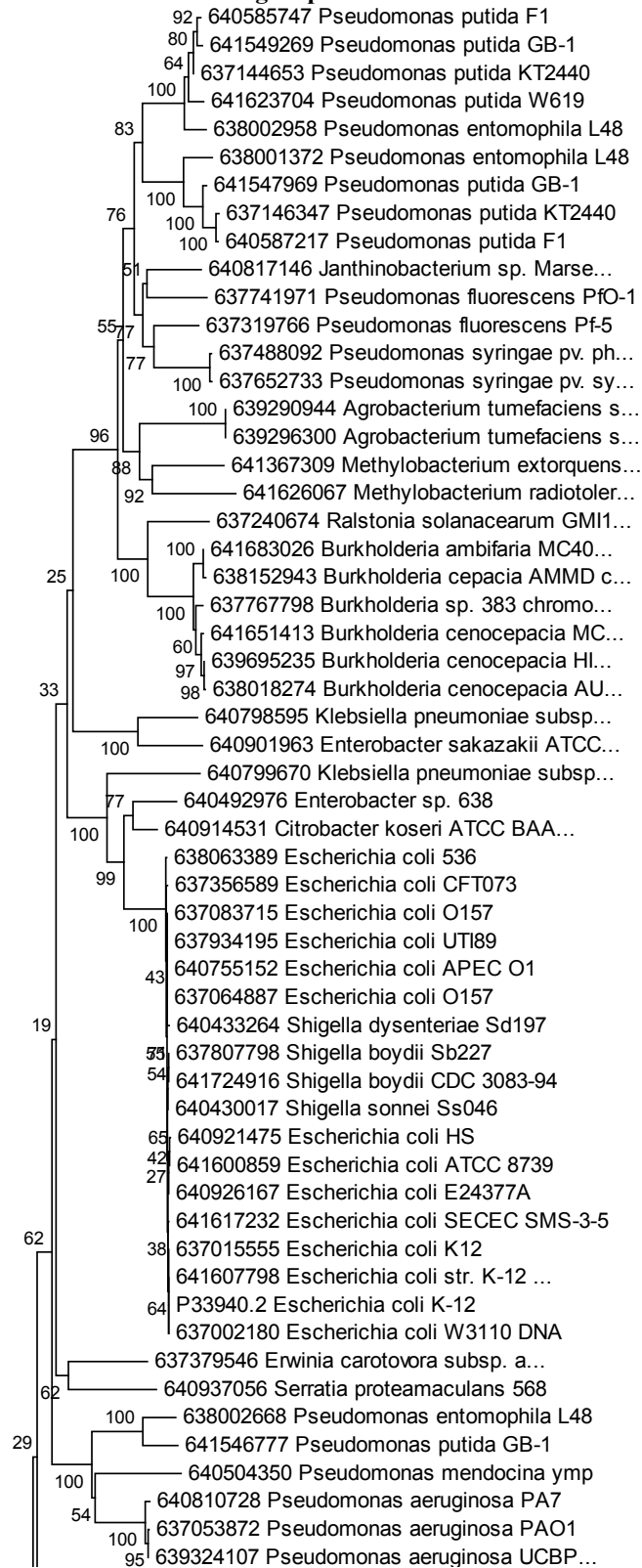




Figure 16 (continued):

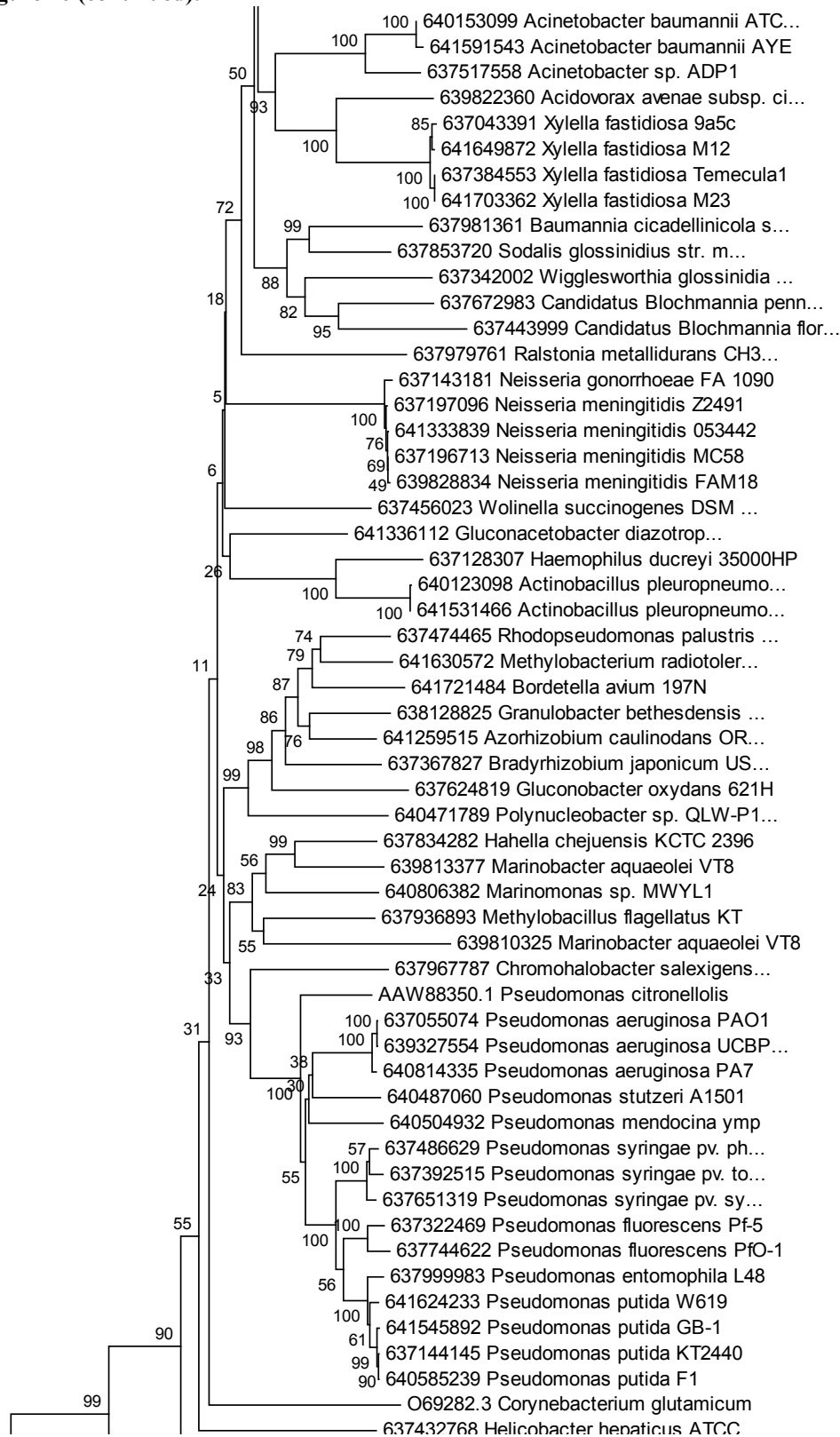
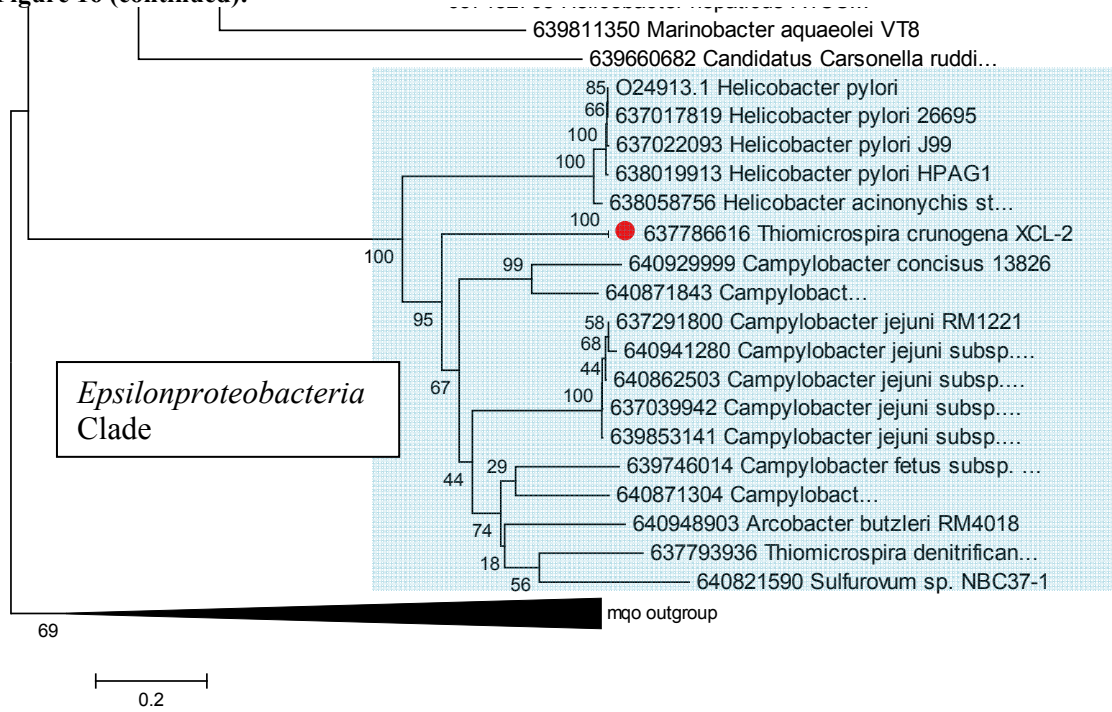


Figure 16 (continued):



### 3.3 Conclusion

Based on the analyses conducted here, *T. crunogena* does have a complete oxidative citric acid cycle, which is unexpected for an obligate autotroph. Although some of the genes (citrate synthase, aconitase) cluster with other proteobacterial autotrophs, no other autotrophic proteobacterium genome sequenced thus far contains only the MQO gene for oxaloacetate formation, and it seems unlikely that reliance on MQO will be widespread among autotrophic proteobacteria, given its irreversibility as well as energy loss. Although complete, this oxidative CAC is quite different from the familiar one present in mitochondria, with two enzyme substitutions (OAOR, MQO) and evidence it was cobbled together via horizontal gene transfers of at least three of the nine steps.

Furthermore, the six steps of the CAC catalyzed by enzymes whose amino acid sequences do cluster with those from other proteobacteria, do so with long branch lengths, which is likely to be due to *Gammaproteobacteria* related to *T. crunogena* being undersampled in genome sequencing efforts, and therefore, our study. It will be of great interest to determine whether any other members of the *Gammaproteobacteria* that are more closely related to *T. crunogena* have a similar cycle, or whether particular steps (NADH-insensitive citrate synthase, OAOR, MQO) are specific adaptations to its habitat or lifestyle.

## References

1. Scott, K.M., et al., *The genome of deep-sea vent chemolithoautotroph Thiomicrospira crunogena XCL-2*. PLoS Biol, 2006. **4**(12): p. e383.
2. Jannasch, H.W., et al., *Thiomicrospira crunogena* sp. nov., a Colorless, Sulfur-Oxidizing Bacterium from a Deep-Sea Hydrothermal Vent. Int J Syst Bacteriol, 1985. **35**(4): p. 422-424.
3. Wirsen, C.O., et al., *Comparison of a new thiomicrospira strain from the mid-atlantic ridge with known hydrothermal vent isolates*. Appl Environ Microbiol, 1998. **64**(10): p. 4057-9.
4. Johnson, K.S., J.J. Childress, and C.L. Beehler, *Short-term temperature variability in the Rose Garden hydrothermal vent field: an unstable deep-sea environment*. Deep Sea Research Part A. Oceanographic Research Papers, 1988. **35**(10-11): p. 1711-1721.
5. Nakagawa, S. and K. Takai, *Deep-sea vent chemoautotrophs: diversity, biochemistry and ecological significance*. FEMS Microbiol Ecol, 2008. **65**(1): p. 1-14.
6. Karl, D.M., C.O. Wirsen, and H.W. Jannasch, *Deep-sea primary production at the Galapagos hydrothermal vents*. Journal Name: Science; (United States); Journal Volume: 207, 1980: p. Medium: X; Size: Pages: 1345-1347.
7. Edwards, K.J., et al., *Isolation and characterization of novel psychrophilic, neutrophilic, Fe-oxidizing, chemolithoautotrophic alpha- and gamma-proteobacteria from the deep sea*. Appl Environ Microbiol, 2003. **69**(5): p. 2906-13.
8. Kelley, D.S., et al., *A serpentinite-hosted ecosystem: the Lost City hydrothermal field*. Science, 2005. **307**(5714): p. 1428-34.
9. Smith, M.A., et al., *Characteristics of the aerobic respiratory chains of the microaerophiles Campylobacter jejuni and Helicobacter pylori*. Arch Microbiol, 2000. **174**(1-2): p. 1-10.
10. Dobrinski, K.P., D.L. Longo, and K.M. Scott, *The carbon-concentrating mechanism of the hydrothermal vent chemolithoautotroph Thiomicrospira crunogena*. J Bacteriol, 2005. **187**(16): p. 5761-6.
11. Ciccarelli, F.D., et al., *Toward automatic reconstruction of a highly resolved tree of life*. Science, 2006. **311**(5765): p. 1283-7.
12. Letunic, I. and P. Bork, *Interactive Tree Of Life (iTOL): an online tool for phylogenetic tree display and annotation*. Bioinformatics, 2007. **23**(1): p. 127-8.
13. Cole, J.R., et al., *The Ribosomal Database Project: improved alignments and new tools for rRNA analysis*. Nucleic Acids Res, 2009. **37**(Database issue): p. D141-5.
14. Tamura, K., et al., *MEGA4: Molecular Evolutionary Genetics Analysis (MEGA)*

- software version 4.0. Mol Biol Evol, 2007. **24**(8): p. 1596-9.
15. Berg, J.M., J.L. Tymoczko, and L. Stryer, *Biochemistry*. 5th ed. 2002, New York: W.H. Freeman. 1 v. (various pagings).
  16. Guest, J.R. and G.C. Russell, *Complexes and complexities of the citric acid cycle in Escherichia coli*. Curr Top Cell Regul, 1992. **33**: p. 231-47.
  17. Owen, O.E., S.C. Kalhan, and R.W. Hanson, *The Key Role of Anaplerosis and Cataplerosis for Citric Acid Cycle Function*. Journal of Biological Chemistry, 2002. **277**(34): p. 30409-30412.
  18. Hasumi, F., Y. Miyamoto, and I. Okura, *Synthesis of glutamate by reductive amination of 2-oxoglutarate with the combination of hydrogenase and glutamate dehydrogenase*. Applied Biochemistry and Biotechnology, 1995. **55**(1): p. 1-4.
  19. Lascelles, J., *The Formation of Porphyrins by Photosynthetic Bacteria*, in *Ciba Foundation Symposium - Porphyrin Biosynthesis and Metabolism*, E.C.P.M. G. E. W. Wolstenholme, Editor. 2008. p. 265-284.
  20. Orgel, L.E., *The implausibility of metabolic cycles on the prebiotic Earth*. PLoS Biol, 2008. **6**(1): p. e18.
  21. Lengeler, J.W., G. Drews, and H.G. Schlegel, *Biology of the prokaryotes*. 1999, Stuttgart ; New York; Malden, MA: Thieme ; Distributed in the USA by Blackwell Science. xxvii, 955 p.
  22. Wood, A.P., J.P. Aurikko, and D.P. Kelly, *A challenge for 21st century molecular biology and biochemistry: what are the causes of obligate autotrophy and methanotrophy?* FEMS Microbiol Rev, 2004. **28**(3): p. 335-52.
  23. Hugler, M., et al., *Evidence for autotrophic CO<sub>2</sub> fixation via the reductive tricarboxylic acid cycle by members of the epsilon subdivision of proteobacteria*. J Bacteriol, 2005. **187**(9): p. 3020-7.
  24. White, D., *The physiology and biochemistry of prokaryotes*. 3rd ed. 2007, New York: Oxford University Press. xix, 628 p.
  25. de Kok, A., et al., *The pyruvate dehydrogenase multi-enzyme complex from Gram-negative bacteria*. Biochim Biophys Acta, 1998. **1385**(2): p. 353-66.
  26. Neveling, U., S. Bringer-Meyer, and H. Sahm, *Gene and subunit organization of bacterial pyruvate dehydrogenase complexes*. Biochim Biophys Acta, 1998. **1385**(2): p. 367-72.
  27. Powles, R. and D. Rawlings, *The pyruvate dehydrogenase complex of the chemolithoautotrophic bacterium Thiobacillus ferrooxidans has an unusual E2-E3 subunit fusion*. Microbiology, 1997. **143** ( Pt 7): p. 2189-95.
  28. Patel, M.S. and L.G. Korotchkina, *The biochemistry of the pyruvate dehydrogenase complex*. Biochemistry and Molecular Biology Education, 2003. **31**(1): p. 5-15.
  29. Murphy, G.E. and G.J. Jensen, *Electron cryotomography of the E. coli pyruvate and 2-oxoglutarate dehydrogenase complexes*. Structure, 2005. **13**(12): p. 1765-73.
  30. Ogasawara, H., et al., *PdhR (Pyruvate Dehydrogenase Complex Regulator) Controls the Respiratory Electron Transport System in Escherichia coli*. J. Bacteriol., 2007. **189**(15): p. 5534-5541.

31. Charon, M.H., et al., *Structure and electron transfer mechanism of pyruvate:ferredoxin oxidoreductase*. Curr Opin Struct Biol, 1999. **9**(6): p. 663-9.
32. Ikeda, T., et al., *Anabolic five subunit-type pyruvate:ferredoxin oxidoreductase from Hydrogenobacter thermophilus TK-6*. Biochem Biophys Res Commun, 2006. **340**(1): p. 76-82.
33. Townson, S.M., J.A. Upcroft, and P. Upcroft, *Characterisation and purification of pyruvate:ferredoxin oxidoreductase from Giardia duodenalis*. Mol Biochem Parasitol, 1996. **79**(2): p. 183-93.
34. Kletzin, A. and M.W. Adams, *Molecular and phylogenetic characterization of pyruvate and 2-ketoisovalerate ferredoxin oxidoreductases from Pyrococcus furiosus and pyruvate ferredoxin oxidoreductase from Thermotoga maritima*. J Bacteriol, 1996. **178**(1): p. 248-57.
35. Furdui, C. and S.W. Ragsdale, *The role of pyruvate ferredoxin oxidoreductase in pyruvate synthesis during autotrophic growth by the Wood-Ljungdahl pathway*. J Biol Chem, 2000. **275**(37): p. 28494-9.
36. Chabriere, E., et al., *Crystal structures of the key anaerobic enzyme pyruvate:ferredoxin oxidoreductase, free and in complex with pyruvate*. Nat Struct Biol, 1999. **6**(2): p. 182-90.
37. Ragsdale, S.W., *Pyruvate ferredoxin oxidoreductase and its radical intermediate*. Chem Rev, 2003. **103**(6): p. 2333-46.
38. Pieulle, L., et al., *Structural and kinetic studies of the pyruvate-ferredoxin oxidoreductase/ferredoxin complex from Desulfovibrio africanus*. Eur J Biochem, 1999. **264**(2): p. 500-8.
39. Becker, A., et al., *Structure and mechanism of the glycyl radical enzyme pyruvate formate-lyase*. Nat Struct Biol, 1999. **6**(10): p. 969-75.
40. Becker, A. and W. Kabsch, *X-ray structure of pyruvate formate-lyase in complex with pyruvate and CoA. How the enzyme uses the Cys-418 thiyl radical for pyruvate cleavage*. J Biol Chem, 2002. **277**(42): p. 40036-42.
41. Lehtio, L. and A. Goldman, *The pyruvate formate lyase family: sequences, structures and activation*. Protein Eng Des Sel, 2004. **17**(6): p. 545-52.
42. Wiegand, G. and S.J. Remington, *Citrate synthase: structure, control, and mechanism*. Annu Rev Biophys Biophys Chem, 1986. **15**: p. 97-117.
43. Li, F., et al., *Re-citrate synthase from Clostridium kluyveri is phylogenetically related to homocitrate synthase and isopropylmalate synthase rather than to Si-citrate synthase*. J Bacteriol, 2007. **189**(11): p. 4299-304.
44. Nguyen, N.T., et al., *Comparative analysis of folding and substrate binding sites between regulated hexameric type II citrate synthases and unregulated dimeric type I enzymes*. Biochemistry, 2001. **40**(44): p. 13177-87.
45. Takahashi, R., et al., *Purification and Some Properties of Citrate Synthase from Ammonia-Oxidizing Chemoautotrophic Nitrosomonas europaea ATCC 25978*. Bulletin of Japanese Society of Microbial Ecology, 1992. **7**(2): p. 47-54.
46. Bond, D.R., et al., *Characterization of citrate synthase from Geobacter sulfurreducens and evidence for a family of citrate synthases similar to those of eukaryotes throughout the Geobacteraceae*. Appl Environ Microbiol, 2005. **71**(7):

- p. 3858-65.
47. Maurus, R., et al., *Insights into the evolution of allosteric properties. The NADH binding site of hexameric type II citrate synthases*. *Biochemistry*, 2003. **42**(19): p. 5555-65.
  48. Lucas, C. and P.D. Weitzman, *Regulation of citrate synthase from blue-green bacteria by succinyl coenzyme A*. *Arch Microbiol*, 1977. **114**(1): p. 55-60.
  49. Taylor, B.F., *Fine control of citrate synthase activity in blue-green algae*. *Arch Mikrobiol*, 1973. **92**(3): p. 245-9.
  50. Francois, J.A., et al., *Structure of a NADH-insensitive hexameric citrate synthase that resists acid inactivation*. *Biochemistry*, 2006. **45**(45): p. 13487-99.
  51. Prodromou, C., P.J. Artymiuk, and J.R. Guest, *The aconitase of Escherichia coli. Nucleotide sequence of the aconitase gene and amino acid sequence similarity with mitochondrial aconitases, the iron-responsive-element-binding protein and isopropylmalate isomerases*. *Eur J Biochem*, 1992. **204**(2): p. 599-609.
  52. Viollier, P.H., et al., *Roles of aconitase in growth, metabolism, and morphological differentiation of Streptomyces coelicolor*. *J Bacteriol*, 2001. **183**(10): p. 3193-203.
  53. Jordan, P.A., et al., *Biochemical and spectroscopic characterization of Escherichia coli aconitases (AcnA and AcnB)*. *Biochem J*, 1999. **344 Pt 3**: p. 739-46.
  54. Varghese, S., Y. Tang, and J.A. Imlay, *Contrasting sensitivities of Escherichia coli aconitases A and B to oxidation and iron depletion*. *J Bacteriol*, 2003. **185**(1): p. 221-30.
  55. Makarova, K.S. and E.V. Koonin, *Filling a gap in the central metabolism of archaea: prediction of a novel aconitase by comparative-genomic analysis*. *FEMS Microbiol Lett*, 2003. **227**(1): p. 17-23.
  56. Kanao, T., et al., *Characterization of isocitrate dehydrogenase from the green sulfur bacterium Chlorobium limicola. A carbon dioxide-fixing enzyme in the reductive tricarboxylic acid cycle*. *Eur J Biochem*, 2002. **269**(7): p. 1926-31.
  57. Steen, I.H., T. Lien, and N.K. Birkeland, *Biochemical and phylogenetic characterization of isocitrate dehydrogenase from a hyperthermophilic archaeon, Archaeoglobus fulgidus*. *Arch Microbiol*, 1997. **168**(5): p. 412-20.
  58. Berg, A., J. Vervoort, and A. de Kok, *Solution structure of the lipoyl domain of the 2-oxoglutarate dehydrogenase complex from Azotobacter vinelandii*. *J Mol Biol*, 1996. **261**(3): p. 432-42.
  59. Bunik, V., A.H. Westphal, and A. de Kok, *Kinetic properties of the 2-oxoglutarate dehydrogenase complex from Azotobacter vinelandii - Evidence for the formation of a precatalytic complex with 2-oxoglutarate*. *European Journal of Biochemistry*, 2000. **267**(12): p. 3583-3591.
  60. Ricaud, P.M., et al., *Three-dimensional structure of the lipoyl domain from the dihydrolipoyl succinyltransferase component of the 2-oxoglutarate dehydrogenase multienzyme complex of Escherichia coli*. *J Mol Biol*, 1996. **264**(1): p. 179-90.
  61. Yamamoto, M., et al., *Role of two 2-oxoglutarate:ferredoxin oxidoreductases in*

- Hydrogenobacter thermophilus* under aerobic and anaerobic conditions. FEMS Microbiol Lett, 2006. **263**(2): p. 189-93.
62. Fukuda, E. and T. Wakagi, *Substrate recognition by 2-oxoacid:ferredoxin oxidoreductase from Sulfolobus sp. strain 7*. Biochim Biophys Acta, 2002. **1597**(1): p. 74-80.
  63. Yun, N.R., et al., *A novel five-subunit-type 2-oxoglutarate:ferredoxin oxidoreductases from Hydrogenobacter thermophilus TK-6*. Biochem Biophys Res Commun, 2002. **292**(1): p. 280-6.
  64. Hughes, N.J., et al., *Helicobacter pylori porCDAB and oorDABC genes encode distinct pyruvate:flavodoxin and 2-oxoglutarate:acceptor oxidoreductases which mediate electron transport to NADP*. J Bacteriol, 1998. **180**(5): p. 1119-28.
  65. Buck, D., M.E. Spencer, and J.R. Guest, *Primary structure of the succinyl-CoA synthetase of Escherichia coli*. Biochemistry, 1985. **24**(22): p. 6245-52.
  66. Fraser, M.E., et al., *A detailed structural description of escherichia coli succinyl-CoA synthetase*. J Mol Biol, 1999. **288**(3): p. 501.
  67. Luo, G.X. and J.S. Nishimura, *Site-directed mutagenesis of Escherichia coli succinyl-CoA synthetase. Histidine 142 alpha is a facilitative catalytic residue*. J Biol Chem, 1991. **266**(31): p. 20781-5.
  68. Lancaster, C.R., *Succinate:quinone oxidoreductases: an overview*. Biochim Biophys Acta, 2002. **1553**(1-2): p. 1-6.
  69. Lancaster, C.R., et al., *Structure of fumarate reductase from Wolinella succinogenes at 2.2 Å resolution*. Nature, 1999. **402**(6760): p. 377-85.
  70. Lemos, R.S., et al., *Quinol:fumarate oxidoreductases and succinate:quinone oxidoreductases: phylogenetic relationships, metal centres and membrane attachment*. Biochim Biophys Acta, 2002. **1553**(1-2): p. 158-70.
  71. Horsefield, R., S. Iwata, and B. Byrne, *Complex II from a structural perspective*. Current Protein & Peptide Science, 2004. **5**(2): p. 107-118.
  72. Estevez, M., et al., *X-ray crystallographic and kinetic correlation of a clinically observed fumarase mutation*. Protein Sci, 2002. **11**(6): p. 1552-7.
  73. Tseng, C.P., et al., *Oxygen- and growth rate-dependent regulation of Escherichia coli fumarase (FumA, FumB, and FumC) activity*. J Bacteriol, 2001. **183**(2): p. 461-7.
  74. Yumoto, N. and M. Tokushige, *Characterization of multiple fumarase proteins in Escherichia coli*. Biochem Biophys Res Commun, 1988. **153**(3): p. 1236-43.
  75. Woods, S.A., S.D. Schwartzbach, and J.R. Guest, *Two biochemically distinct classes of fumarase in Escherichia coli*. Biochim Biophys Acta, 1988. **954**(1): p. 14-26.
  76. Flint, D.H., *Escherichia coli fumarase A catalyzes the isomerization of enol and keto oxalacetic acid*. Biochemistry, 1993. **32**(3): p. 799-805.
  77. Flint, D.H., *Initial kinetic and mechanistic characterization of Escherichia coli fumarase A*. Arch Biochem Biophys, 1994. **311**(2): p. 509-16.
  78. Mizobata, T., et al., *Purification and Characterization of a Thermostable Class II Fumarase from Thermus thermophilus*. Archives of Biochemistry and Biophysics, 1998. **355**(1): p. 49-55.



79. van der Rest, M.E., C. Frank, and D. Molenaar, *Functions of the membrane-associated and cytoplasmic malate dehydrogenases in the citric acid cycle of Escherichia coli*. J Bacteriol, 2000. **182**(24): p. 6892-9.
80. Goward, C.R. and D.J. Nicholls, *Malate dehydrogenase: a model for structure, evolution, and catalysis*. Protein Sci, 1994. **3**(10): p. 1883-8.
81. Molenaar, D., et al., *Functions of the membrane-associated and cytoplasmic malate dehydrogenases in the citric acid cycle of Corynebacterium glutamicum*. J Bacteriol, 2000. **182**(24): p. 6884-91.
82. Park, S.J., P.A. Cotter, and R.P. Gunsalus, *Regulation of malate dehydrogenase (mdh) gene expression in Escherichia coli in response to oxygen, carbon, and heme availability*. J Bacteriol, 1995. **177**(22): p. 6652-6.
83. Kather, B., et al., *Another unusual type of citric acid cycle enzyme in Helicobacter pylori: the malate:quinone oxidoreductase*. J Bacteriol, 2000. **182**(11): p. 3204-9.
84. Crooks, G.E., et al., *WebLogo: a sequence logo generator*. Genome Res, 2004. **14**(6): p. 1188-90.
85. Finn, R.D., et al., *The Pfam protein families database*. Nucleic Acids Res, 2008. **36**(Database issue): p. D281-8.
86. Cole, J.R., et al., *The Ribosomal Database Project (RDP-II): previewing a new autoaligner that allows regular updates and the new prokaryotic taxonomy*. Nucleic Acids Res, 2003. **31**(1): p. 442-3.
87. Textor, S., et al., *Propionate oxidation in Escherichia coli: evidence for operation of a methylcitrate cycle in bacteria*. Arch Microbiol, 1997. **168**(5): p. 428-36.
88. Baba, T., et al., *Construction of Escherichia coli K-12 in-frame, single-gene knockout mutants: the Keio collection*. Mol Syst Biol, 2006. **2**: p. 2006 0008.
89. Hugler, M., et al., *Autotrophic CO<sub>2</sub> fixation pathways in archaea (Crenarchaeota)*. Arch Microbiol, 2003. **179**(3): p. 160-73.
90. O'Brien, R.W. and B.L. Taylor, *Formation and dissimilation of oxalacetate and pyruvate Pseudomonas citronellolis grown on noncarbohydrate substrates*. J Bacteriol, 1977. **130**(1): p. 131-5.
91. Molenaar, D., M.E. van der Rest, and S. Petrovic, *Biochemical and genetic characterization of the membrane-associated malate dehydrogenase (acceptor) from Corynebacterium glutamicum*. Eur J Biochem, 1998. **254**(2): p. 395-403.
92. Kretschmar, U., et al., *Malate:quinone oxidoreductase is essential for growth on ethanol or acetate in Pseudomonas aeruginosa*. Microbiology, 2002. **148**(Pt 12): p. 3839-47.
93. Man, W.J., et al., *THE EFFECT OF REPLACING THE CONSERVED ACTIVE-SITE RESIDUES HIS-264, ASP-312 AND ARG-314 ON THE BINDING AND CATALYTIC PROPERTIES OF ESCHERICHIA-COLI CITRATE SYNTHASE*. Biochemical Journal, 1994. **300**: p. 765-770.
94. Tang, Y., et al., *Switching aconitase B between catalytic and regulatory modes involves iron-dependent dimer formation*. Mol Microbiol, 2005. **56**(5): p. 1149-58.
95. Hurley, J.H., et al., *Catalytic mechanism of NADP(+)-dependent isocitrate dehydrogenase: implications from the structures of magnesium-isocitrate and*

- NADP<sup>+</sup> complexes*. Biochemistry, 1991. **30**(35): p. 8671-8.
96. Knapp, J.E., et al., *Crystal structure of the truncated cubic core component of the Escherichia coli 2-oxoglutarate dehydrogenase multienzyme complex*. Journal of Molecular Biology, 1998. **280**(4): p. 655-668.
  97. Wolodko, W.T., et al., *THE CRYSTAL-STRUCTURE OF SUCCINYL-COA SYNTHETASE FROM ESCHERICHIA-COLI AT 2.5-ANGSTROM RESOLUTION*. Journal of Biological Chemistry, 1994. **269**(14): p. 10883-10890.
  98. Weaver, T., *Structure of free fumarate C from Escherichia coli*. Acta Crystallogr D Biol Crystallogr, 2005. **61**(Pt 10): p. 1395-401.
  99. Madern, D., *Molecular evolution within the L-malate and L-lactate dehydrogenase super-family*. Journal of Molecular Evolution, 2002. **54**(6): p. 825-840.
  100. Sawers, G., *The aerobic/anaerobic interface*. Curr Opin Microbiol, 1999. **2**(2): p. 181-7.
  101. Sawers, G. and G. Watson, *A glycyl radical solution: oxygen-dependent interconversion of pyruvate formate-lyase*. Mol Microbiol, 1998. **29**(4): p. 945-54.
  102. Atteia, A., et al., *Pyruvate formate-lyase and a novel route of eukaryotic ATP synthesis in Chlamydomonas mitochondria*. J Biol Chem, 2006. **281**(15): p. 9909-18.
  103. Hawkins, C.F., A. Borges, and R.N. Perham, *A common structural motif in thiamin pyrophosphate-binding enzymes*. FEBS Lett, 1989. **255**(1): p. 77-82.
  104. Lessard, I.A. and R.N. Perham, *Expression in Escherichia coli of genes encoding the E1 alpha and E1 beta subunits of the pyruvate dehydrogenase complex of Bacillus stearothermophilus and assembly of a functional E1 component (alpha 2 beta 2) in vitro*. J Biol Chem, 1994. **269**(14): p. 10378-83.
  105. Green, J.D., et al., *Three-dimensional structure of a lipoyl domain from the dihydrolipoyl acetyltransferase component of the pyruvate dehydrogenase multienzyme complex of Escherichia coli*. J Mol Biol, 1995. **248**(2): p. 328-43.
  106. Russell, G.C. and J.R. Guest, *Site-directed mutagenesis of the lipoate acetyltransferase of Escherichia coli*. Proc Biol Sci, 1991. **243**(1307): p. 155-60.
  107. Zhu, P.P. and A. Peterkofsky, *Sequence and organization of genes encoding enzymes involved in pyruvate metabolism in Mycoplasma capricolum*. Protein Sci, 1996. **5**(8): p. 1719-36.
  108. Yu, X., et al., *Structures of the human pyruvate dehydrogenase complex cores: a highly conserved catalytic center with flexible N-terminal domains*. Structure, 2008. **16**(1): p. 104-14.
  109. Arjunan, P., et al., *Crystal structure of the thiamin diphosphate-dependent enzyme pyruvate decarboxylase from the yeast Saccharomyces cerevisiae at 2.3 Å resolution*. J Mol Biol, 1996. **256**(3): p. 590-600.

## Appendices

Appendix 1: Biochemically Characterized Genes of the Citric Acid Cycle Used as Query Sequences for BLAST Searches of IMG

<u>Enzyme</u>	<u>COG ID</u>	<u>Species</u>	<u>Genbank accession #</u>
Si-citrate synthase	COG0372	<i>Pyrobaculum aerophilum</i>	Q8ZWP2
		<i>Escherichia coli</i>	1K3P_A
		<i>Thermotoga maritima</i>	Q9WYC6
		<i>Pyrococcus furiosus</i>	1AJ8_A
		<i>Sulfolobus solfataricus</i>	1O7X_A
		<i>Sus scrofa</i>	P00889
Re-citrate synthase	COG0119	<i>Clostridium kluyveri</i> DSM 555	YP_001394363
Aconitase A	COG1048	<i>Bacillus subtilis</i>	P09339
		<i>Mycobacterium avium</i>	O08451
		<i>Rattus norvegicus</i>	NP_077374
Aconitase B	COG1049	<i>Escherichia coli</i>	1L5J_B
Aconitase X	COG1679,		
	COG1786	<i>Aeropyrum pernix</i>	NP_148375
		<i>Archaeoglobus fulgidus</i>	NP_071158
		<i>Pseudomonas aeruginosa</i>	NP_249950
Monomeric IDH	COG0473	<i>Azotobacter vinelandii</i>	1J1W A
Multimeric IDH	COG0538	<i>Thermotoga Maritima</i>	1ZOR A
		<i>Bacillus subtilis</i>	1HQS A
		<i>Aeropyrum Pernix</i>	1XGV A
2-OGDH -E1 subunit	COG0567	<i>Pseudomonas putida</i>	AAC23516
		<i>Azotobacter vinelandii</i>	P20707
		<i>Bacillus subtilis</i>	P23129
		<i>Corynebacterium glutamicum</i>	Q8NRC3*
-E2 subunit	COG0508	<i>Pseudomonas putida</i>	AAC23516
		<i>Azotobacter vinelandii</i>	P20707
		<i>Bacillus subtilis</i>	P23129
-E3 subunit	COG1249	<i>Stenotrophomonas maltophilia</i> K279a	CAQ46640
		<i>Leishmania major</i>	CAJ08475
2-subunit OAOR -subunit alpha	COG0674	<i>Hydrogenobacter thermophilus</i>	BAB21494
-subunit beta	COG1013	<i>Hydrogenobacter thermophilus</i>	BAB21495
4-subunit OAOR -subunit alpha	COG0674	<i>Helicobacter pylori</i>	AAC38211
		<i>Methanothermobacter marburgensis</i>	AAB85529
-subunit beta	COG1013	<i>Helicobacter pylori</i>	AAC38212

Appendix 1 (continued):

		<i>Methanothermobacter marburgensis</i>	AAB85530
-subunit Gamma	COG1014	<i>Helicobacter pylori</i> <i>Methanothermobacter marburgensis</i>	AAC38213 AAB85531
-subunit delta	COG1144	<i>Helicobacter pylori</i> <i>Methanothermobacter marburgensis</i>	AAC38210 AAB85528
5-subunit OAOR			
-subunit alpha	COG0674	<i>Hydrogenobacter thermophilus</i>	BAB62133
-subunit beta	COG1013	<i>Hydrogenobacter thermophilus</i>	BAB62134
-subunit gamma	COG1014	<i>Hydrogenobacter thermophilus</i>	BAB62135
-subunit delta	COG1144	<i>Hydrogenobacter thermophilus</i>	BAB62136
-subunit epsilon	-	<i>Hydrogenobacter thermophilus</i>	BAB62132
Succinyl-coA			
-subunit alpha	COG0074	<i>Escherichia coli</i> <i>Sus scrofa</i> <i>Trichomonas vaginalis</i>	P0AGE9 1EUDA P53401
-subunit beta	COG0045	<i>Escherichia coli</i> <i>Sus scrofa</i> <i>Trichomonas vaginalis</i>	P07460 2FP4_B AAA30326
SDH-FRD Type A			
-subunit alpha	COG1053	<i>Halobacterium sp. NRC-1</i> <i>Mycobacterium tuberculosis H37Rv</i> <i>Thermoplasma acidophilum DSM</i> <i>1728</i> <i>Archaeoglobus fulgidus DSM 4304</i>	NP_280171 NP_217835 NP_394461 NP_069515
-subunit beta	COG0479	<i>Halobacterium sp. NRC-1</i> <i>Mycobacterium tuberculosis H37Rv</i> <i>Thermoplasma acidophilum DSM</i> <i>1728</i> <i>Archaeoglobus fulgidus DSM 4304</i>	NP_280172 NP_217836 NP_394462 NP_069516
-subunit gamma	COG2009, COG2048	<i>Halobacterium sp. NRC-1</i> <i>Mycobacterium tuberculosis H37Rv</i> <i>Thermoplasma acidophilum DSM</i> <i>1728</i> <i>Archaeoglobus fulgidus DSM 4304</i>	NP_280174 NP_217833 NP_394463 NP_069517
-subunit delta	COG2142	<i>Halobacterium sp. NRC-1</i> <i>Mycobacterium tuberculosis H37Rv</i> <i>Thermoplasma acidophilum DSM</i> <i>1728</i>	NP_280173 NP_217834 NP_394464

Appendix 1 (continued):

		<i>Archaeoglobus fulgidus</i> DSM 4304	NP_069518
SDH-FRD Type B			
-subunit alpha	COG1053	<i>Campylobacter jejuni</i> subsp. <i>jejuni</i> CG8486	ZP_01810183
		<i>Bacillus subtilis</i> subsp. <i>subtilis</i> str. 168	NP_390722
		<i>Chlamydomophila pneumoniae</i> CWL029	NP_224984
-subunit beta	COG0479	<i>Campylobacter jejuni</i> subsp. <i>jejuni</i> CG8486	ZP_01810184
		<i>Bacillus subtilis</i> subsp. <i>subtilis</i> str. 168	NP_390721
		<i>Chlamydomophila pneumoniae</i> CWL029	NP_224985
-subunit gamma	COG2009, COG2048	<i>Campylobacter jejuni</i> subsp. <i>jejuni</i> CG8486	ZP_01810182
		<i>Bacillus subtilis</i> subsp. <i>subtilis</i> str. 168	NP_390723
		<i>Chlamydomophila pneumoniae</i> CWL029	NP_224983
SDH-FRD Type C			
-subunit alpha	COG1053	<i>Rhodoferrax fermentans</i> <i>Escherichia coli</i> O157:H7 str. Sakai <i>Rickettsia prowazekii</i> str. Madrid E	BAA31215 NP_308775 NP_220520
-subunit beta	COG0479	<i>Rhodoferrax fermentans</i> <i>Escherichia coli</i> O157:H7 str. Sakai <i>Rickettsia prowazekii</i> str. Madrid E	BAA31216 NP_308776 NP_220521
-subunit gamma	COG2009, COG2048	<i>Rhodoferrax fermentans</i> <i>Escherichia coli</i> O157:H7 str. Sakai <i>Rickettsia prowazekii</i> str. Madrid E	BAA31213 NP_308773 NP_220518
-subunit delta	COG2142	<i>Rhodoferrax fermentans</i> <i>Escherichia coli</i> O157:H7 str. Sakai <i>Rickettsia prowazekii</i> str. Madrid E	BAA31214 NP_308774 NP_220519
SDH-FRD Type D			
-subunit alpha	COG1053	<i>Escherichia coli</i> str. K-12 substr. MG1655 <i>Haemophilus influenzae</i> Rd KW20	NP_418578 NP_438995
-subunit beta	COG0479	<i>Escherichia coli</i> str. K-12 substr. MG1655 <i>Haemophilus influenzae</i> Rd KW20	NP_418577 NP_438994
-subunit gamma	COG2009, COG2048	<i>Escherichia coli</i> str. K-12 substr. MG1655 <i>Haemophilus influenzae</i> Rd KW20	NP_418576 NP_438993

Appendix 1 (continued):

-subunit delta	COG2142	<i>Escherichia coli</i> str. K-12 substr. MG1655 <i>Haemophilus influenzae</i> Rd KW20	NP_418575 NP_438992
SDH-FRD Type E			
-subunit alpha	COG1053	<i>Campylobacter jejuni</i> subsp. <i>jejuni</i> CF93-6 <i>Sulfolobus acidocaldarius</i> <i>Synechocystis</i> sp. PCC 6803	ZP_01067418 CAA70249 NP_440839
-subunit beta	COG0479	<i>Campylobacter jejuni</i> subsp. <i>jejuni</i> 84-25 <i>Sulfolobus acidocaldarius</i> <i>Synechocystis</i> sp. PCC 6803	ZP_01100272 CAA70250 NP_442463
-subunit gamma	COG2009, COG2048	<i>Sulfolobus acidocaldarius</i>	CAA70251
-subunit delta	COG2142	<i>Sulfolobus acidocaldarius</i>	CAA70252
Fumarase			
-Class I	COG1951, COG1838	<i>Endoriftia persephone</i> <i>Bradyrhizobium</i> sp. ORS278 <i>Escherichia coli</i> <i>Escherichia coli</i>	ABG77122 CAL78714 AAA23827 CAA25204
-Class II	COG0114	<i>Bacillus subtilis</i> <i>Escherichia coli</i>	CAA25849 2FUS_A
Malate Dehydrogenase	COG0039	<i>Sus Scrofa</i> <i>Prosthecochloris vibrioformis</i> <i>Aeropyrum Pernix</i> <i>Cryptosporidium Parvum</i>	4MDH 1GV1 2D4A 2HJR
Malate Quinone Oxidoreductase	COG0579	<i>Pseudomonas citronellolis</i> <i>Corynebacterium glutamicum</i> <i>Helicobacter pylori</i> <i>Escherichia coli</i> K-12	AAW88350 O69282 O24913 P33940
PDH (homodimeric)			
-E1 subunit	COG2609	<i>Escherichia coli</i> <i>Pseudomonas aeruginosa</i> <i>Azotobacter vinelandii</i> <i>Ralstonia eutropha</i>	NP_285810 AAC45353 CAA75394 AAA21598
-E2 subunit	COG0508	<i>Escherichia coli</i> <i>Haemophilus influenzae</i> <i>Azotobacter vinelandii</i> <i>Pseudomonas aeruginosa</i>	NP_285811 □□□□39388 CAA30987 AAC45354

Appendix 1 (continued):

-E3 subunit	COG1249	<i>Escherichia coli</i> <i>Haemophilus influenzae</i> <i>Ralstonia eutropha</i>	NP 285812 NP 439387 AAA21600
PDH (heterodimeric)			
-E1 alpha	COG1071	<i>Zymomonas mobilis</i> <i>Homo sapiens</i> <i>Acidithiobacillus ferrooxidans</i>	CAA73384 NP 000275 AAB41626
-E1 beta	COG0022	<i>Zymomonas mobilis</i> <i>Homo sapiens</i> <i>Acidithiobacillus ferrooxidans</i>	CAA73385 NP 000916 AAB41627
-E2	COG0508	<i>Zymomonas mobilis</i> <i>Homo sapiens</i> <i>Geobacillus stearothermophilus</i>	CAA63808 NP 001922 CAA37630
-E3	COG1249	<i>Homo sapiens</i> <i>Geobacillus stearothermophilus</i>	1ZY8 CAA37631
Pyruvate Formate Lyase	COG1882	<i>Escherichia coli</i> <i>Shewanella oneidensis</i> <i>Thermoanaerobacterium</i> <i>saccharolyticum</i> <i>Streptococcus mutans</i> <i>Lactococcus lactis</i>	1MZO AAN55926  ACA51671 BAA09085 O32799
1-subunit PAOR	COG0674	<i>Desulfovibrio africanus</i> <i>Pantoea agglomerans</i>	CAA70873 CAA55302
2-subunit PAOR			
-subunit alpha	COG0674, COG1014	<i>Thermoanaerobacterium</i> <i>saccharolyticum</i> <i>Halobacterium salinarum</i>	ACA51672 CAA45825
-subunit beta	COG1013	<i>Thermoanaerobacterium</i> <i>saccharolyticum</i> <i>Halobacterium salinarum</i>	ACA51673 CAA45826
4-subunit PAOR			
-subunit alpha	COG0674	<i>Pyrococcus furiosus</i> <i>Helicobacter pylori</i>	CAA59505 AAC38206
-subunit beta	COG1013	<i>Pyrococcus furiosus</i> <i>Helicobacter pylori</i>	CAA59506 AAC38207
-subunit gamma	COG1014	<i>Pyrococcus furiosus</i> <i>Helicobacter pylori</i>	CAA59500 AAC38204
-subunit delta	COG1144	<i>Pyrococcus furiosus</i> <i>Helicobacter pylori</i>	CAA59504 AAC38205



Appendix 1 (continued):

5-subunit PAOR			
-subunit alpha	COG0674	<i>Hydrogenobacter thermophilus</i>	BAA95605
-subunit beta	COG1013	<i>Hydrogenobacter thermophilus</i>	BAA95606
-subunit Gamma	COG1014	<i>Hydrogenobacter thermophilus</i>	BAA95607
-subunit delta	COG1144	<i>Hydrogenobacter thermophilus</i>	BAA95604
-subunit epsilon	-	<i>Hydrogenobacter thermophilus</i>	BAA95603

\*This species has a fused E1 and E2 subunits.

## Appendix 2: Paralogous Genes with an Alternative Function

<u>Enzyme</u>	<u>Paralogs with Alternative Function</u>
Si-citrate synthase (both types)	homocitrate synthase 2-methylcitrate synthase
Re-citrate synthase	2-isopropylmalate synthase
Aconitase A	3-isopropylmalate synthase large subunit
Aconitase B	3-isopropylmalate synthase large subunit
Aconitase X	3-isopropylmalate synthase large subunit
Isocitrate Dehydrogenase	3-isopropylmalate dehydrogenase tartrate dehydrogenase
2-OGDH	
-E1	heterodimeric PDH E1 alpha Branched chain dehydrogenase Acetoin dehydrogenase
-E2	alphaketobutyrate dehydrogenase Branched chain dehydrogenase PDH homodimeric E2 PDH heterodimeric E2 Acetoin dehydrogenase
-E3	methionine degrading enzyme glutathione reductase tryptathione reductase thioredoxin reductase
2-subunit OAOR	
-subunit alpha	2-subunit PAOR, alpha subunit 2-oxoisovalerate oxidoreductase, beta subunit phenylglyoxylate:acceptor oxidoreductase 4-subunit OAOR, alpha subunit 4-subunit PAOR, alpha subunit
-subunit beta	4-subunit IOR, alpha subunit

Appendix 2 (continued):

4-subunit OAOR	
-all subunits	4-subunit IOR 4-subunit PAOR 4-subunit VOR 4-subunit PGOR
-subunit alpha	2-subunit OAOR, alpha subunit 2-subunit PAOR, alpha subunit 1-subunit PAOR
Succinyl-coA Synthetase	-
Succinate Dehydrogenase	
-subunit alpha	L-aspartate oxidase
-subunit beta	-
Fumarase	
Class 1	tartrate dehydratase
Class 2	argininosuccinate lyase
Malate dehydrogenase	inosine-5'-monophosphate dehydrogenase
Malate Quinone Oxidoreductase	FAD dependent oxidoreductase sarcosine oxidase, beta subunit
PDH (homodimeric)	
-E1	alphaketobutyrate dehydrogenase methionine degrading enzyme
-E2	alphaketobutyrate dehydrogenase Branched chain dehydrogenase 2-OGDH E2 Acetoin dehydrogenase
-E3	methionine degrading enzyme glutathione reductase tryptathione reductase thioredoxin reductase
PDH (heterodimeric)	

Appendix 2 (continued):

-E1 alpha	2-OGDH E1 Branched chain dehydrogenase Acetoin dehydrogenase
-E1 beta	Branched chain dehydrogenase Acetoin dehydrogenase
-E2	alphaketobutyrate dehydrogenase Branched chain dehydrogenase 2-OGDH E2 Acetoin dehydrogenase
-E3	methionine degrading enzyme glutathione reductase tryptathione reductase thioredoxin reductase
1-subunit PAOR	4-subunit PAOR, alpha subunit 4-subunit OAOR, alpha subunit 4-subunit VOR, alpha subunit 4-subunit PGOR, alpha subunit
2-subunit PAOR	
-subunit alpha	2-subunit OAOR, alpha subunit 4-subunit OAOR, alpha subunit 4-subunit VOR, alpha subunit 4-subunit PGOR, alpha subunit 4-subunit PAOR, alpha subunit
-subunit beta	4-subunit IOR, alpha subunit
4-subunit PAOR	
-all subunits	4-subunit IOR 4-subunit OAOR 4-subunit VOR 4-subunit PGOR
-subunit alpha	2-subunit OAOR, alpha subunit 2-subunit PAOR, alpha subunit 1-subunit PAOR, alpha subunit

### Appendix 3: Active Site Residues for Alignment Verification

Enzyme	Subunit	Organism	Conserved Residue(s)	Role	Reference
Si-citrate synthase	N/A	<i>Sus scrofa</i>	his174, his 238, his 320, arg 329, arg 401, arg 421, phe 397	stabilize citrate-enzyme interaction, substrate binding and catalysis	[42]
		<i>Escherichia coli</i>	His264, His229, His-306, Arg-314, Arg-387 and Arg-407	stabilize citrate-enzyme interaction, substrate binding and catalysis	[93]
Re-citrate synthase	N/A		no info		-
Aconitase A + B	N/A	<i>Escherichia coli</i>	D100, H101, H147, D165, S166, H167, N170, N258, E262, C434, N446, R447, R452, C518, C521, S642, S643 and R644	coordination of the [4Fe-4S] centre, substrate recognition and catalysis	[51, 94]
Aconitase X	N/A	<i>Pseudomonas aeruginosa</i>	C276, P279, Y280, W11, E13, S14, A16, P60, C19, S29, G32, G15, G25, S26, C27	active center, structurally conserved regions	[55]
Monomeric IDH	N/A	<i>Archaeoglobus fulgidus</i>	I43, S119, R125, R135, R159, Y166, K236, C263, D290, D314, D318, L327, G328, H346, A349, V358, N359, D400	substrate binding and catalysis	[57]
Multimeric IDH	N/A	<i>Escherichia coli</i>	I43, S119, R125, C133, R135, R159, Y166, C200, C207, K236, D290, C308, D314, D318, I327, G328, C339, H346, A349, V358, N359, D400, C413	substrate binding and catalysis	[95]
2-OGDH	E1	<i>Escherichia coli</i>	no info	substrate binding and catalysis	[96]
	E2		threonine 323, histidine 375, Asp379		
OAOR					
2-subunit			no info		
4-subunit			no info		
Succinyl-coA Synthetase	alpha	<i>Escherichia coli</i>	K or R242, G248, L or P276	dimerization	[67]
	alpha		D103, Y158, E159, T237, K242, G248, L276	binding CoA	

Appendix 3 (continued):

SDH-FRD (all forms)	alpha		G14, F15, T16, G17, S18, Q19, G20, P40, G41, K42, V72, P73, F76, S or A80	accepting phosphoryl	
	alpha		H246	site of phosphorylation	
	alpha		H142	assisting H246	
	beta	<i>Escherichia coli</i>	N199, D213	coordinate the Mg necessary to bind NDPs	[97]
	beta		Y6, Q7, R or G70, N94, R116, R225, A or E231, E or D249, F319	dimerization	
	beta		R348, D274, E242, L374	conserved residues	
Fumarase		<i>Escherichia coli</i>	H242, R286, H354 and R399 (FAD-binding domain); 3 clusters of 4 cysteines (FeS cluster)	substrate binding and catalysis	[71]
Malate Dehydrogenase	Class I		no info		
	Class II	<i>Escherichia coli</i>	Asn326, Lys324, Ser98, Thr100, Asn141, His188, Glu331 and His188	substrate binding and catalysis	[75, 98]
Malate Quinone Oxidoreductase		<i>Escherichia coli</i>	R102, R109, D168, R171, and H195	substrate binding and catalysis	[99]
PAOR			no info		
1-subunit	N/A	<i>D. africanus</i>	812, 815, 840, 1071 (4 cysteines) 689-699 (4 cysteines) 745-755 (4 cysteines)	iron-sulfur cluster iron-sulfur cluster iron-sulfur cluster	[31, 34, 36-38]
2-subunit	alpha	<i>Halobacterium salinarum</i>	183-189 (GDILEQN)	aldehyde-binding motif--can be variable	
	beta	<i>Halobacterium salinarum</i>	30, 33, 64, 212 (4 cysteines)	iron-sulfur cluster	
	beta	<i>Halobacterium salinarum</i>	105-108 (GDG)	TPP-binding	
4-subunit	beta	<i>Pyrococcus furiosus</i>	21, 24, 69, 224 (4 cysteines)	iron-sulfur cluster	
	beta	<i>Pyrococcus furiosus</i>	109-112 (GDG)	TPP-binding	
	gamma	<i>Pyrococcus furiosus</i>	161-170 (GELGEKNA)	aldehyde-binding motif--can be variable	
	delta	<i>Pyrococcus furiosus</i>	53-63 (4 cysteines)	iron-sulfur cluster	
	delta	<i>Pyrococcus furiosus</i>	83-93 (4 cysteines)	iron-sulfur cluster	

Appendix 3 (continued):

PFL	N/A	<i>E. coli</i>	734 (glycine) 418 and 419 (2 cysteines)	glycine radical form S-C bond with C2 of pyruvate	[39, 41, 100-102]
PDH					
Heterodimeric	E1 alpha	<i>G. stearothermophilus</i>	173 (GDG)	binds TPP	[26, 103, 104]
Homodimeric	E1	<i>E. coli</i>	229-231 (GDG)	binds TPP	[25, 26, 105-109]
	E1	<i>E. coli</i>	258-260 (NCN)	binds TPP	
	E2	<i>G. stearothermophilus</i>	398-400 (DHR)	H for transferring acetyl group to CoA	
		<i>E. coli</i>	602-604 (DHR)	H for transferring acetyl group to CoA	
		<i>E. coli</i>	39; 141; 242 [GDKASME; G(D/E)X13(D/S)K X10 (G/C)]	lipoyl prosthetic group is covalently bonded to the lysine (K) residues here; some E2s have more than one location that is lipoylated, others do not. This sequence can vary; the key bit is the lysine residue.	
		<i>G. stearothermophilus</i>	27-54 [G(D/E)X13(D/S)K X10 (G/C)]	lipoyl binding domain	
	E3	<i>E. coli</i>	13-18; 182-187 (GXGXXG)	binds ADP of FAD	
		<i>G. stearothermophilus</i>	16-21; 183-188 (GXGXXG)	binds ADP of FAD	
		<i>E. coli</i>	45-50 (CXXXXC)	redox-sensitive disulfide center	
		<i>G. stearothermophilus</i>	47-52 (CXXXXC)	redox-sensitive disulfide center	

#### Appendix 4: Pfams Whose HMM Logos Were Used to Verify Alignments

<u>Enzyme</u>	<u>Pfam</u>
Si-citrate synthase	pfam00285
Re-citrate synthase	pfam00682
Aconitase A	pfam00330, pfam00694
Aconitase B	pfam00330, pfam06434
Aconitase X	pfam01989, pfam04412
Monomeric IDH	pfam03971
Multimeric IDH	pfam00180
2-OGDH	
-E1 subunit	pfam00676, pfam02779
-E2 subunit	pfam00198, pfam00364, pfam02817
-E3 subunit	pfam02852, pfam07992
2-subunit OAOR	
-subunit alpha	pfam01558, pfam01855, pfam02780
-subunit beta	pfam02775
4-subunit OAOR	
-subunit alpha	pfam01855, pfam02780
-subunit beta	pfam02775
-subunit gamma	pfam01558
-subunit delta	pfam00037
5-subunit OAOR subunit epsilon	None available
Succinyl-coA	
-subunit alpha	pfam02629



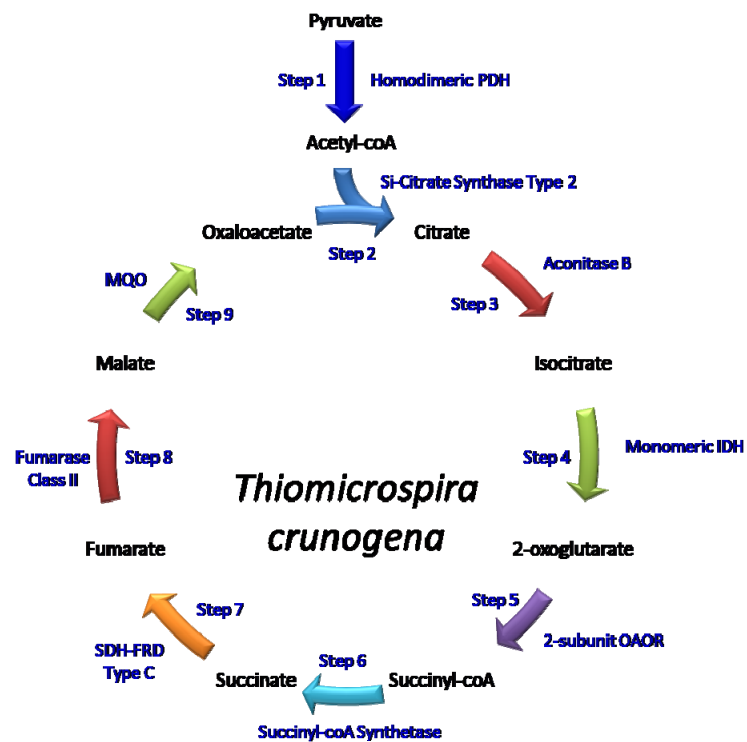
#### Appendix 4 (continued)

-subunit beta	pfam08442, pfam00549
SDH-FRD (all forms)	
-subunit alpha	pfam01266, pfam02910, pfam00890
-subunit beta	pfam00037, pfam00111
-subunit gamma	pfam02300
-subunit delta	pfam02313
Fumarase	
-Class 1	pfam05681, pfam05683
-Class 2	pfam00206, pfam10415
Malate Dehydrogenase	pfam00056, pfam02866
Malate Quinone Oxidoreductase	pfam01266, pfam06039
PDH (homodimeric)	
-E1 subunit	pfam00456
-E2 subunit	pfam00198, pfam00364, pfam02817
-E3 subunit	pfam02852, pfam07992
PDH (heterodimeric)	
-E1 alpha	pfam00676
-E1 beta	pfam02779, pfam02780
-E2	pfam00198, pfam00364, pfam02817
-E3	pfam02852, pfam07992
Pyruvate Formate Lyase	pfam02901, pfam01228
1-subunit PAOR	pfam01855, pfam01558, pfam00037, pfam02775

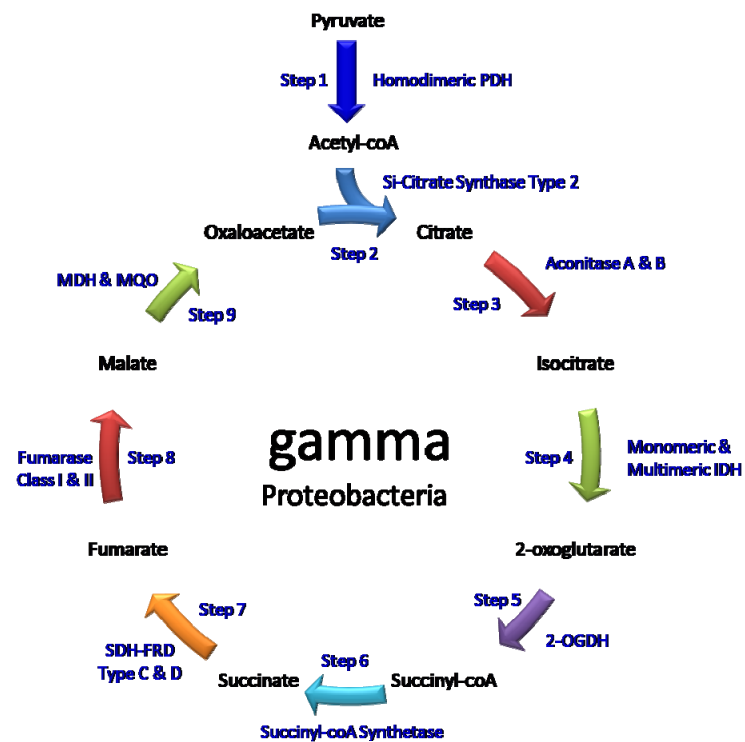
#### Appendix 4 (continued)

2-subunit PAOR	
-subunit alpha	pfam01558, pfam01855
-subunit beta	pfam02775
4-subunit PAOR	
-subunit alpha	pfam01855
-subunit beta	pfam02775
-subunit gamma	pfam01558
-subunit delta	pfam00037
5-subunit PAOR subunit epsilon	None available

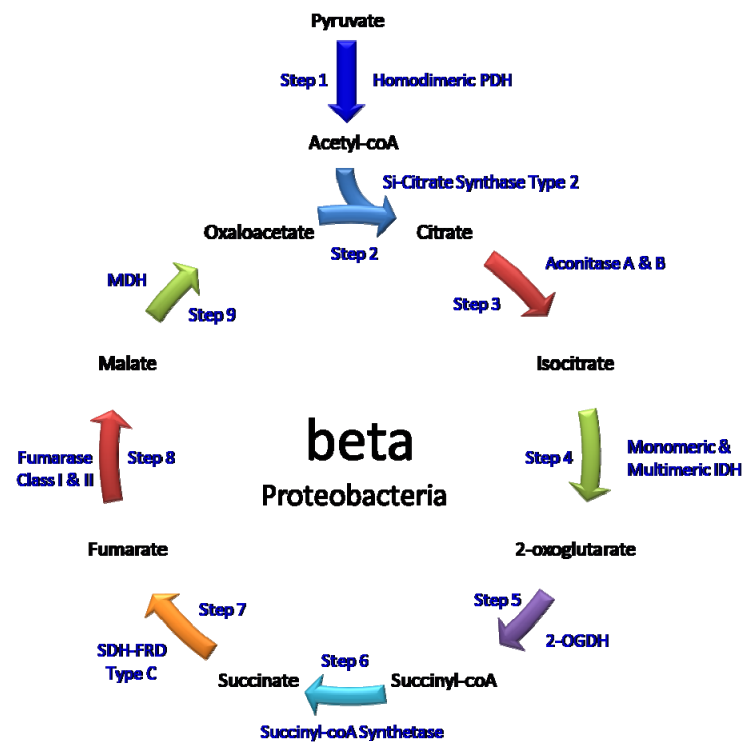
Appendix 5: The citric acid cycle of *T. crunogena*



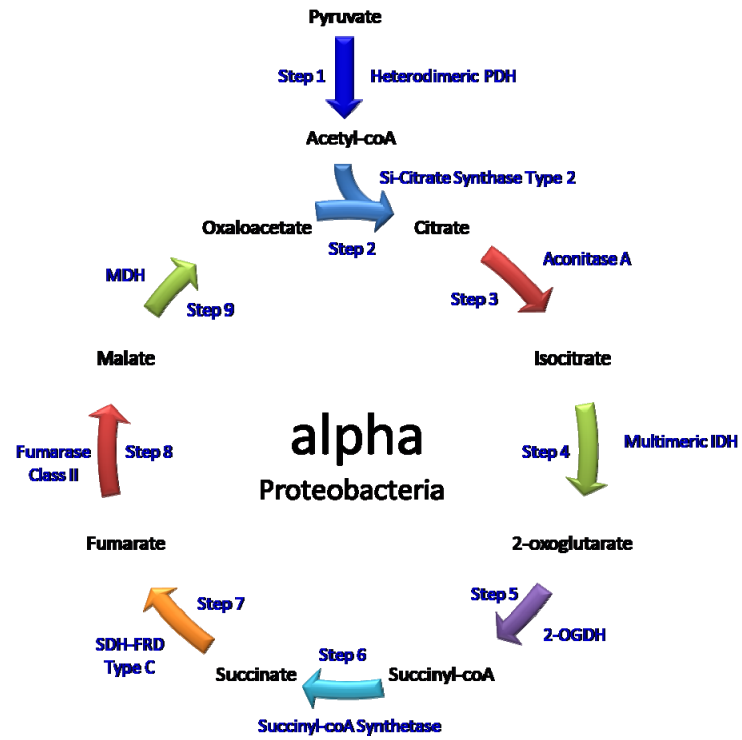
Appendix 6: The canonical citric acid cycle of *Gammaproteobacteria*



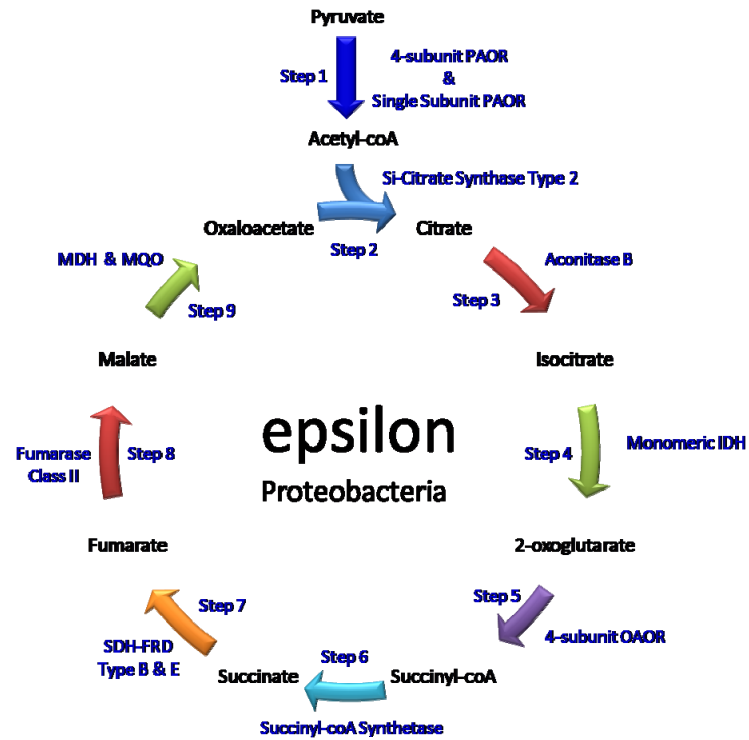
## Appendix 7: The canonical citric acid cycle of *Betaproteobacteria*



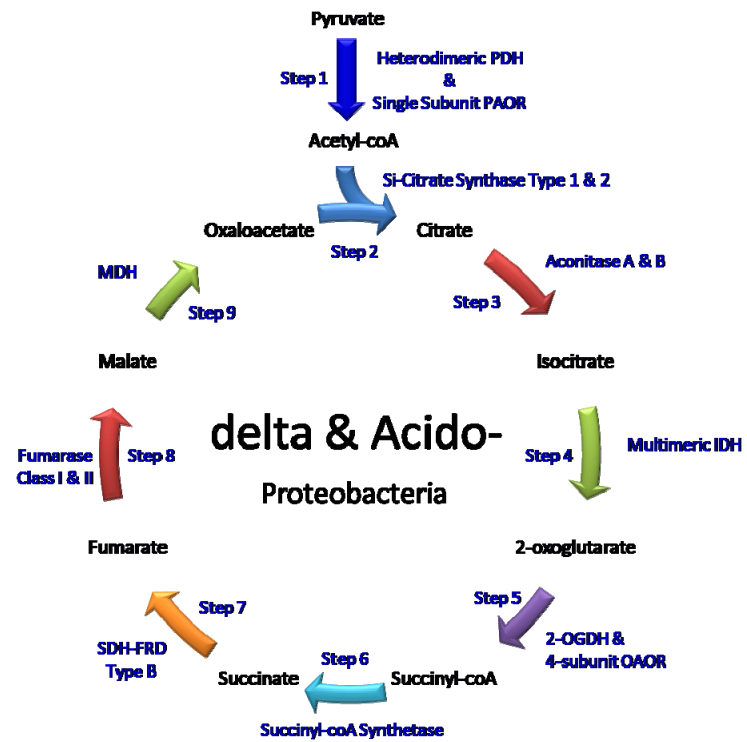
Appendix 8: The canonical citric acid cycle of *Alphaproteobacteria*.



Appendix 9: The canonical citric acid cycle of *Epsilonproteobacteria*.



Appendix 10: The canonical citric acid cycle of *Delta*- and *Acido*-proteobacteria.

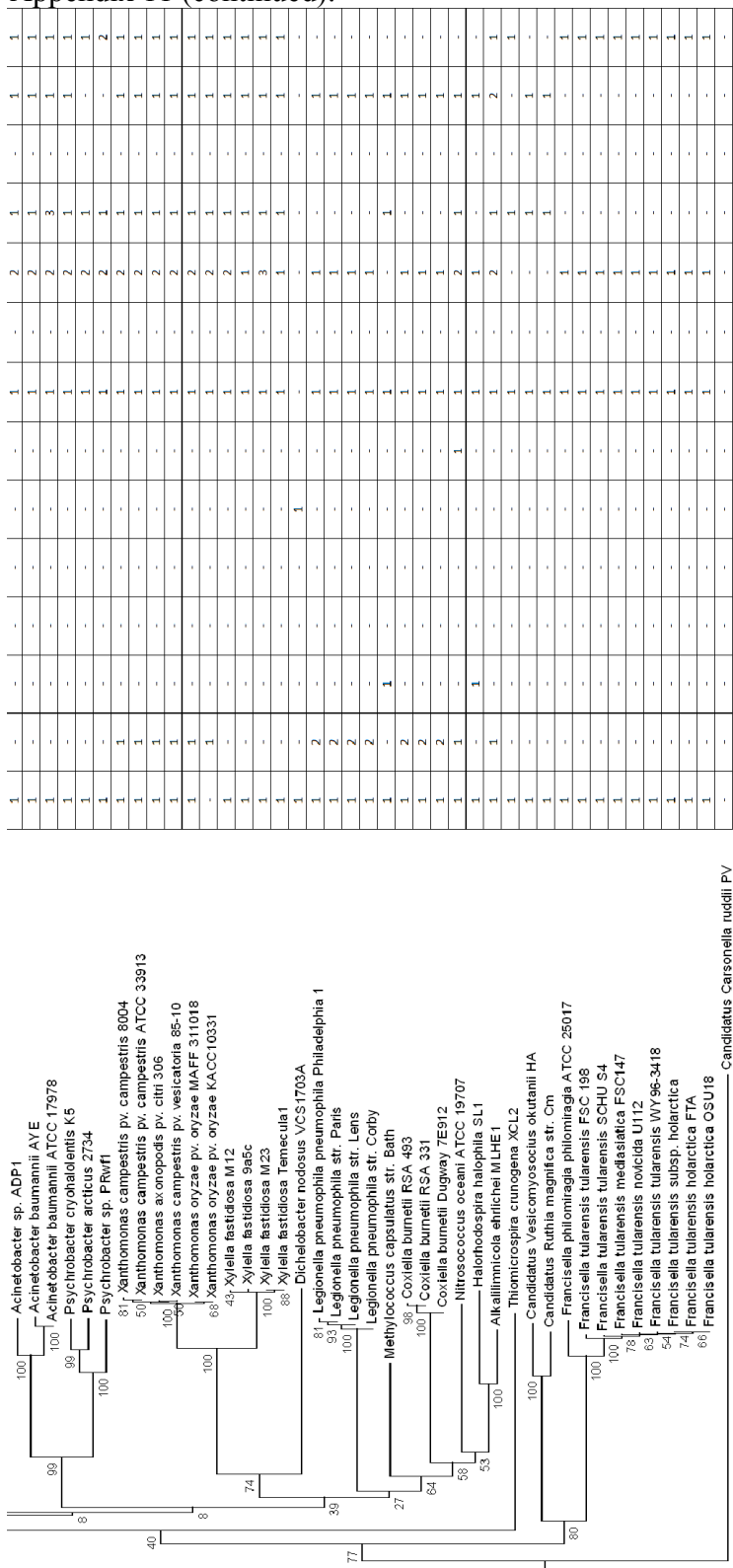




[illegible]

[illegible]

# Appendix 11 (continued):



75

75

[illegible]

[illegible]

[illegible]

[illegible]





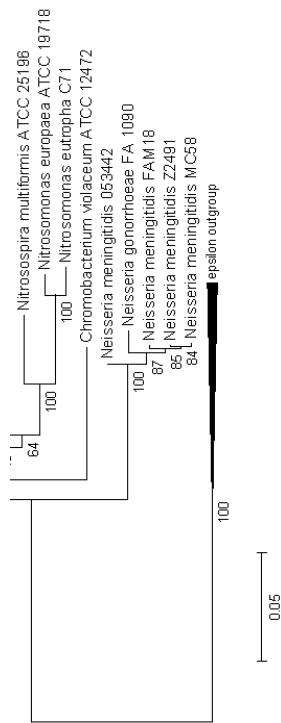
[illegible]

[illegible]



Appendix 16 (continued):

1	-	-	-	2	-	-	-	1	-	-	-	1	1	-
1	-	-	2	2	-	-	-	1	-	-	-	1	1	-
1	-	-	2	-	-	-	-	1	-	-	-	1	1	-
1	-	-	1	1	-	-	1	1	-	1	1	1	1	-
1	-	-	1	1	-	-	-	1	-	-	1	1	-	1
1	-	-	1	1	-	-	-	1	-	-	-	1	-	1
1	-	-	1	1	-	-	-	1	-	-	-	1	-	1
1	-	-	1	1	-	-	-	1	-	-	-	1	-	1
1	-	-	1	1	-	-	-	1	-	-	-	1	-	1
1	-	-	1	1	-	-	-	1	-	-	-	1	-	1
1	-	-	1	1	-	-	-	1	-	-	-	1	-	1
1	-	-	1	1	-	-	-	1	-	-	-	1	-	1



[illegible]

[illegible]

Appendix 18: Citric acid cycle genes (2-oxoglutarate to oxaloacetate) present for each species in the *Epsilon*-, *Delta*-, and *Acido-proteobacteria*. The phylogenetic trees adjacent to these tables were made using 16S RNA sequences and show the evolutionary relatedness and distance between the species in each class.

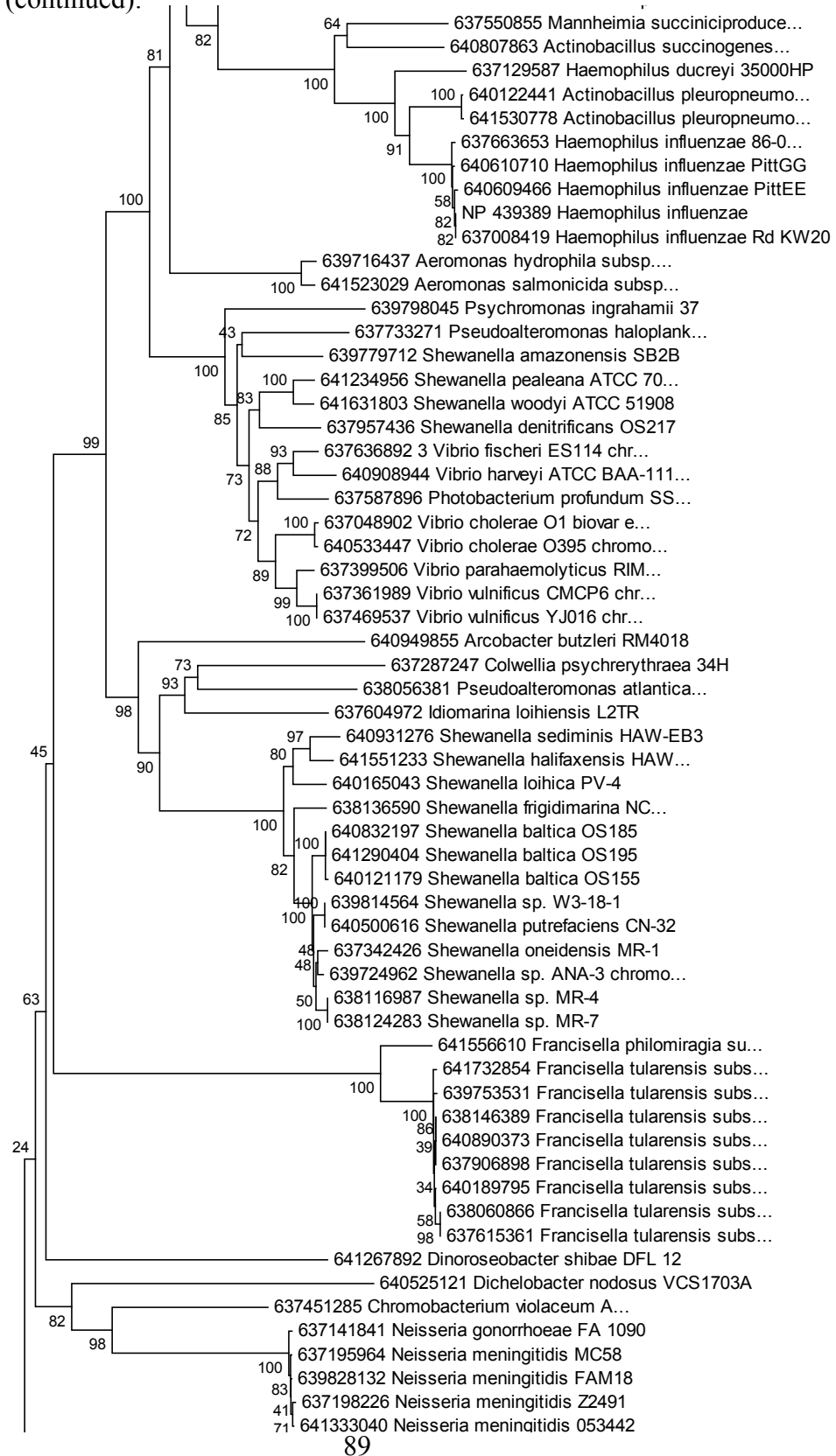
2OG --- Succinyl-CoA				Succinyl-CoA --- Succinate		Succinate --- Fumarate				Fumarate --- Malate		Malate --- Oxaloacetate		
2OG Dehydrogenase	Two Subunit OAOR		Four Subunit OAOR		Succinyl-CoA Synthetase	Sdh-Trd Type A	Sdh-Trd Type B	Sdh-Trd Type C	Sdh-Trd Type D	Sdh-Trd Type E	Fumarase Class I	Fumarase Class II	Malate Dehydrogenase	Malate Oxidoreductase
	-	-	-	-	-	-	-	-	-	-	-	-	-	-
-	-	-	-	-	-	-	-	-	-	-	-	-	-	-
-	-	-	-	-	-	-	-	-	-	-	-	-	-	-
-	-	-	-	-	-	-	-	-	-	-	-	-	-	-
-	-	-	-	-	-	-	-	-	-	-	-	-	-	-
-	-	-	-	-	-	-	-	-	-	-	-	-	-	-
-	-	-	-	-	-	-	-	-	-	-	-	-	-	-
-	-	-	-	-	-	-	-	-	-	-	-	-	-	-
-	-	-	-	-	-	-	-	-	-	-	-	-	-	-
-	-	-	-	-	-	-	-	-	-	-	-	-	-	-
-	-	-	-	-	-	-	-	-	-	-	-	-	-	-
-	-	-	-	-	-	-	-	-	-	-	-	-	-	-
-	-	-	-	-	-	-	-	-	-	-	-	-	-	-
-	-	-	-	-	-	-	-	-	-	-	-	-	-	-
-	-	-	-	-	-	-	-	-	-	-	-	-	-	-
-	-	-	-	-	-	-	-	-	-	-	-	-	-	-
-	-	-	-	-	-	-	-	-	-	-	-	-	-	-
-	-	-	-	-	-	-	-	-	-	-	-	-	-	-
-	-	-	-	-	-	-	-	-	-	-	-	-	-	-
-	-	-	-	-	-	-	-	-	-	-	-	-	-	-
-	-	-	-	-	-	-	-	-	-	-	-	-	-	-
-	-	-	-	-	-	-	-	-	-	-	-	-	-	-
-	-	-	-	-	-	-	-	-	-	-	-	-	-	-
-	-	-	-	-	-	-	-	-	-	-	-	-	-	-
-	-	-	-	-	-	-	-	-	-	-	-	-	-	-
-	-	-	-	-	-	-	-	-	-	-	-	-	-	-
-	-	-	-	-	-	-	-	-	-	-	-	-	-	-
-	-	-	-	-	-	-	-	-	-	-	-	-	-	-
-	-	-	-	-	-	-	-	-	-	-	-	-	-	-
-	-	-	-	-	-	-	-	-	-	-	-	-	-	-
-	-	-	-	-	-	-	-	-	-	-	-	-	-	-
-	-	-	-	-	-	-	-	-	-	-	-	-	-	-
-	-	-	-	-	-	-	-	-	-	-	-	-	-	-
-	-	-	-	-	-	-	-	-	-	-	-	-	-	-
-	-	-	-	-	-	-	-	-	-	-	-	-	-	-
-	-	-	-	-	-	-	-	-	-	-	-	-	-	-
-	-	-	-	-	-	-	-	-	-	-	-	-	-	-
-	-	-	-	-	-	-	-	-	-	-	-	-	-	-
-	-	-	-	-	-	-	-	-	-	-	-	-	-	-
-	-	-	-	-	-	-	-	-	-	-	-	-	-	-
-	-	-	-	-	-	-	-	-	-	-	-	-	-	-
-	-	-	-	-	-	-	-	-	-	-	-	-	-	-
-	-	-	-	-	-	-	-	-	-	-	-	-	-	-
-	-	-	-	-	-	-	-	-	-	-	-	-	-	-
-	-	-	-	-	-	-	-	-	-	-	-	-	-	-
-	-	-	-	-	-	-	-	-	-	-	-	-	-	-
-	-	-	-	-	-	-	-	-	-	-	-	-	-	-
-	-	-	-	-	-	-	-	-	-	-	-	-	-	-
-	-	-	-	-	-	-	-	-	-	-	-	-	-	-
-	-	-	-	-	-	-	-	-	-	-	-	-	-	-
-	-	-	-	-	-	-	-	-	-	-	-	-	-	-
-	-	-	-	-	-	-	-	-	-	-	-	-	-	-
-	-	-	-	-	-	-	-	-	-	-	-	-	-	-
-	-	-	-	-	-	-	-	-	-	-	-	-	-	-
-	-	-	-	-	-	-	-	-	-	-	-	-	-	-
-	-	-	-	-	-	-	-	-	-	-	-	-	-	-
-	-	-	-	-	-	-	-	-	-	-	-	-	-	-
-	-	-	-	-	-	-	-	-	-	-	-	-	-	-
-	-	-	-	-	-	-	-	-	-	-	-	-	-	-
-	-	-	-	-	-	-	-	-	-	-	-	-	-	-
-	-	-	-	-	-	-	-	-	-	-	-	-	-	-
-	-	-	-	-	-	-	-	-	-	-	-	-	-	-
-	-	-	-	-	-	-	-	-	-	-	-	-	-	-
-	-	-	-	-	-	-	-	-	-	-	-	-	-	-
-	-	-	-	-	-	-	-	-	-	-	-	-	-	-
-	-	-	-	-	-	-	-	-	-	-	-	-	-	-
-	-	-	-	-	-	-	-	-	-	-	-	-	-	-
-	-	-	-	-	-	-	-	-	-	-	-	-	-	-
-	-	-	-	-	-	-	-	-	-	-	-	-	-	-
-	-	-	-	-	-	-	-	-	-	-	-	-	-	-
-	-	-	-	-	-	-	-	-	-	-	-	-	-	-
-	-	-	-	-	-	-	-	-	-	-	-	-	-	-
-	-	-	-	-	-	-	-	-	-	-	-	-	-	-
-	-	-	-	-	-	-	-	-	-					



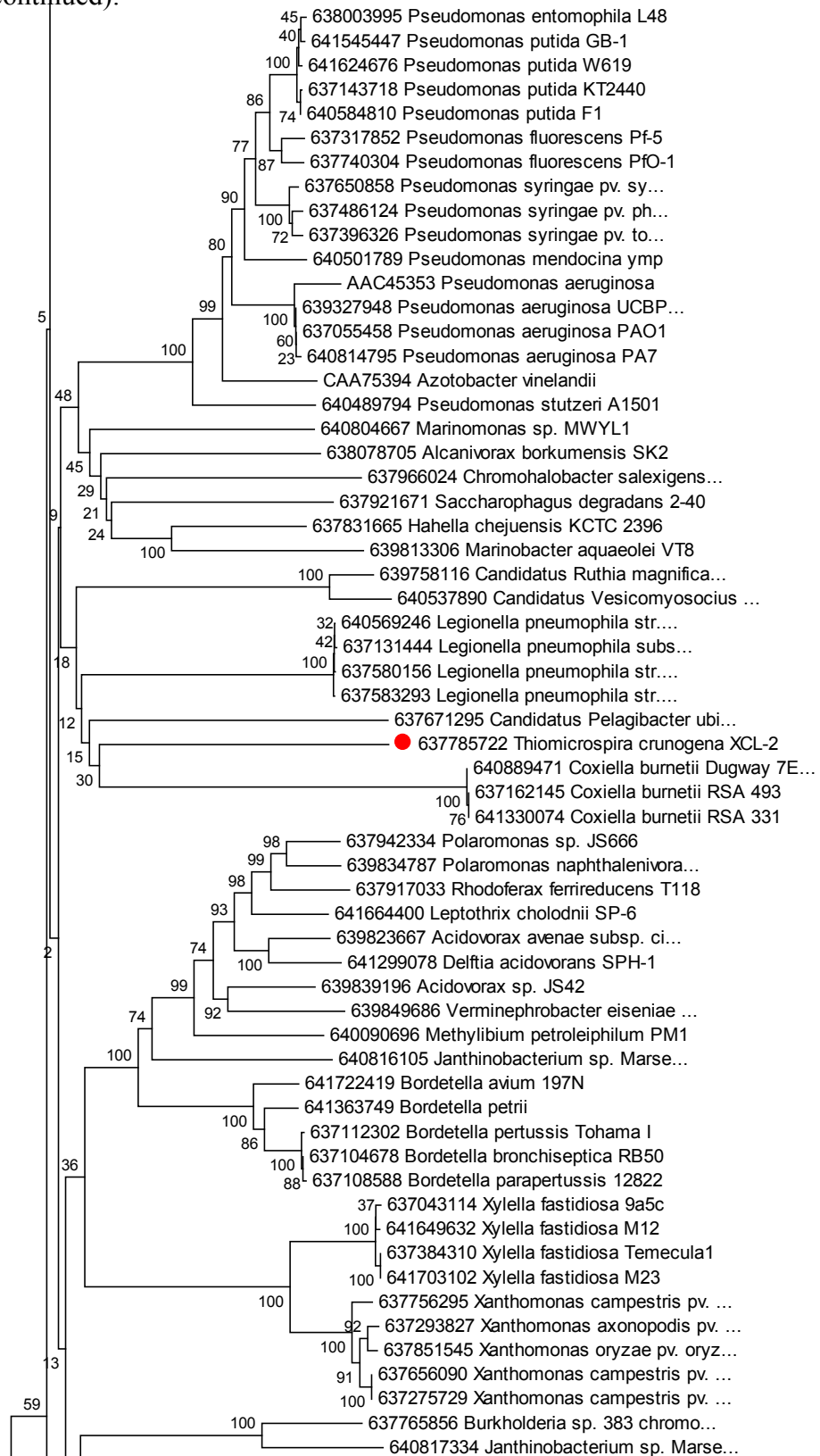
Appendix 19: Phylogeny of homodimeric pyruvate dehydrogenase sequences, using genes encoding methionine degradation enzyme as an outgroup.



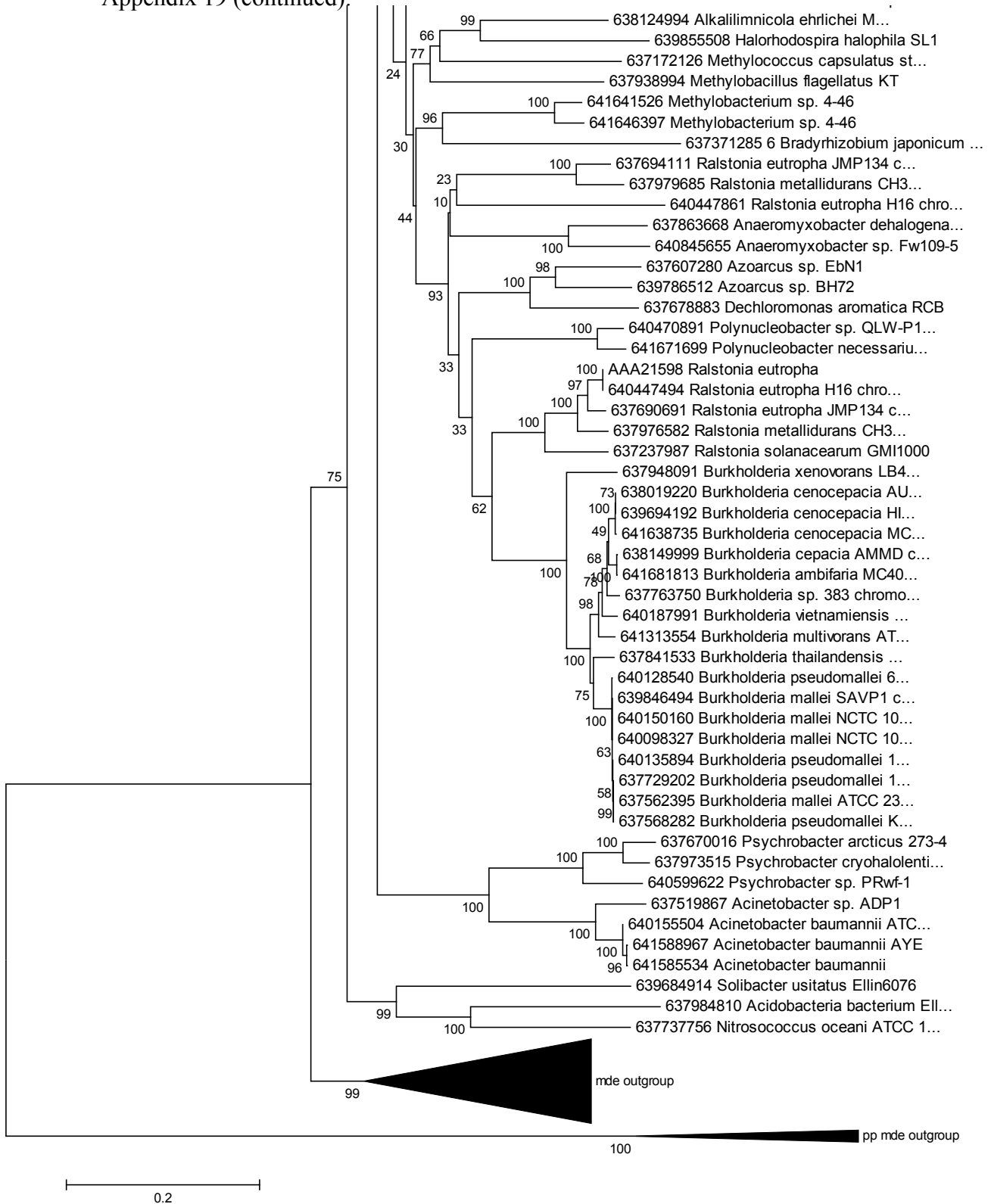
Appendix 19 (continued):



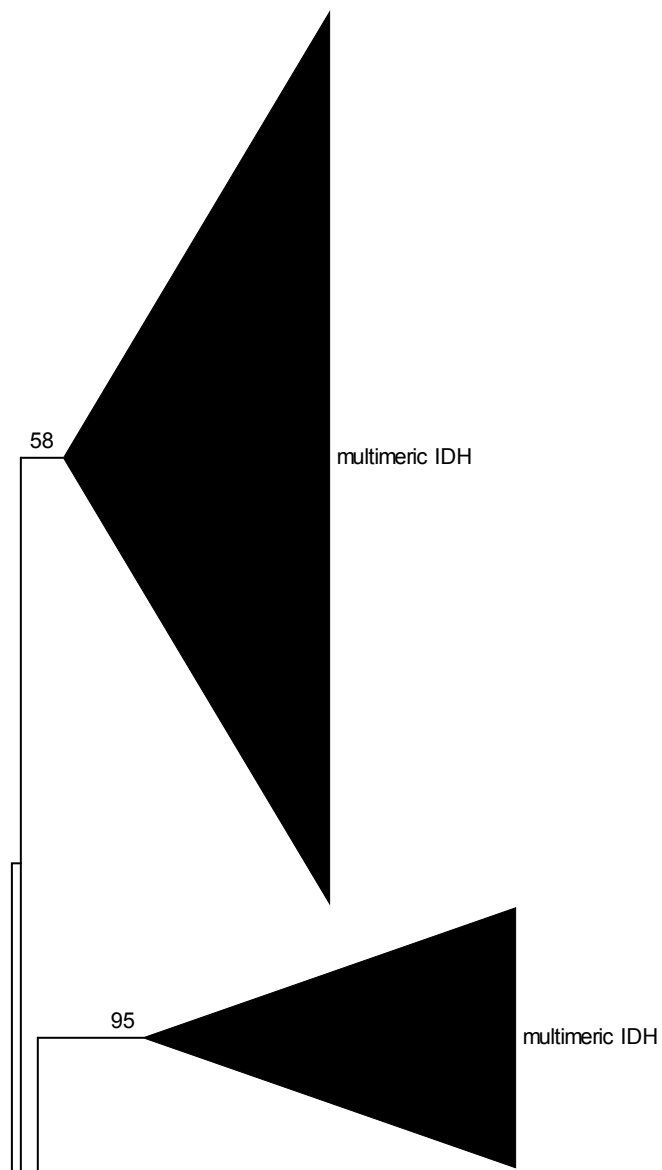
Appendix 19 (continued):



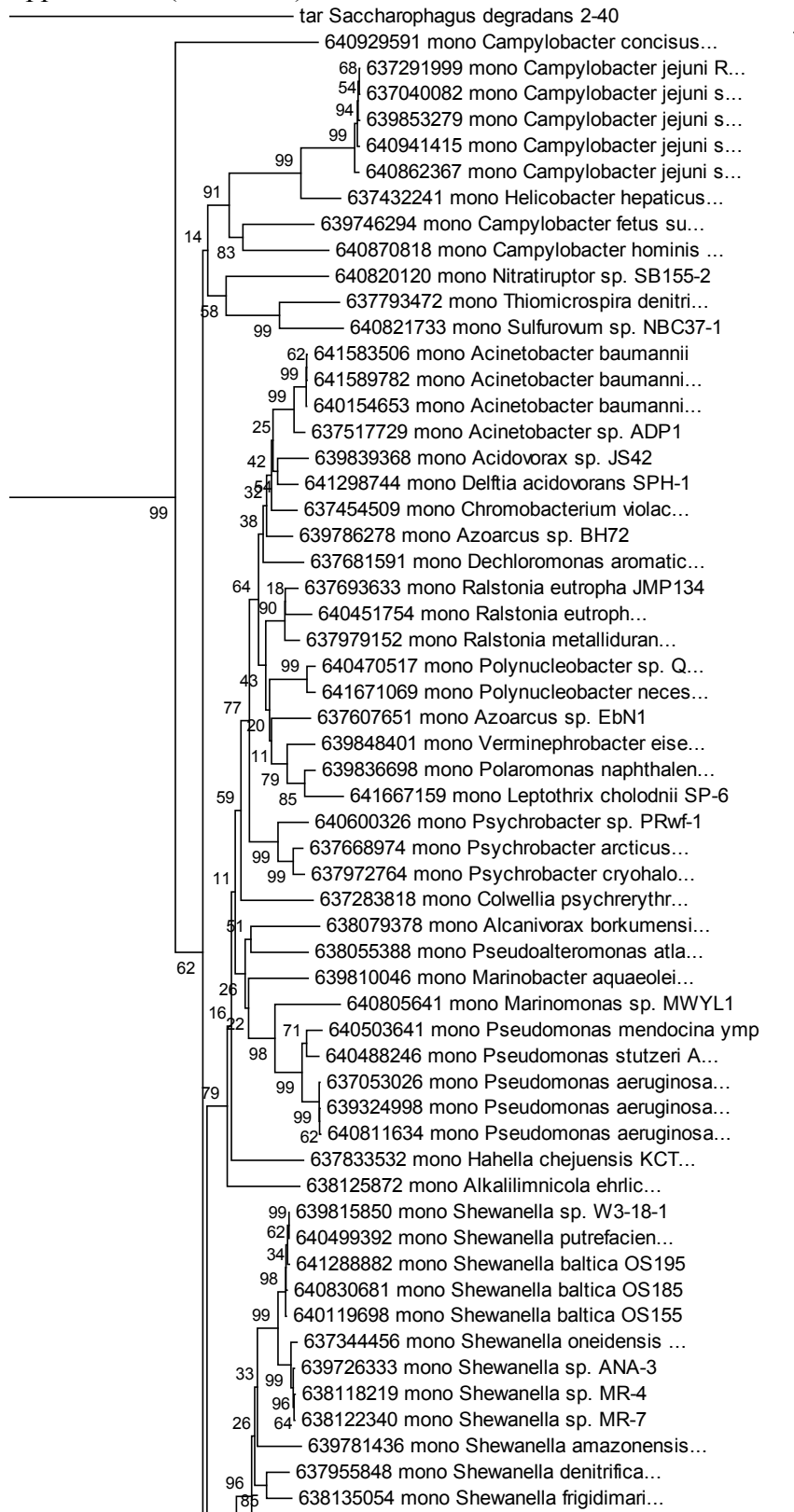
Appendix 19 (continued):



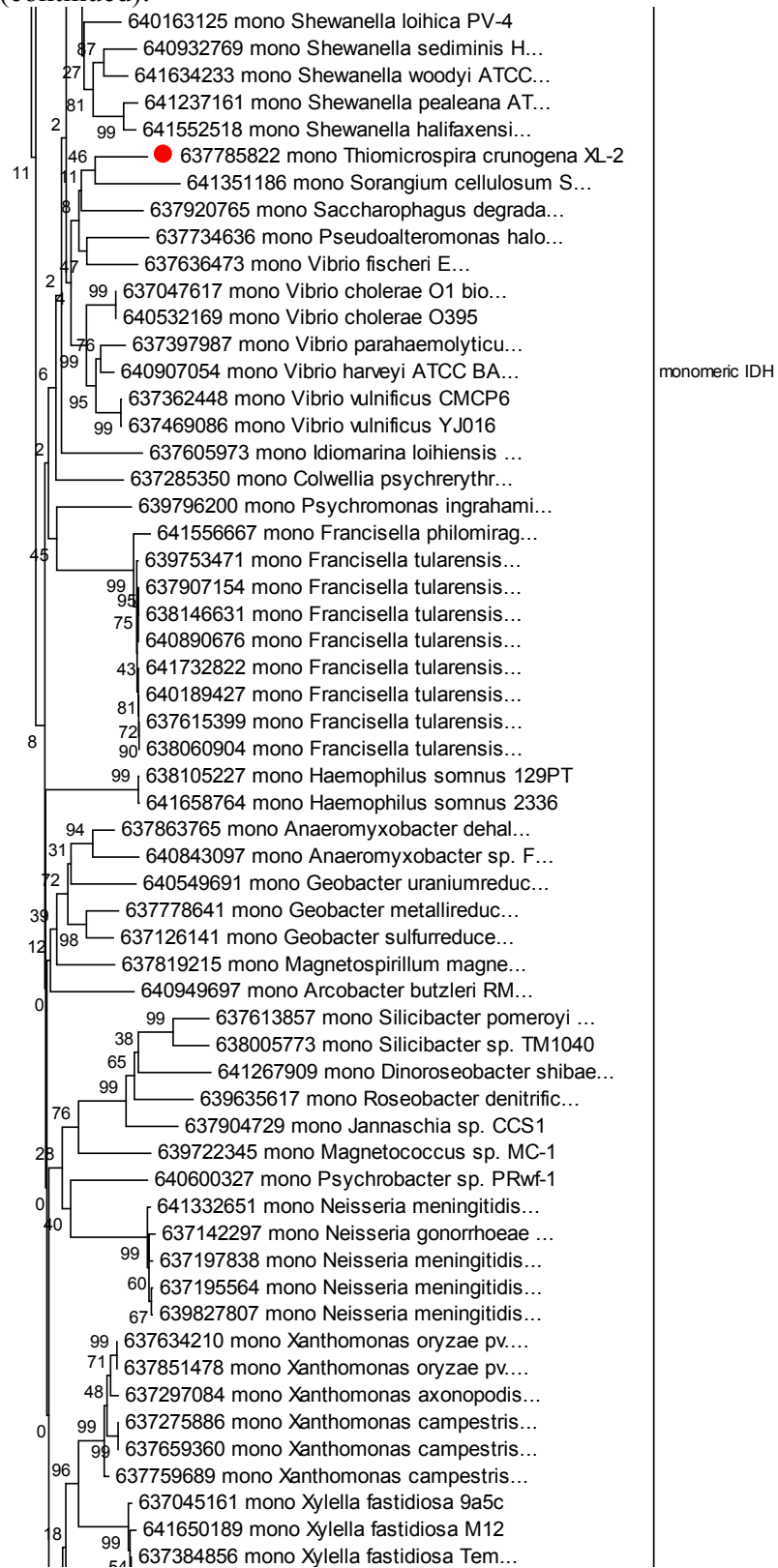
Appendix 20: Phylogeny of isocitrate dehydrogenase sequences, using genes encoding 3-isopropylmalate and tartrate dehydrogenases as an outgroup.



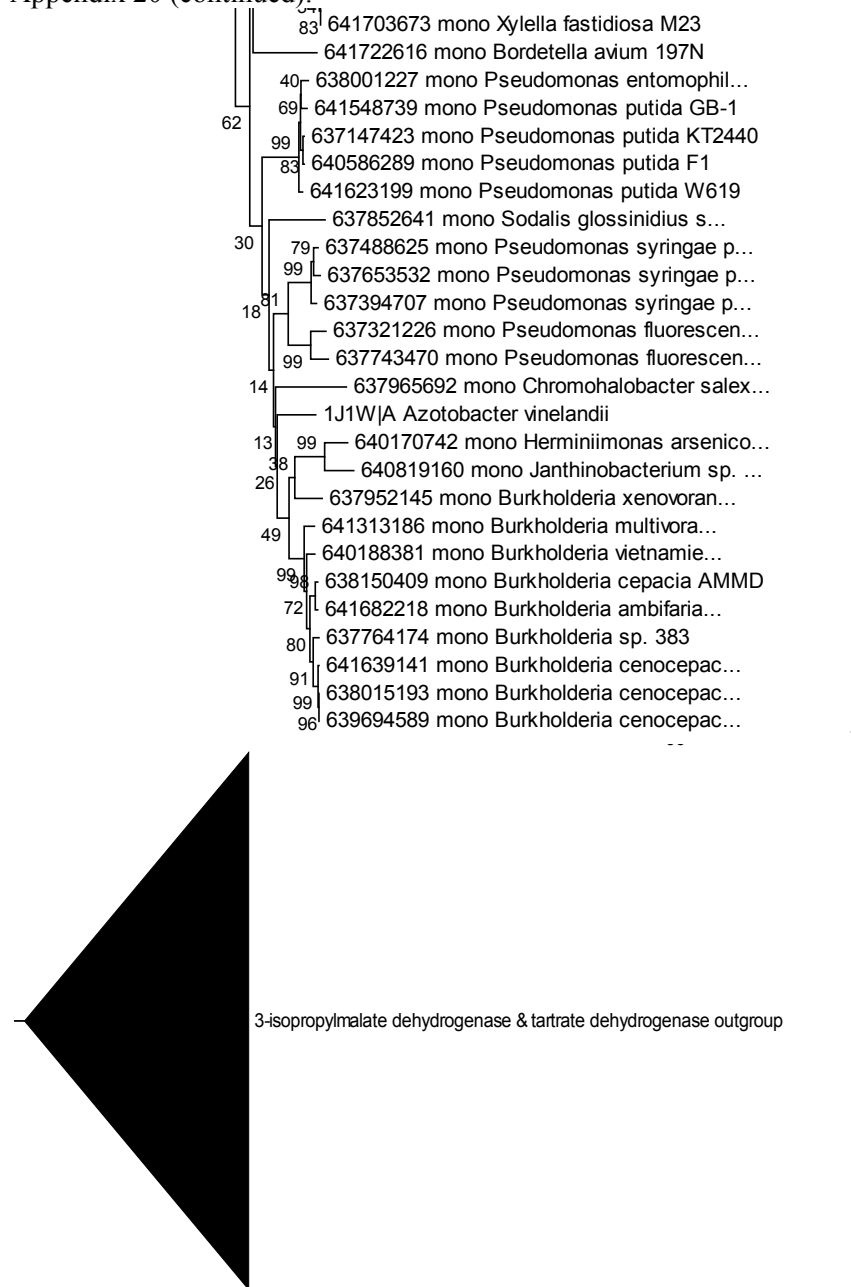
Appendix 20 (continued):



Appendix 20 (continued):

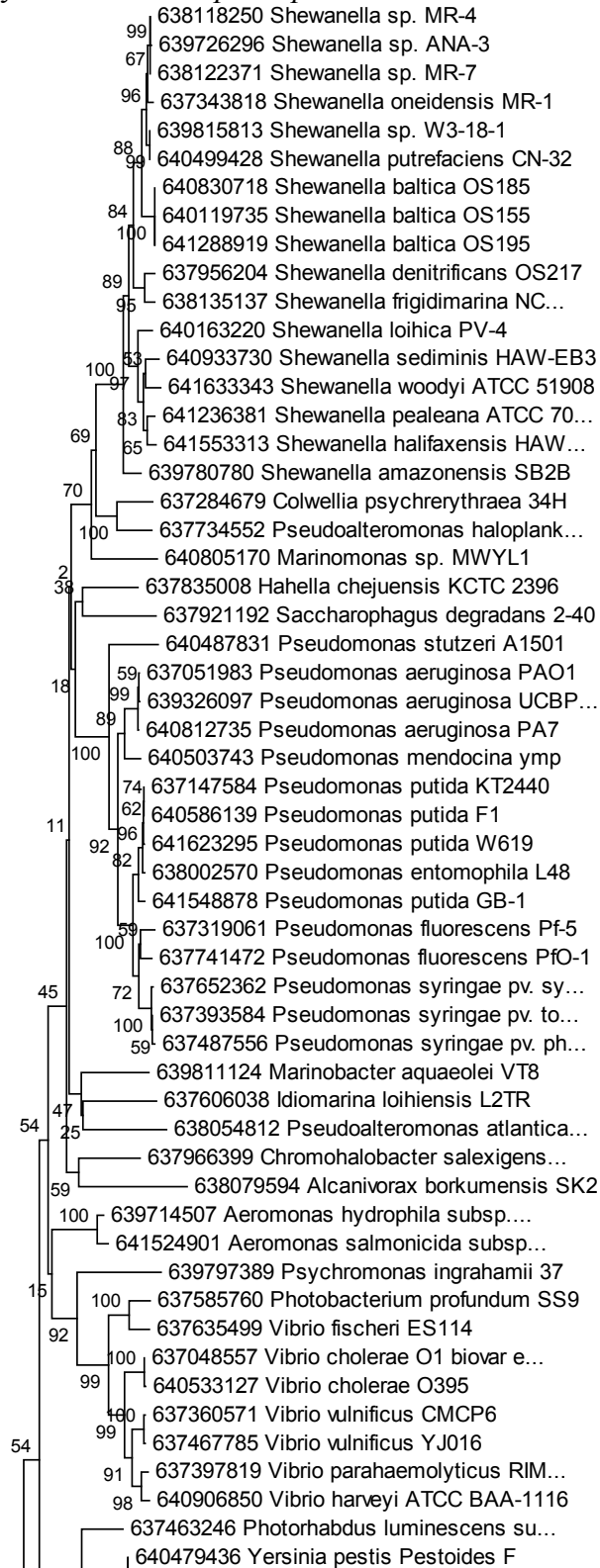


Appendix 20 (continued):

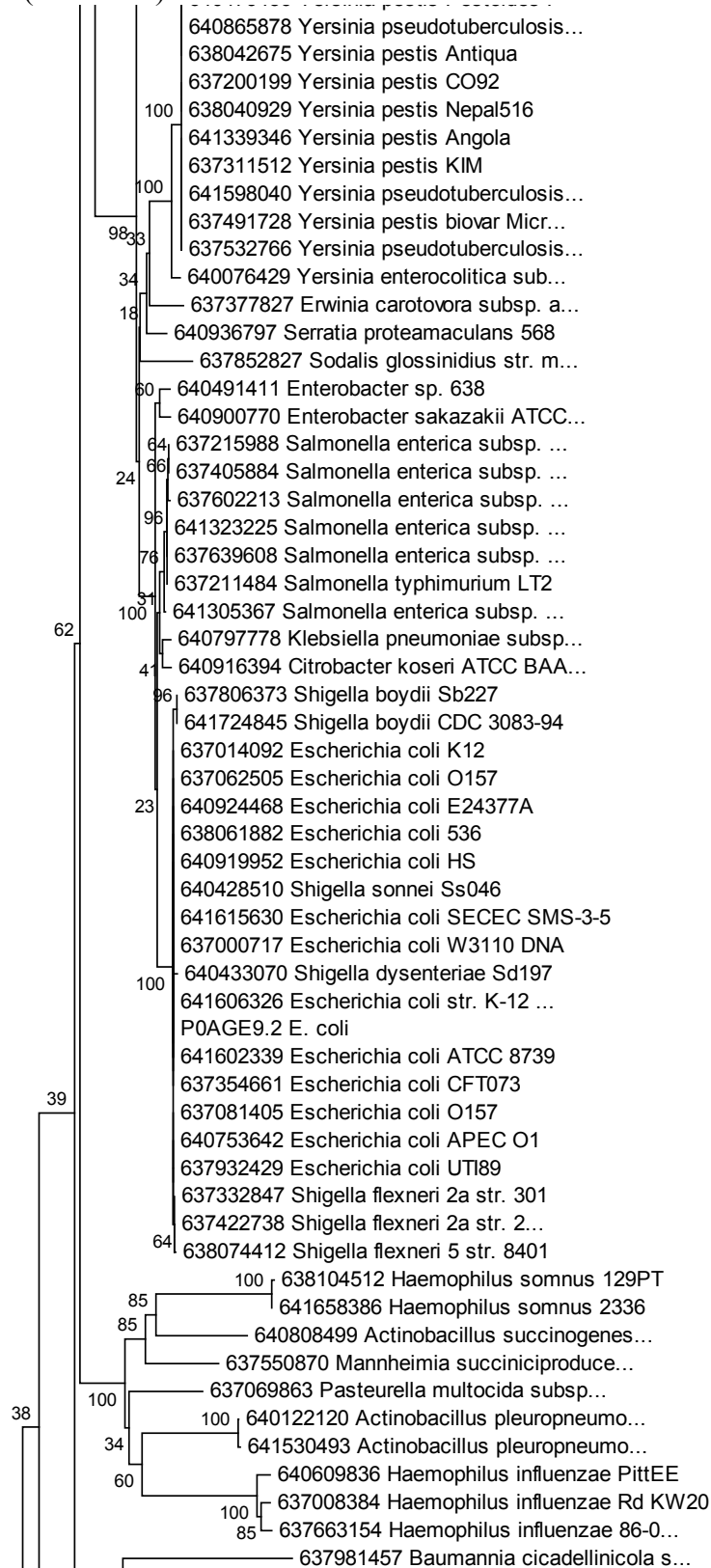




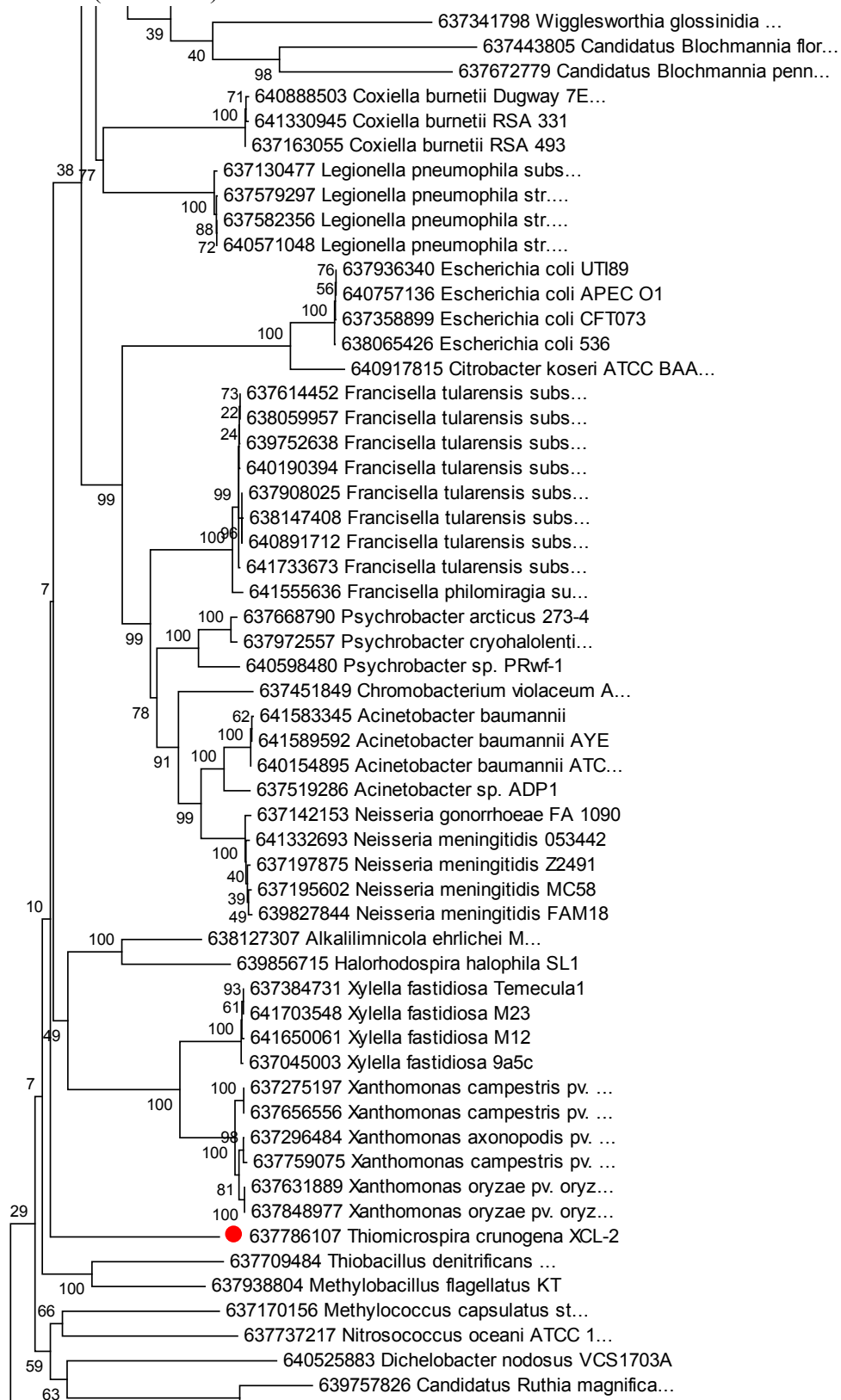
Appendix 21: Phylogeny of succinyl-coA synthetase sequences, using sequences of succinyl-coA synthetase from *Epsilonproteobacteria* as the outgroup.



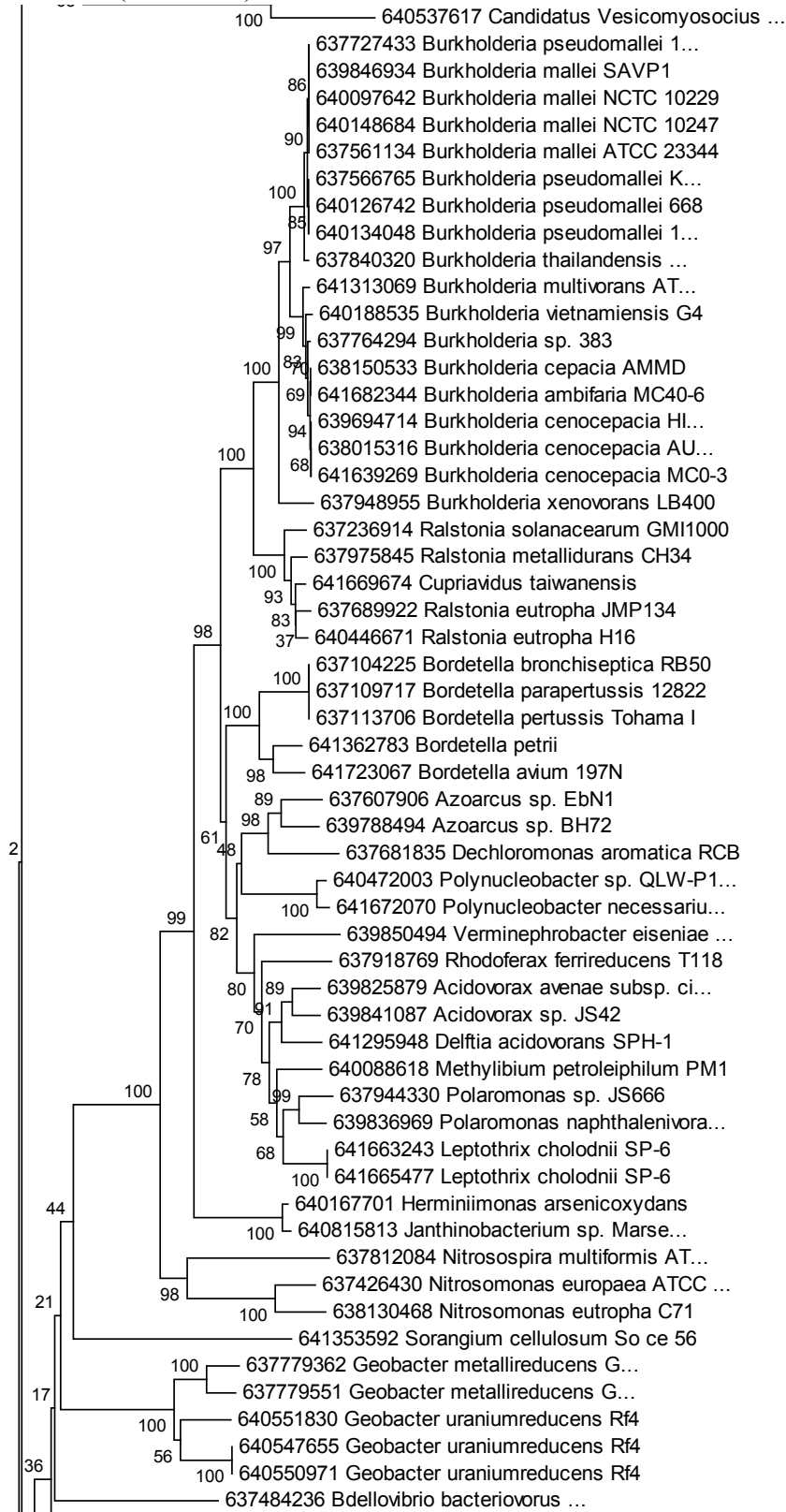
Appendix 21 (continued):



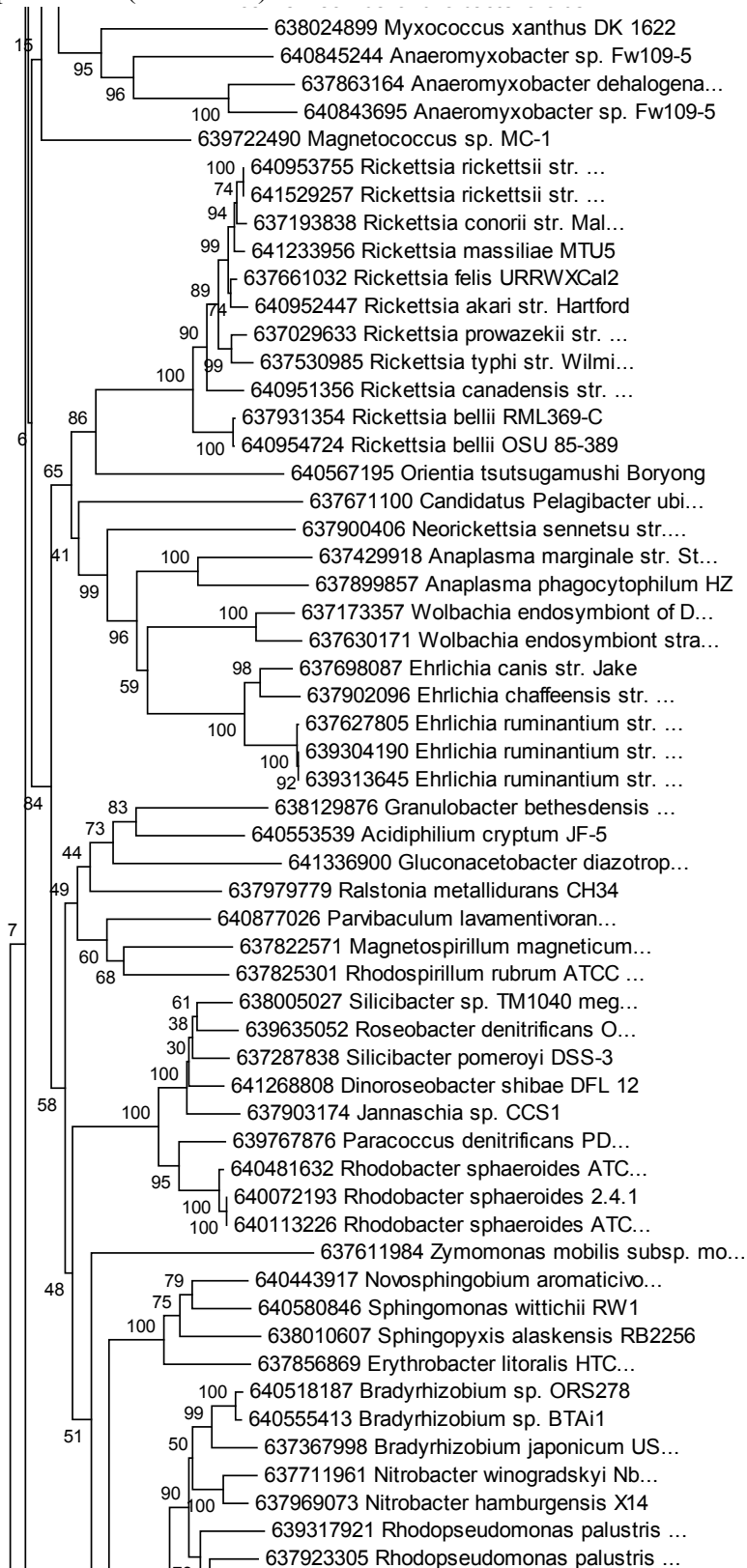
Appendix 21 (continued):



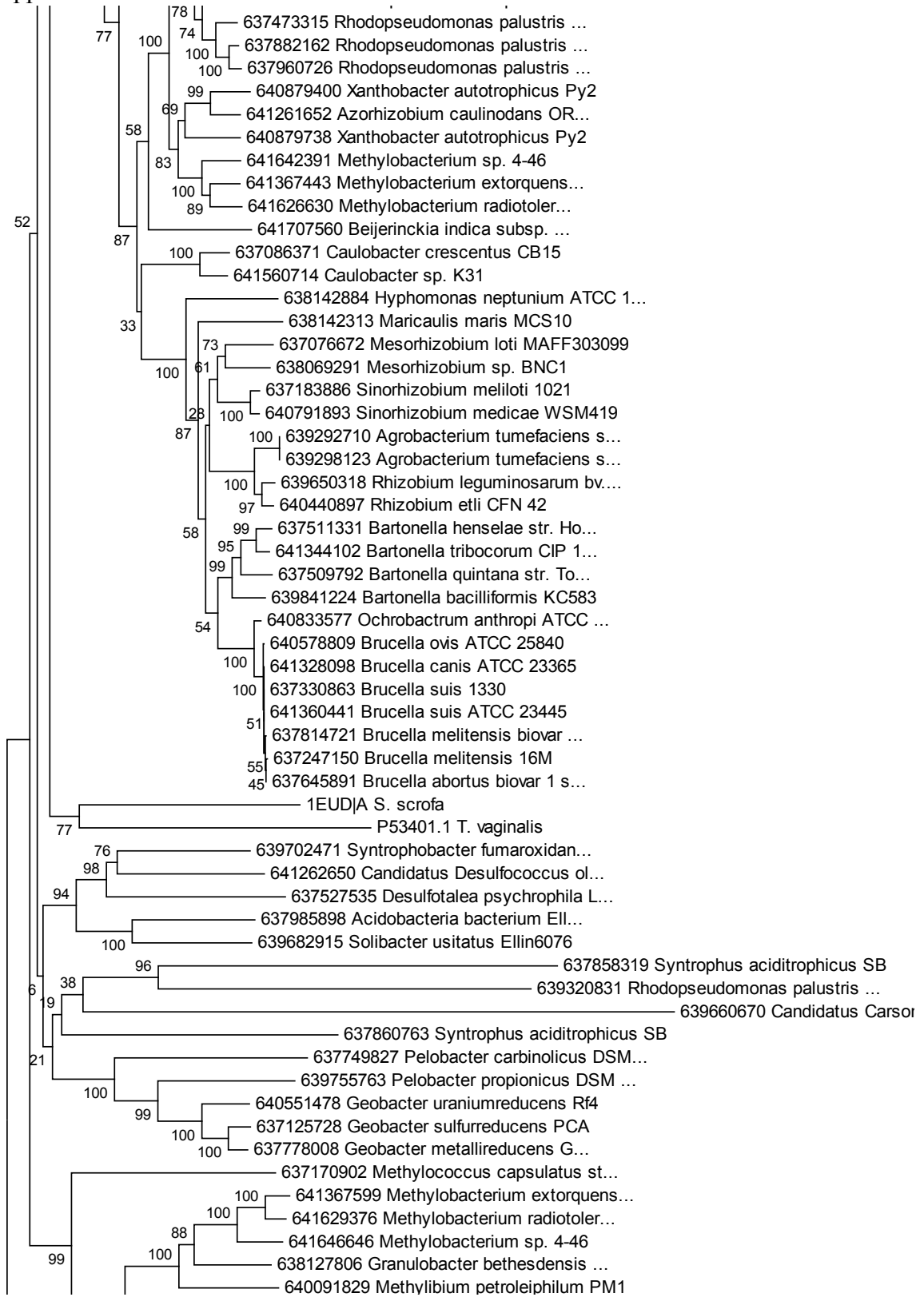
Appendix 21 (continued):



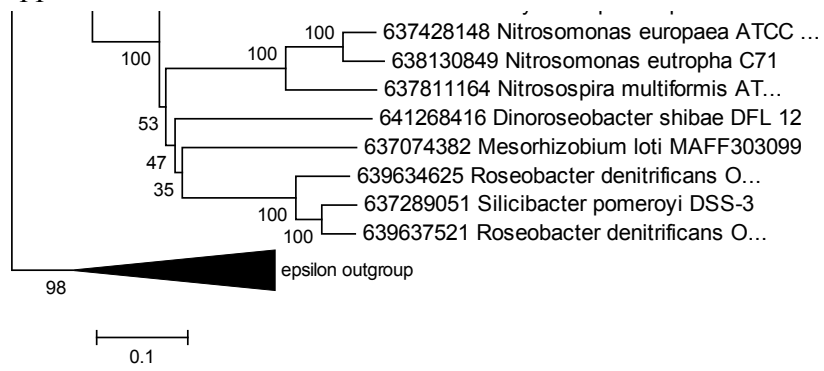
Appendix 21 (continued):



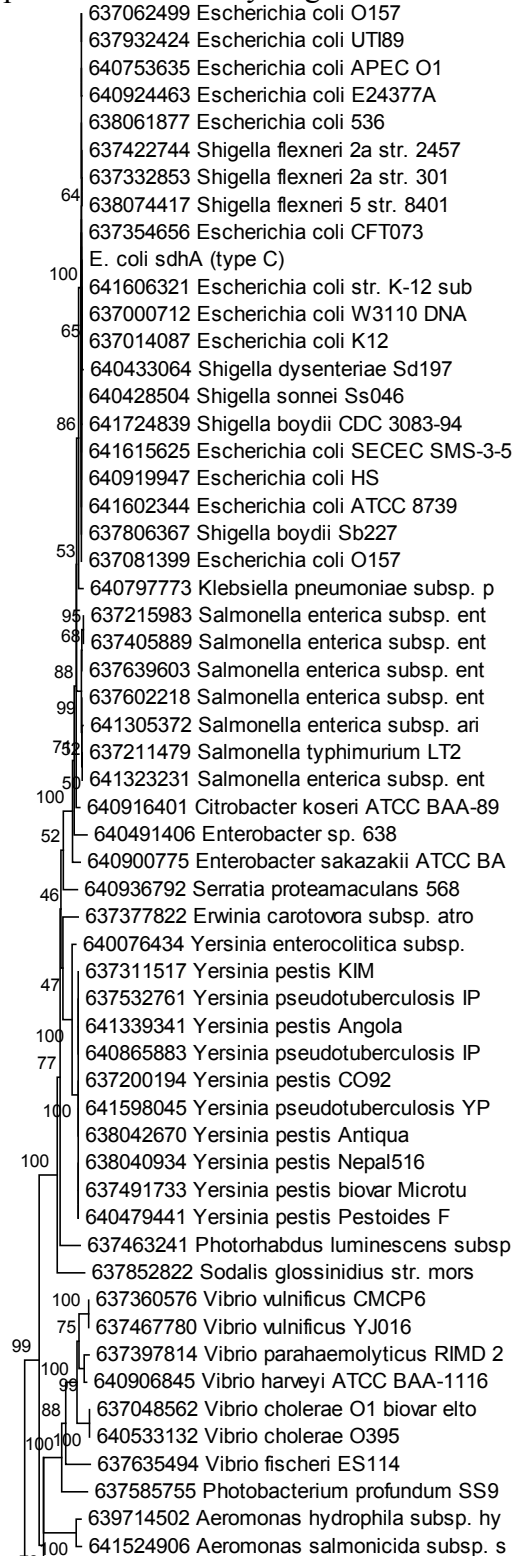
# Appendix 21:



# Appendix 21:

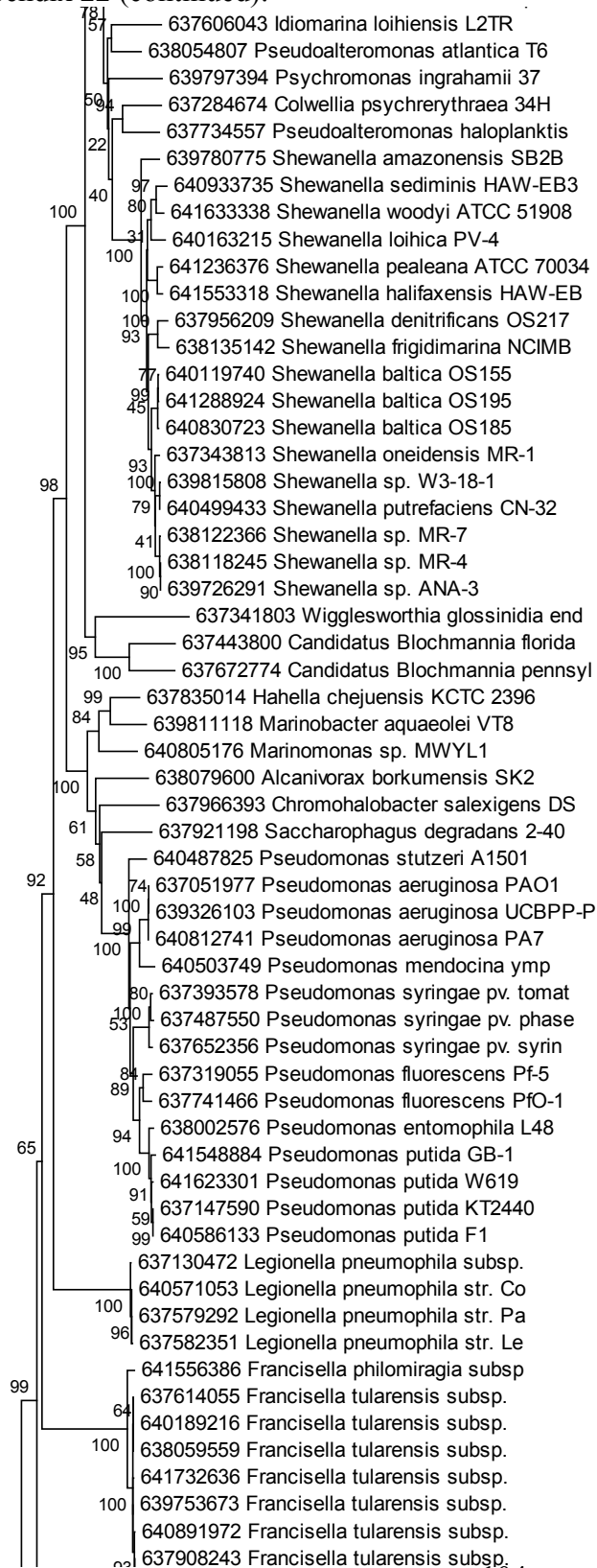


Appendix 22: Phylogeny of succinate dehydrogenase/fumarate reductase sequences, using Type D succinate dehydrogenase/fumarate reductase sequences as an outgroup.

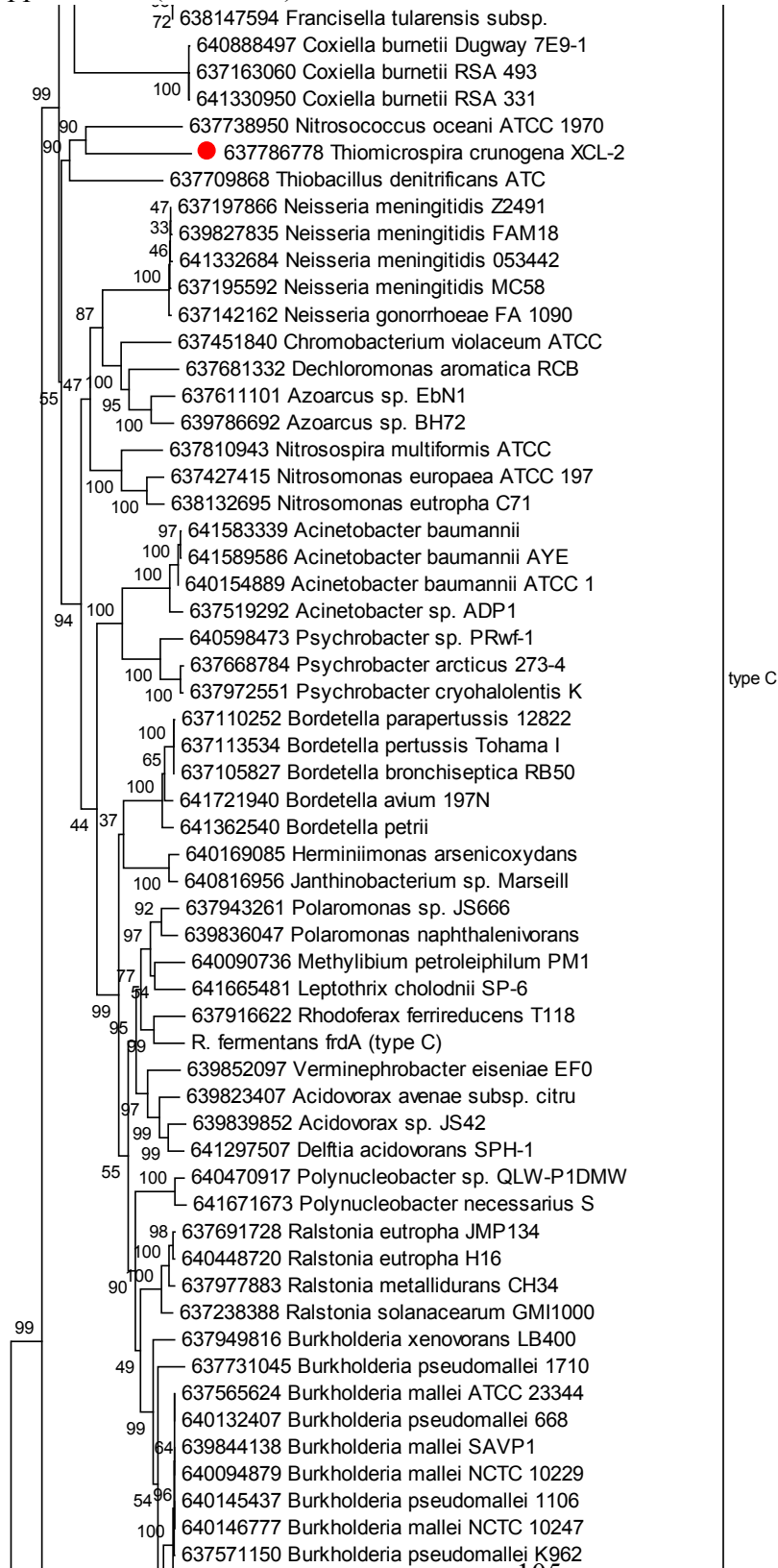




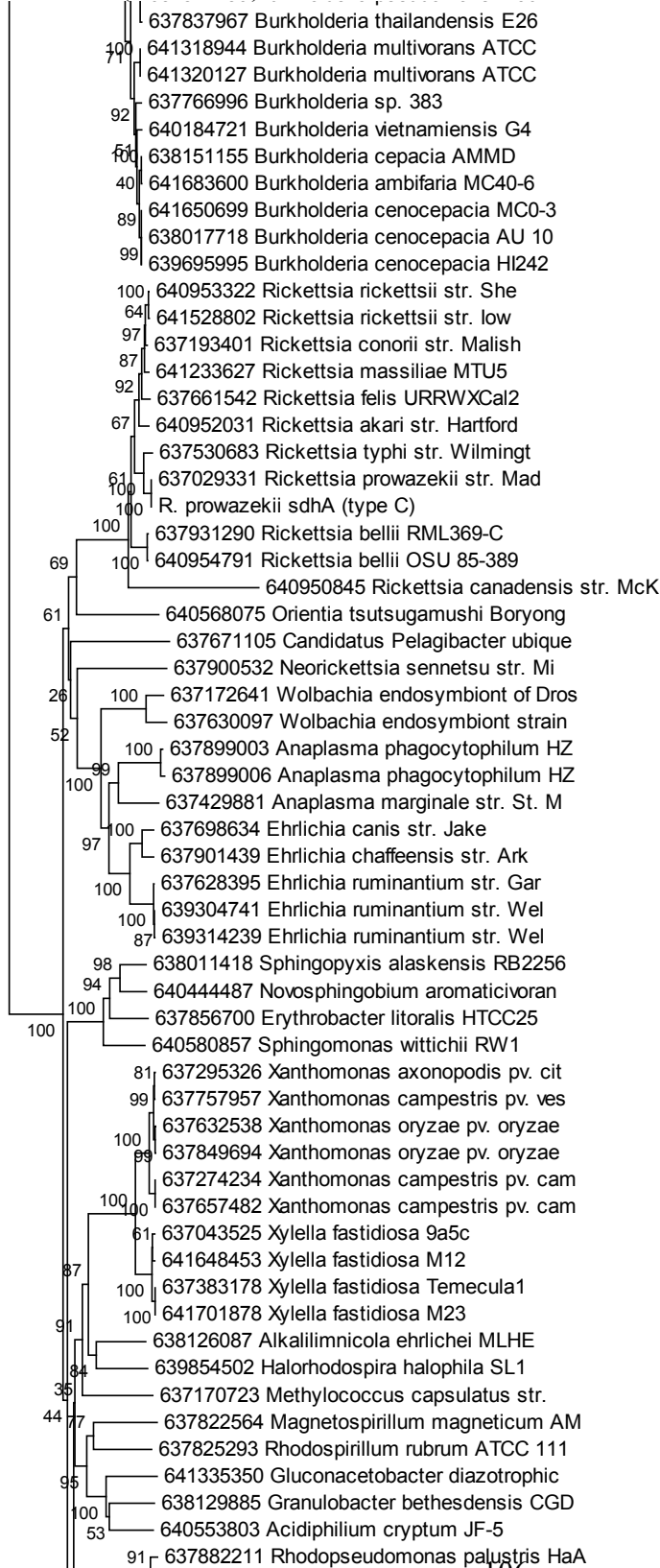
Appendix 22 (continued):



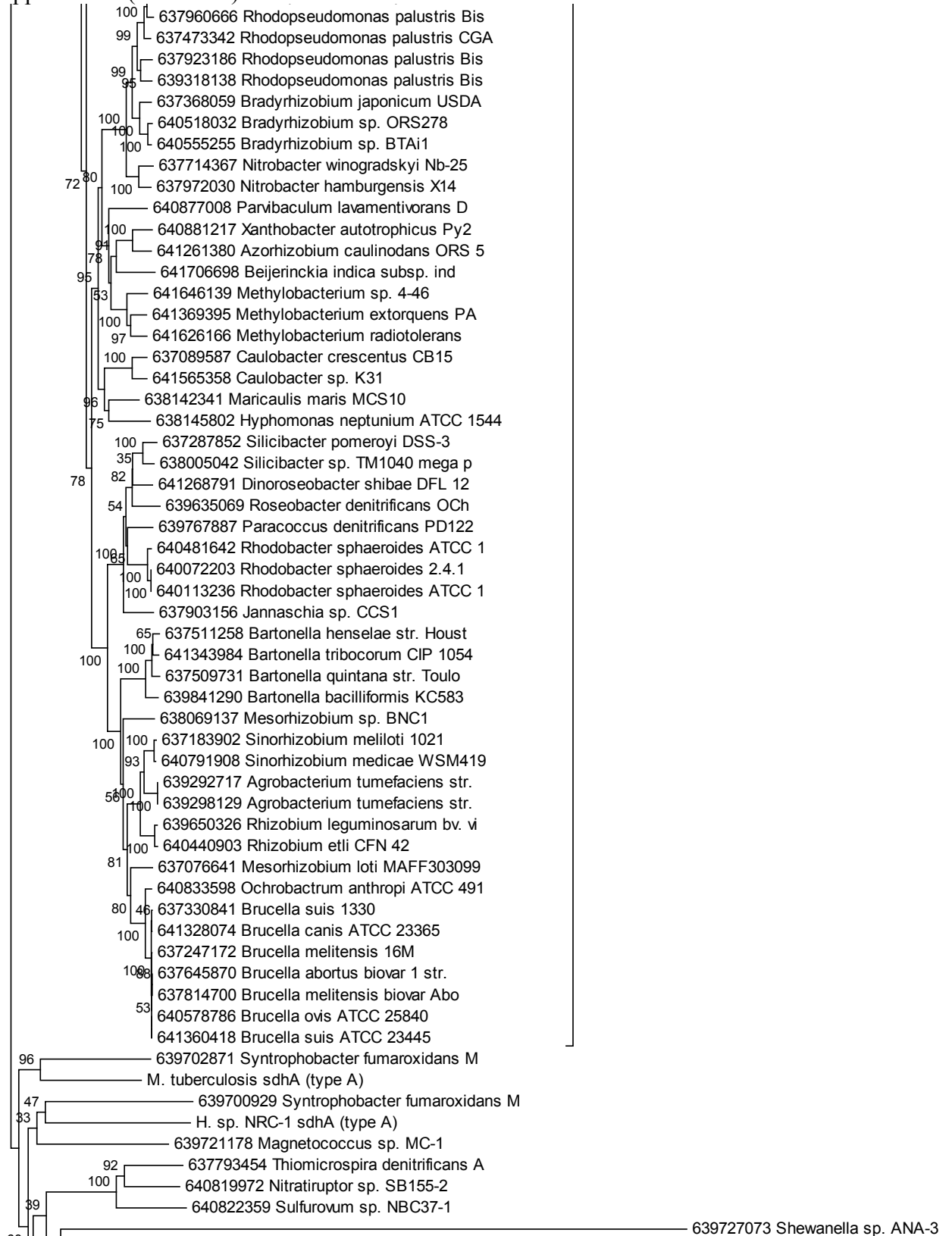
# Appendix 22 (continued):



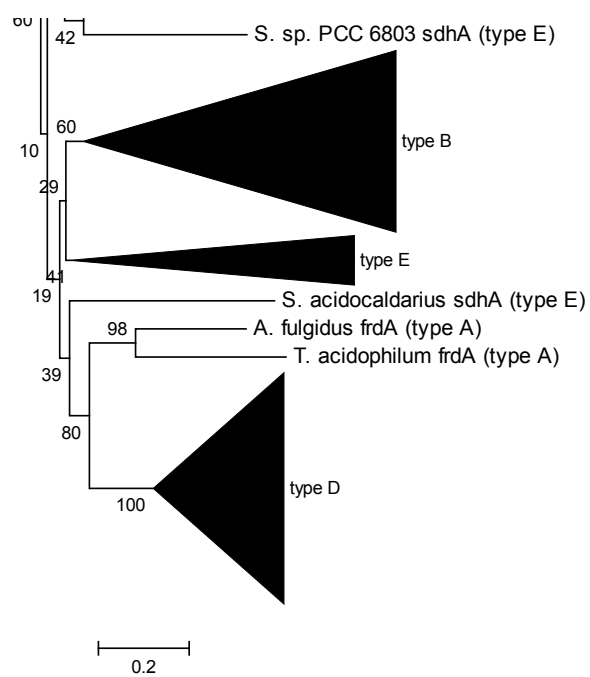
Appendix 22 (continued):



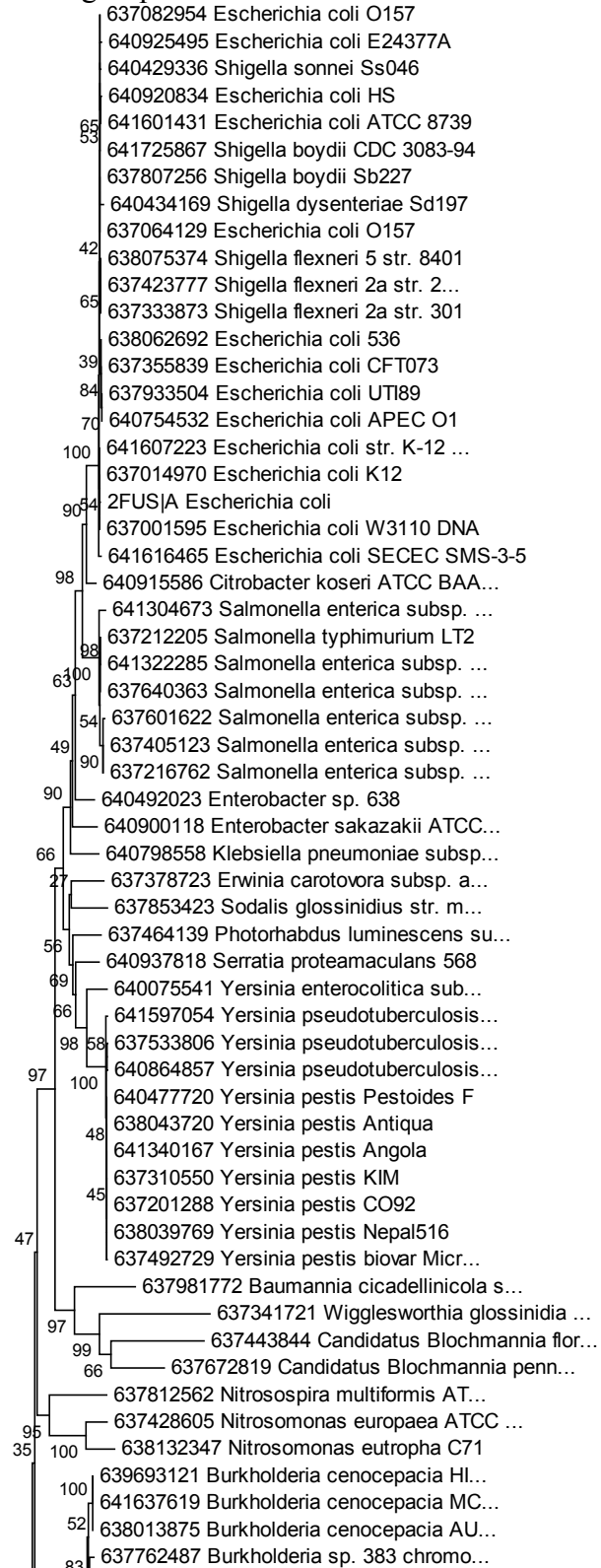
Appendix 22 (continued):



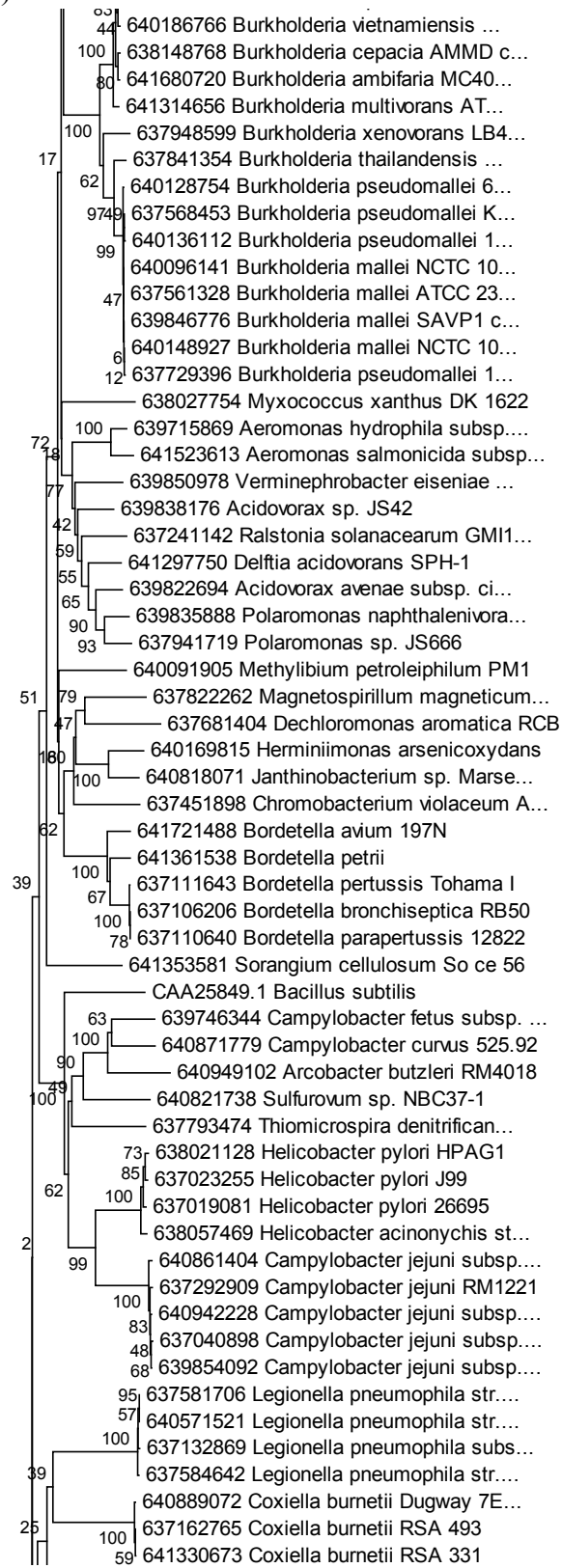
Appendix 22 (continued):



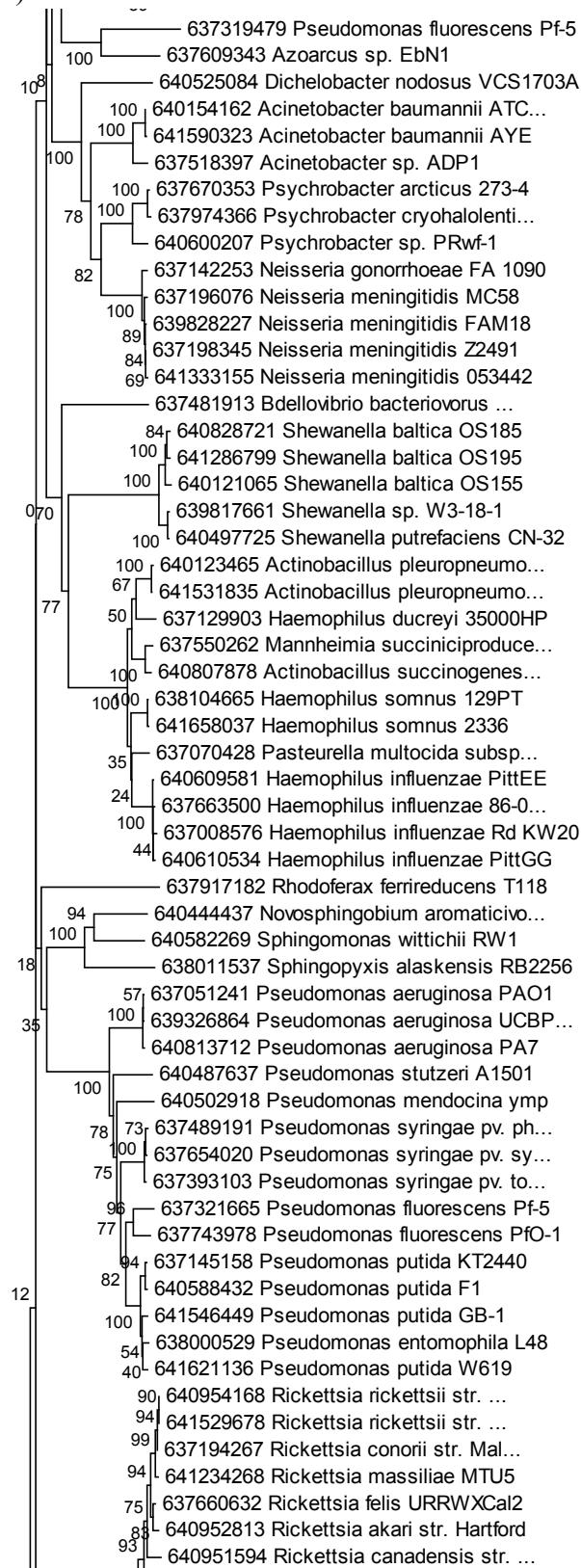
Appendix 23: Phylogeny of class II fumarase sequences, using genes encoding argininosuccinate lyase as an outgroup.



Appendix 23 (continued):

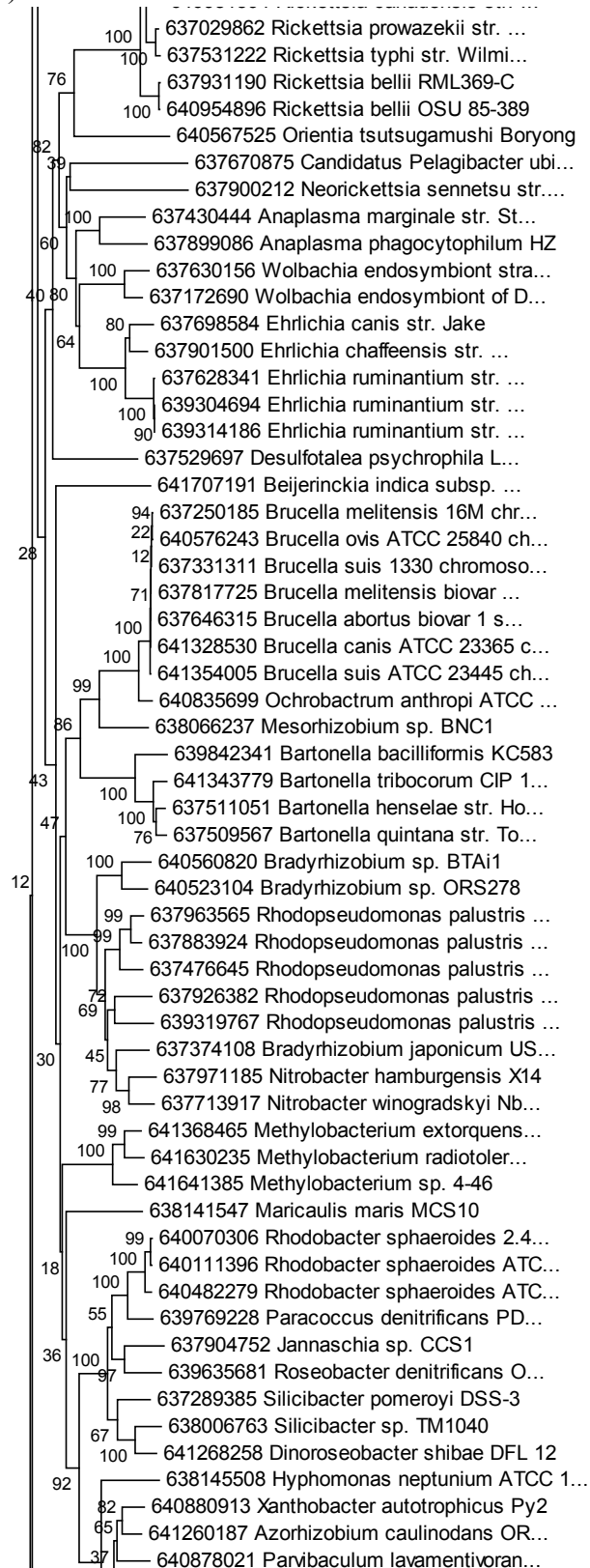


Appendix 23 (continued):

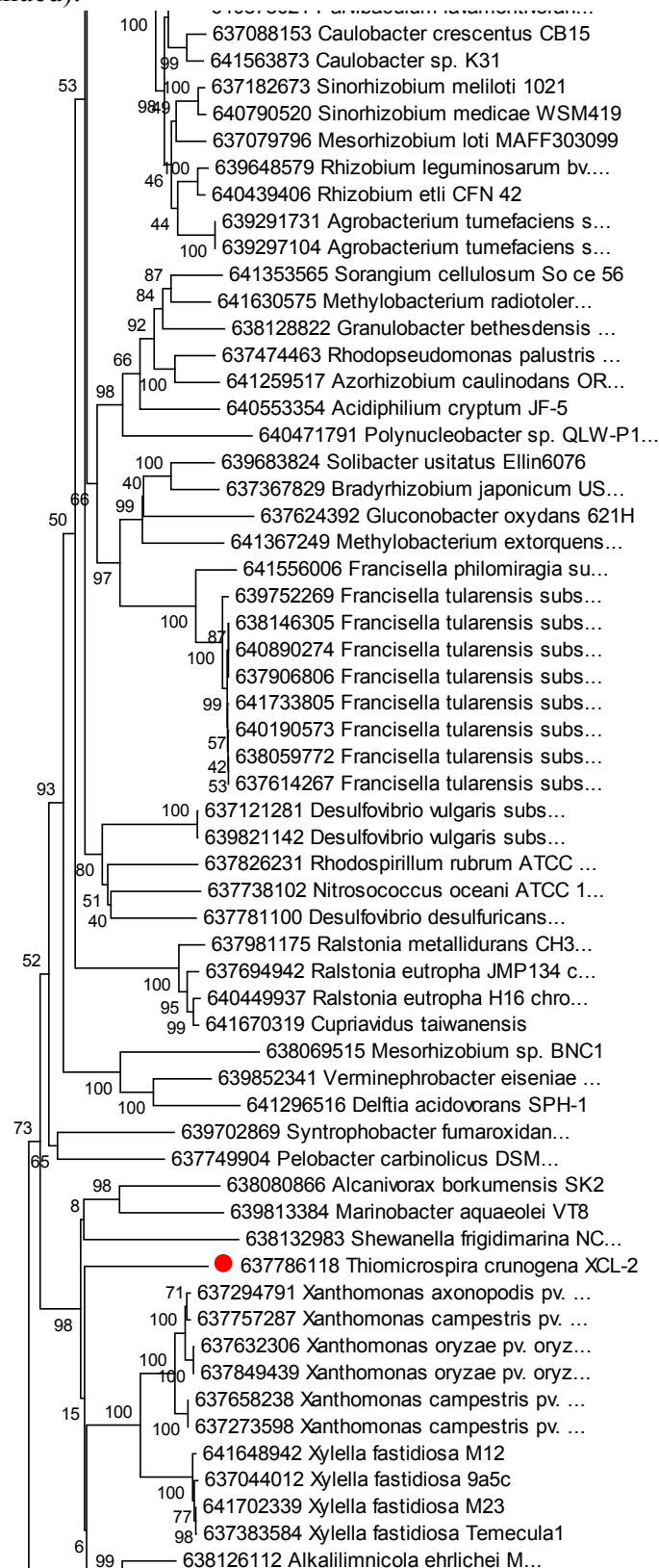




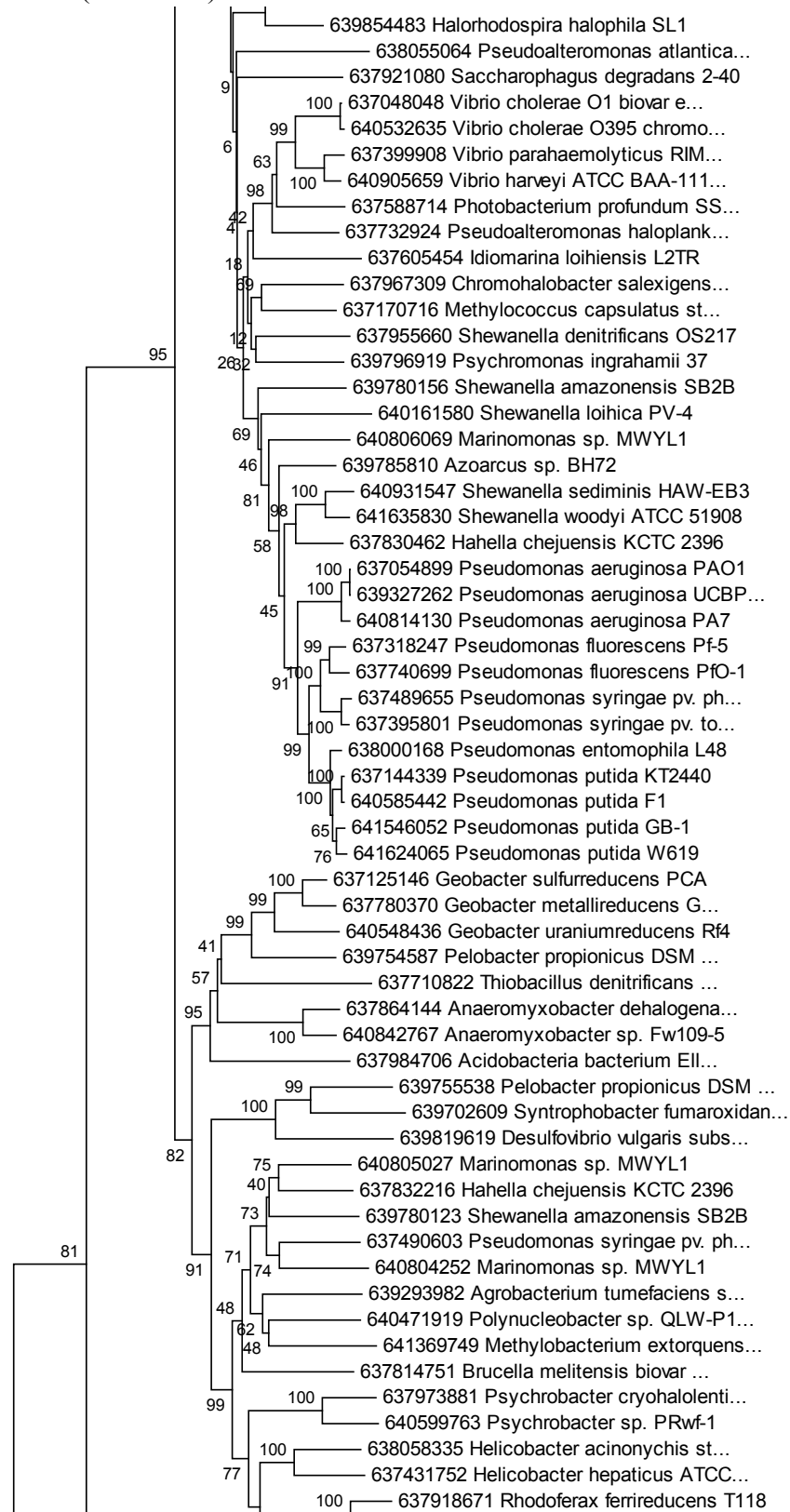
Appendix 23 (continued):



Appendix 23 (continued):



Appendix 23 (continued):



Appendix 23 (continued):

